G.A. Dantuma

Hydraulic conductivity determination with direct push methods

TU Delft

Hydraulic conductivity determination with direct push methods

By

G.A. Dantuma

in partial fulfilment of the requirements for the degree of

Master of Science
in Applied Earth Sciences

at the Delft University of Technology,
to be defended on Monday May 30, 2016 at 16:00.

Supervisor:	Prof. dr. ir. T.J. Heimovaara	TU Delft
Thesis committee:	Dr. A. Askerinejad	TU Delft
	Dr. D.V. Voskov	TU Delft
	Ir./ MSc. B. Snacken	Fugro

This thesis is confidential and cannot be made public until May 30, 2021.

Acknowledgements

Hereby I would like to thank everybody who supported me during the whole thesis process. First my supervisors at Fugro, Barbara Snacken and Herman Wolfs who spend a lot of time on my thesis. Unfortunately Herman couldn't support any more for the last months. Second all the committee members at the university, Timo Heimovaara, Amin Askerinejad and Denis Voskov. The new insight, comments and ideas kept me on track and helped when I got stuck.

I would also thank Bas Berbee for his first introduction in the topic and showing me the research he has done. Also I would like to thank Ahmed Tohami for showing me the HPT in the truck and in practice at the sight in Velp. Seeing it being used in practice showed me the possibilities and limitations of the probe and it was a great opportunity to discuss these subjects with people who use the probe in practice. Of some of the details of the probe I had different thoughts based on the available documents. Seeing it in practice has cleared some misunderstandings for me.

And of course all my family and friends who supported me.

Abstract

The topic of this thesis covers hydraulic conductivity determination with direct push methods. The most known direct push method is the Cone Penetration Test. Based on this technique a method was developed to determine the hydraulic conductivity. This method is based on water injection from the side of the probe into the soil. Pressure transducers are installed around the injection screen or pressure is measured at surface level. The soil prevents water from freely exiting the probe, causing a pressure increase. This pressure increase is measured at the pressured transducers or at surface level. Low hydraulic conductivity will result in a higher pressure increase than higher hydraulic conductivity. Also the flowrate of the water injection is important, because a larger flowrate will cause larger pressure increases. The ratio flowrate/pressure is a measure of the hydraulic conductivity. But how to relate this ratio to the absolute hydraulic conductivity is something that is not always clear. In this thesis are several methods are given and analysed. Also the effects that take place on the soil around the injection probe and injection screen are analysed and given in this thesis.

Preface

This thesis is the result of a master graduation project for the master Geo-Engineering at the TU Delft. The topic of research is 'Hydraulic conductivity determination with direct push methods'. This topic was introduced to me by Fugro Geoservices, who have and use a direct push method to determine the hydraulic conductivity of the subsurface. This tool is called the Hydraulic Profiling Tool, or HPT. This so called probe can be used in normal CPT trucks and is therefore a very fast method compared to conventional methods used to determine the hydraulic conductivity. Also a normal CPT cone can be connected to the HPT probe, meaning that also other soil parameters then the hydraulic conductivity are retrieved.

In this thesis some of the available described methods are given and analysed in the finite element program Comsol. All these methods are described in the literature review and then analysed. In the third part the focus is more on the HPT probe and what effects take place in the soil around the probe.

Symbols

μ	dynamic viscosity of water [kg/ms]
a (HRK)	correction factor [-]
a (ellipsoid)	horizontal radius of ellipsoid [m]
a	radius of probe [m]
A	surface area of flow path [m^2]
a_s	effective radius of the spherical injection zone [m]
b (HRK)	correction factor [-]
b (ellipsoid)	vertical radius of ellipsoid [m]
b	thickness of soil column [m]
B_q	pore pressure ratio [-]
C	correction factor. See detailed info in probe description [-]
d	D_{50}, medium diameter of soil particles[m]
D_{50}	median of soil particles size [m]
DPIL(in equation)	ratio, injection flowrate / induced pressure head [m^2/s]
dV	volume change per unit time in tip process zone [m^3/s]
F_r	sleeve friction [-]
f_s	sleeve friction defined in units of stress [kPa]
g_const	gravitational constant [m^2/s]
g	gravitational constant [m^2/s]
h	head [m]
h_i	head at location i[m]
h_{total}	total head [m]
$h_{hydrostatic}$	hydrostatic head [m]
i_a	hydraulic gradient at location radius a [-]
k	hydraulic conductivity [m/s]

$k_{average}$	average hydraulic conductivity [m/s]
k_D	dimensionless hydraulic conductivity index [-]
K_{DPIL}	relative hydraulic conductivity, DPIL probe [-]
k_h	horizontal hydraulic conductivity [m/s]
k_v	vertical hydraulic conductivity [m/s]
l	length [m]
n	stress exponent [-]
p	pore water pressure [Pa]
P	measured pressure near injection point [kPa or m]
p_a	absolute pore water pressure [Pa]
p_{atmos}	atmospheric pressure [kPa]
p_{inj}	injection pressure [kPa]
p_{li}	pressure exerted by a water column of length l_i (see Figure 2.11)
p_s	hydrostatic pore pressure [kPa]
P_{trans}	pressure measured at the transducer on the surface [kPa]
Q	flowrate [m^3/s]
q	variable, based on *a* and *b*, to calculate surface area of ellipsoid [-]
Q_{inlet}	flowrate within sphere [m^3/s]
Q_{out}	flowrate out of sphere [m^3/s]
q_t	corrected cone resistance [kPa]
Q_t	normalized cone resistance [-]
r	radius or radial distance [m]
Re	the Reynolds number [-]
rho_w	unit weight of water [kN/m^3]
R_{total}	resistance to water injection [-]
R_{tube}	resistance of tube [-]

U	advancement rate of the probe [m/s]
v	velocity of fluid[m/s]
x	linear distance [m]
z	distance pressure measuring location on probe beneath or above injection point [m]
α	constant of proportionality that should be equal or less than 1.0, to correct k_D [-]
β	constant to correct k_D [-]
γ_w	unit weight of water [N/m^3]
Δh	pressure head difference [m]
σ'_v	effective in situ stress [kPa]
σ'_{v0}	effective initial in situ stress [kPa]
σ_v	in situ stress [kPa]
υ	kinematic viscosity [m^2/s]
λ	coefficient of anisotropy [-]
ρ *(anisotropy)*	radial distance from point source [-]
ρ	unit weight [kN/m^3]

Abbreviations

CPT	Cone Penetration Test
DPIL	Direct Push Injection Logger
DPP	Direct Push Permeameter
HPT	Hydraulic Profiling Tool
HRK	High Resolution-K probe
PT	Pressure Transducer

Contents

1 Introduction

1.1 Introduction to the research

This thesis is the result of master graduation project on the topic: 'Hydraulic conductivity determination with direct push methods'. In this chapter an introduction is given to this topic, where it originates from and how the research will be done.

1.2 Context of the research

The topic originates from Fugro, which uses a direct push method to determine the hydraulic conductivity. This tool is called the hydraulic profiling tool or HPT. The HPT is based on the in the geotechnical field common used direct push methods. The most common known technique is the Cone Penetration Test (CPT).

1.2.1 Why would one want to determine the hydraulic conductivity?

The hydraulic conductivity is important to be known in several geotechnical and (geo)hydrological cases. Some are given in this paragraph.

Piping

Piping is the process of water leakage under a dike (Figure 1.1), caused by a difference in hydraulic head between the two sides of a dike. Dikes are usually made up out of an impermeable material such as clay. But below the dike permeable material such as sand can be present, forming an aquifer. The difference in head causes water flow through the aquifer. The water therefore ends up at the other side of the dike, where the head is lower. In practice it starts with small wells. But the problem lies in the fact that this water can also take soil particle with it, creating internal erosion of the dike. In the worst case scenario, a whole dike fails. Recently piping has become a more trending topic in the Netherlands. Therefore, detection methods to find possible locations where piping can take place are becoming more important. Piping can only take place if the soil below the dike is able to let water flow. So the hydraulic conductivity has to be determined, along the whole dike. A fast method is needed to analyse the whole dike and direct push methods can be the solution to do this analysis in a faster way than conventional methods.

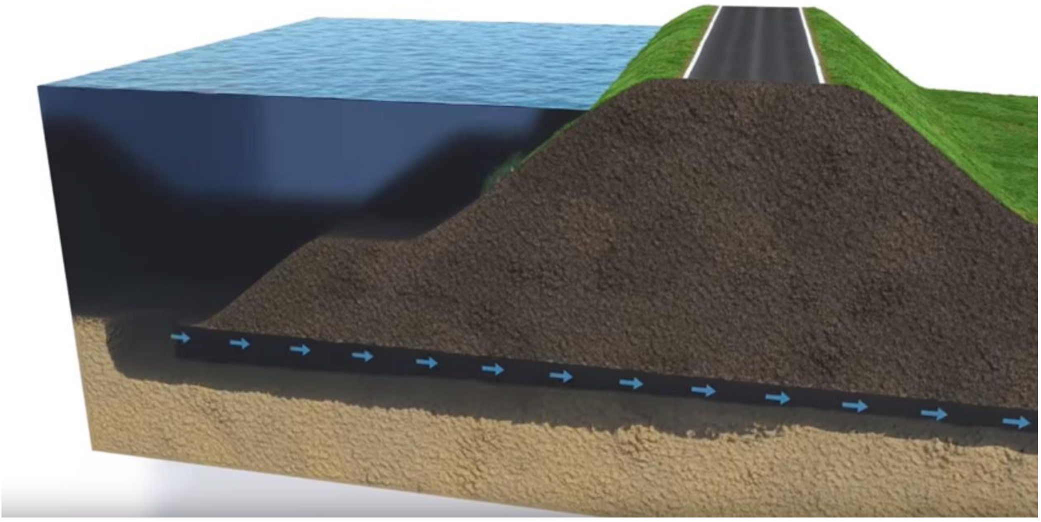

Figure 1.1: Piping under a dike, arrows indicate flow direction (WR, 2014)

Another examples are:

- the extraction and/or injection of water around building pits
- Shallow extraction wells for drinking water or production water
- Stability of foundations and constructions
- Soil remediation

1.2.2 Conventional methods for hydraulic conductivity determination

Before direct push methods were introduced to determine the hydraulic conductivity, multiple methods were already available. These methods are referred in this thesis as *conventional methods.* The most commonly used conventional methods are:

- Slug test

With a slug test a borehole is made in the subsurface. At the depth of the layer that needs to be analysed, a filter is placed. When the situation is stationary, the water level is then decreased, or increases, and the time it takes to reach a stationary situation is measured. Based on the development of the water height in the borehole, the hydraulic conductivity is determined.

- Falling head test

With a falling head test, undisturbed samples are taken at the depth of interest. These samples are analysed in the laboratory. The problem with this test is that the sample are tested in the same direction as they were sampled. This means that the vertical hydraulic conductivity is determined, while often in practice the horizontal hydraulic conductivity is of more interest.

- Grain size analysis

In a grain size analysis samples are taken at the depth of interest. These samples are disturbed, because the interest is not in the sample itself, but on the size of the grains. Based on the distribution of these grains, the hydraulic conductivity can be estimated. These methods are empirical relations and have proven these can be largely out of range of the absolute hydraulic conductivity.

Only the slug test is an in-situ test, the other two are based on an analysis of disturbed samples. Direct push methods are also in-situ methods and have the great advantage to the slug test that they can be performed in a much shorter time frame and are also less labour-intensive.

1.2.3 What are direct push methods

Direct push methods are tools which can be moved into the subsurface without drilling or removal of soil to make a path for the tool. The most common example is the Cone Penetration Test or CPT. The CPT consist of a conical shaped tip which is connected to a load cell, situation in the rod above the cone. This load cell measures the resistance encountered by the cone tip during advancement into the soil. Along the rod, just above the cone, a friction sleeve is attached. This sleeve measures the friction that the soil exerts on the sleeve. This is to distinguish the difference between weak soils such as peat or clay, which both have almost no tip resistance. Peat has a higher friction than clay and based on the friction ratio (equation (2.9)) the difference can be distinguished between peat and clay.

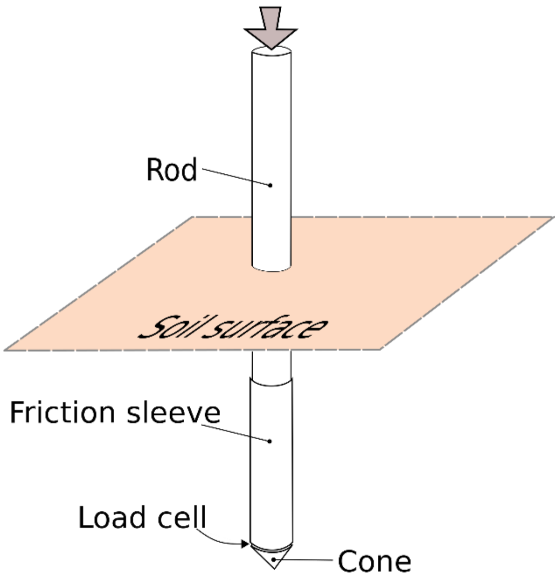

Figure 1.2: Cone penetration test probe

The probe moves into the subsurface by failure of the soil below the tip. This creates a zone of disturbed soil around the cone. This process can be seen in Figure 1.3.

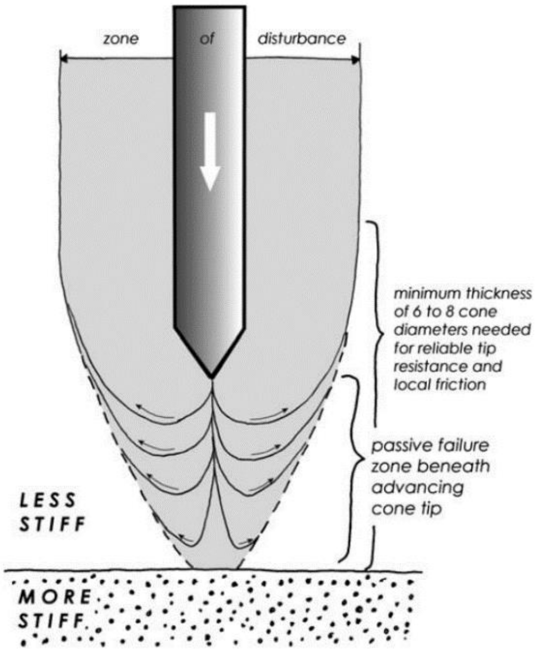

Figure 1.3: Failure of soil around the cone, forming a zone of disturbance (Rodgers, 2006)

CPT cones nowadays are fitted with one or more water pressure transducers, usually called u1, u2 and u3. The u1 is located in the tip of the cone, u2 just above the cone and u3 just above the friction sleeve. Exact locations can be seen in Figure 1.4. Note that not all these are standard present on a probe.

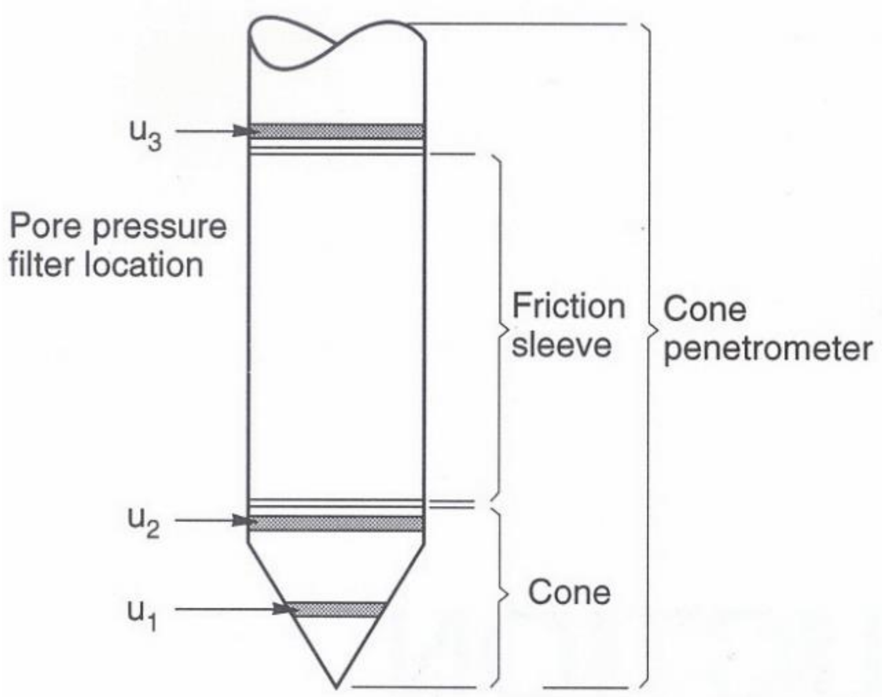

da

Figure 1.4: CPT cone with u1, u2 and u3 locations (Lunne et al., 1997)

1.2.4 Hydraulic conductivity determination with direct push methods

Because direct push methods require a lot less time to perform compared to conventional methods and because they give in-situ information, direct push methods are tested and used for hydraulic conductivity determination since the beginning of the 1980s (Rietsema, 1983).

Three types of hydraulic conductivity determination methods are distinguished:

1. Hydraulic conductivity determination based on CPT and standard water pressure transducer (u1 or u2) data.
2. Hydraulic conductivity determination based on water injection during continuous advancement into the soil.
3. Hydraulic conductivity determination based on water injection during stationary conditions, this means no movement of the probe and no excess pore pressures caused by previous movement of the cone.

The water is injected through a screen situated in the probe, with some probes having extra pressure transducers installed at the injection screen or above or below the screen. In chapter Literature review2 different examples of these methods are given.

1.3 Research questions

Based on the literature review in chapter 2, the following research questions were formed.

1.3.1 Main research question

- ***Are analytical solutions the appropriate method to determine the hydraulic conductivity?*** *According to field experience lateral hydraulic conductivity is generally higher than vertical hydraulic conductivity. Which would indicate that the assumption of a perfect spherical flow is not valid.*

This question is answered by creating a model of a direct push device with finite element software and simulated in different scenarios. Soil types, heterogeneity, anisotropy, injection rates, boundary conditions can all be varied to create different kinds of conditions. Comsol will be used to answer this question. Comsol is a very versatile software package which has the capability to include other kind of physics besides groundwater flow. At this moment Darcy's law is the only kind of physics that will be used. When a stable model is created the different methods and relations are modelled and simulated to test how well they determine the hydraulic conductivity.

1.3.2 Sub research questions

- ***How are the results affected by the compaction and creation of smear zone around the probe/cone?***

First a literature study is done. This literature can be used to give a first conclusion on the soils hydraulic conductivity. This can then be assessed in a Comsol model. If the smear zone is very thin, this might lead to limitations of the finite element method, due to the refinement of the grid near the probe. The change in anisotropy related to the deformation of the soil around the cone is something that can't be simulated in finite element code and that has to be assumed based on laboratory tests.

- ***If the system could be redesigned, where and how many pressure transducers would lead to a better hydraulic conductivity determination and at which location should water be injected?***

This is analysed in Comsol. The model can be adapted and a redesigned tool can be implemented and tested.

- *There are systems that inject from a point screen in 1D (HPT and DPIL) and systems that inject from a cylindrical screen(DPP).* ***Which method is preferred and how does the geometry affect the k-Q/P relations mentioned above?***

Idem to the question above. The system can be redesigned if needed. Experience from practice and the used different injection rates should also be taken into account.

- ***Which injection flowrates are recommended?*** *Should the injection flowrates be adjusted to different soil types in relation to short-circuiting? Can Darcy's law be assumed with the used injection flowrates of the HPT system? Should the injection rate be increased with depth? Until which depth can the HPT direct push methods be used?*

The Reynolds number can be calculated for different soil types and injection flowrates. Flowrates can be varied in the model and analysed on effect on the final result. The depth of injection can be varied in the model and its effect on the injection rate and induced pressure head.

1.4 Content of report

First a literature review is given, with most of the available direct push methods used for hydraulic conductivity estimation, now and in the past. These methods are then analysed in Comsol, in which a model of the probes is created. First an elaboration is given on how the model is created and validated. Then the results are given, tools are compared and other effects taking place around the probe are analysed. Finally, a conclusion is made and recommendations are given for further research.

2 Literature review

2.1 Introduction

There are multiple ways to determine the hydraulic conductivity of the subsurface. The faster methods are direct push techniques, where a probe with measurements devices is pushed in the subsurface. In a relatively short period of time a large amount of data can be obtained. The main advantage of these techniques compared to conventional hydraulic conductivity tests, is that the soils characteristics are measured in-situ and that much time is saved. Most of these direct push devices inject water, increasing the pore water pressure around the device. This pressure increase is measured with one or more pressure transducers, at surface level or in-situ. The injection flowrate (Q) into the soil and the measured pressures (P) can be used to determine the hydraulic conductivity of the soil. There are multiple ways to relate the Q/P to the hydraulic conductivity(k). These are:

- Hydraulic conductivity determination based on standard u1 or u2 pressure transducers from CPT data
- Hydraulic conductivity determination based on <u>non-moving</u> direct push methods with water injection
- Hydraulic conductivity determination based on <u>moving</u> direct push methods with water injection

Existing relations are given in this report and are analysed to see what they are based on. Side-effects are also taken into account, such as the increase in pore pressure that is created by the displacement of the soil by the probe and the smear zone that is created by it.

2.2 Darcy's law for spherical flow

The basis for a scientific approach for describing groundwater flow was made by Henry Darcy (Darcy, 1956). Most methods given in the next chapter use Darcy's law, ending up with an analytical solution of the form:

$$k = \frac{Q}{4\pi \Delta h r} \qquad (2.1)$$

With:
k = hydraulic conductivity [m/s]
Q = flowrate [m^3/s]
Δh = pressure head difference [m]
r = radius at which pressure is measured [m]

Equation (2.1) is based on Darcy's law (Darcy, 1856):

$$Q = kA\frac{dh}{dx} \tag{2.2}$$

With:
A = surface area of flow path [m^2]
$\frac{dh}{dx}$ = Pressure difference over linear distance x

In equation (2.1) the flow from the injection point of the probe is assumed to be a point source from which the water dissipates in spherical direction around the point source. Note that in practice all the sources are never a perfect point source, because the injection screens are not spherically shaped.

Changing from 1-dimensional flow to spherical flow:

The limit of the pressure difference over a certain radius of the sphere is:

$$\lim_{\Delta r \to 0} \frac{h(r + \Delta r) - h(r)}{\Delta r} = \frac{dh}{dr} \tag{2.3}$$

Combining (2.2) and (2.3) leads to:

$$\frac{Q}{4\pi r^2} = k\frac{dh}{dr} \tag{2.4}$$

Integrating both sides with respect to r and h:

$$\int_0^r \frac{Q}{r^2} dr = \int_{h1}^{h2} 4\pi k dh \tag{2.5}$$

$$\frac{Q}{r} = -4\pi k(h_2 - h_1) \tag{2.6}$$

$$Q = 4\pi k \Delta h r \tag{2.7}$$

$$k = \frac{Q}{4\pi \Delta h r} \tag{2.8}$$

Please note that the pressure head difference is the pressure head induced by the injection of water, this means that the hydrostatic pressure must be extracted from the measured total head.

With this approach 2 assumptions are made:

- Water flow or pressure distribution follows a perfect spherical path within the soil from the injection point outwards. From field experience (Kruseman and de Ridder, 2000) however it is known that for most soft soils the horizontal conductivity tends to be higher than the vertical hydraulic conductivity. Rietsema (1983) and Bruggeman (1994) show that when pressure is measured directly above or below the injection point the calculated $k = k_h$.
- There is no turbulent flow during water injection. Darcy flow within a porous media only holds for Re <10 (Bear, 1972, Figure 2.1), which is a very low number.

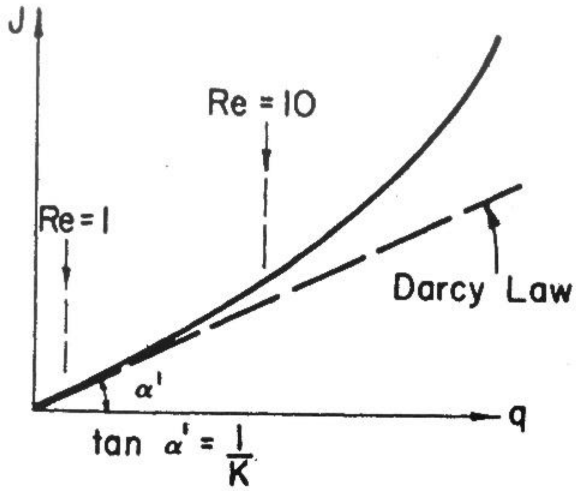

Figure 2.1: Darcy's solution compared to real values, showing increasing deviation of the hydraulic gradient(J) for higher specific discharge(q) (Bear, 1972)

2.3 Hydraulic conductivity determination based on CPT data

The CPT probe is used for determining soil parameters of the subsurface. But these properties can also give an indication of the hydraulic conductivity (Lee et al. (2008), Robertson (2010) and Chai et al. (2011)) during advancement into the subsurface. The probe displaces soil and water, creating an increase in pore pressure around the cone. This pore pressure increase, along with the cone resistance and sleeve friction measurements can be used to give an indication of the hydraulic conductivity.

2.3.1 On-the-fly method (Elsworth, 2005 and Lee et al. ,2008)

Elsworth (2005) and Lee et al. (2008) call this method the on-the-fly method. This on-the-fly method gives the hydraulic conductivity based on the standard data that is acquired by a CPT probe with water pressure transducer installed.

The CPT profile gives cone resistance, sleeve friction, and pore pressure p. By Robertson (1990) these can be defined in dimensionless form as the pore pressure ratio, B_q, cone resistance, Q_t, and sleeve friction, F_r:

$$B_q = \frac{p - p_s}{q_t - \sigma_{v0}}; \qquad Q_t = \frac{q_t - \sigma_{v0}}{\sigma'_{v0}}; \qquad F_r = \frac{f_s}{q_t - \sigma_{v0}} \tag{2.9}$$

Bq = Pore pressure ratio [-]
Q_t = Normalized cone resistance [-]
F_r = Sleeve friction [-]
p = Absolute pore fluid pressure [kPa]
p_s = Hydrostatic pore pressure [kPa]
q_t = Corrected cone resistance [kPa]
σ_{v0} = Initial in situ stress [kPa]
σ'_{v0}= Effective initial in situ stress [kPa]
f_s = Sleeve friction defined in units of stress [kPa]

p-p_s is defined as the penetration induced pore pressure, with p_s as the hydrostatic pore pressure relative to the pressure p measured at the penetrometer face.

The advancement of the penetrometer can be seen as a continuous injection of water. The amount of water displacement depends on the diameter of the probe, $2a$ (with a = radius of the probe), and the advancement rate U of the probe. The fluid volume injected per unit time is then equal to $\pi a^2 U$. Assuming that the pore fluid dissipates spherically around the cone, that there is no pore pressure change in the surrounding area and that there is no storage capacity, results in equation (2.10)(Lee et al. 2008).

$$p - p_s = \frac{\gamma_w}{4\pi k a} dV = \frac{U a \gamma_W}{4k} \tag{2.10}$$

γ_w = unit weight of water [N/m^3]
k = hydraulic conductivity [m/s]
a = radius of probe [m]
dV = volume change per unit time in tip process zone [m^3/s]
U = advancement rate of the probe [m/s]

The penetration-induced excess pore pressure, p-p_s, can be normalized by σ_{v0}, resulting in:

$$\frac{p - p_s}{\sigma'_{v0}} = \frac{U a \gamma_W}{4k\sigma'_{v0}} = \frac{1}{k_D} \tag{2.11}$$

With k_D as the dimensionless hydraulic conductivity index. This index can also be written as:

$$\frac{p - p_s}{\sigma'_{v0}} = \frac{p - p_s}{q_t - \sigma_{v0}} \frac{q_t - \sigma_{v0}}{\sigma'_{v0}} = B_q Q_t = \frac{1}{k_D} \tag{2.12}$$

Or:

$$k_D = \frac{1}{B_q Q_t} \tag{2.13}$$

Equation (2.13) only holds for partially drained soils (Elsworth, 2005), this means that the hydraulic conductivity is low enough to allow excess pore pressure to be generated by the cone. In case the hydraulic conductivity is too high, no excess pore pressure will be generated and/or measured.

This dimensionless hydraulic conductivity can be related to the absolute hydraulic conductivity by:

$$k = \frac{k_D U a \gamma_W}{4\sigma'_{v0}} \tag{2.14}$$

2.3.2 On-the fly method (Chai et al. 2011)

Chai et al., (2011) used the on-the-fly method and improved it in order to obtain better results within finer type of soils. Resulting in the following relation:

$$p - p_s = (p_a - p_s)\frac{a}{r} \tag{2.15}$$

With:
p = pore water pressure [Pa]
p_s = hydrostatic water pressure [Pa]
p_a = absolute pore water pressure [Pa]
a =radius of probe
r =radius

The hydraulic gradient that is created by the advancement of the cone is defined as:

$$i|_{r=a} = i_a = \frac{1}{\gamma_w} * \frac{dp}{dr}\bigg|_{r=a} = \frac{p_a - p_s}{a\gamma_w} = B_q Q_t \frac{\sigma'_{v0}}{a\gamma_w} = \frac{1}{K_D} * \frac{\sigma'_{v0}}{a\gamma_w} \qquad (2.16)$$

With:
i_a = hydraulic gradient at location radius a [-]

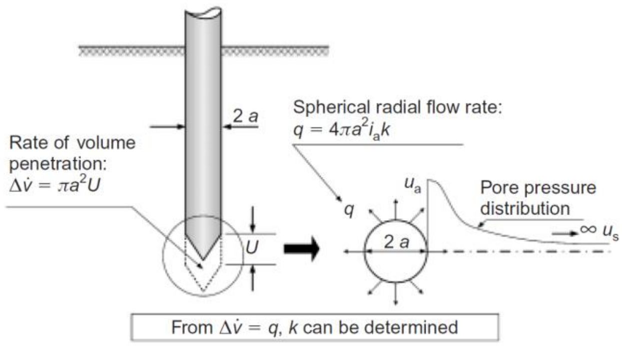

Figure 2.2: On-the-fly method visualised (Chai et al., 2011)

By equating the rate of volume penetration (volume displaced by the probe or *ΔV*) to the spherical radial flow rate(*q)* (Figure 2.2) the hydraulic conductivity can be determined:

$$4\pi a^2 k i_a = \alpha_1 \pi a^2 U \qquad (2.17)$$

With α_1 as the constant of proportionality that should be equal or less than 1.0, look at Figure 2.4 to what values α_1 equals. Combining equation (2.16) and (2.17) and introducing $k'_D = \alpha_1 k_D$ results in the following:

$$k'_D = \alpha_1 k_D = \frac{\alpha_1}{B_q Q_t} = \frac{4k\sigma'_{v0}}{a\gamma_w U} \qquad (2.18)$$

Because water cannot flow into the cone, instead of spherical flow only half spherical flow is assumed.

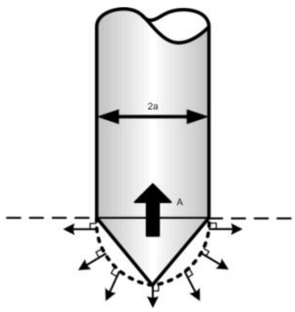

Figure 2.3: Half spherical flow according to Chai et al (2011)

Based on the half spherical flow and equation (2.17):

$$2\pi a^2 k i_a = \alpha_1 \pi a^2 U \quad \text{or} \quad \alpha_1 k_D = \frac{2k\sigma'_{v0}}{a\gamma_w U} \qquad (2.19)$$

For α_1=1, the equation becomes:

$$k_D = \frac{2k\sigma'_{v0}}{a\gamma_w U} \tag{2.20}$$

Field data and equation (2.13) proposed by Lee et al. (2008) were compared. There was a deviation in final result (Figure 2.4 left) . Equation (2.13) is only valid for $B_qQ_t < 0.45$. If $B_qQ_t > 0.45$, values of α of *0.044* and a value of β of *4.91* were empirically determined by fitting the results of k_D to the values of B_qQ_t. The result of equation (2.13) and (2.21) is plotted in Figure 2.4. The data which is shown in Figure 2.4 are 6 data sets, with k-values ranging from 3.0E-9 to 9.0E-3 m/s.

$$k_D = \frac{0.044}{(B_qQ_t)^{4.91}} \qquad (B_qQ_t > 0.45) \tag{2.21}$$

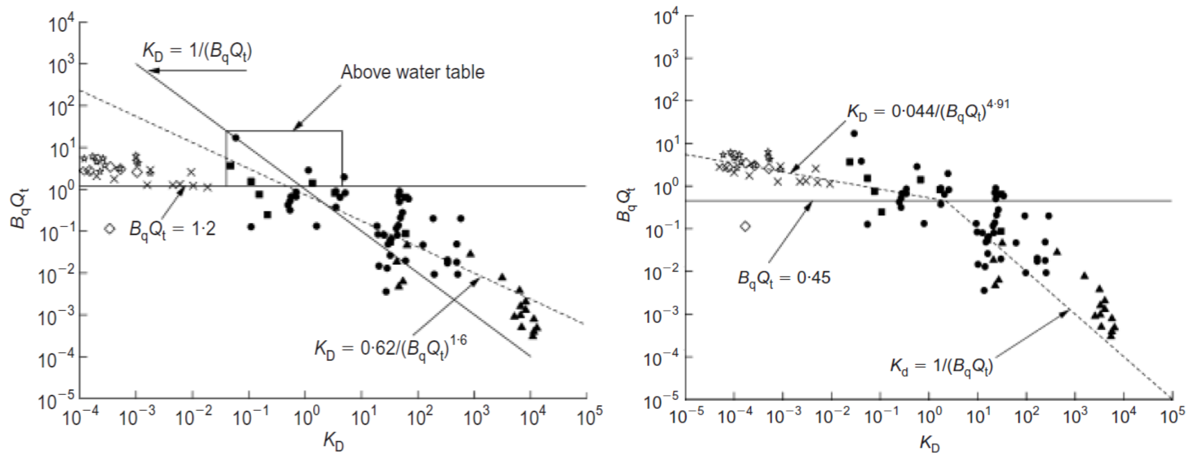

Figure 2.4: Dimensionless hydraulic conductivity (K_D) determination based on CPT testing (left: Elsworth 2005 and right: Chai et al., 2011). On the left is the result of Elsworth. Because of the deviation on result for the are on the left side of the graph, Chai et al. suggested to use 2 approaches with B_qQ_t = 0.45 as a boundary. This improved solution is shown in the right graph by the dashed line. The different types of indicator indicate the type of dataset.

2.3.3 Hydraulic conductivity based on CPT-u data

Another method for determining the permeability based on CPT data is given by Robertson (2010).

The relation is also based on CPT data:

$$When\ 1.0 < I_c \leq 3.27 \qquad k = 10^{(0.952 - 3.04 I_c)} \tag{2.22}$$

$$When\ 3.27 < I_c \leq 4.0 \qquad k = 10^{(-4.52 - 1.37 I_c)} \tag{2.23}$$

With:
k = Hydraulic conductivity [m/s]

$I_c = [(3.47 - log\ Q_{tn})^2 + (log\ F_r + 1.22)^2]^{0.5}$

In which:
F_r = Sleeve friction (Robertson, 1990)
Q_{tn} = Normalized cone resistance

$$Q_{tn} = [\frac{q_t - \sigma_{v0}}{p_{atmos}}](\frac{p_{atmos}}{\sigma'_{v0}})^n \tag{2.24}$$

q_t = Corrected cone resistance [kPa]
σ_{v0} = Initial in situ stress [kPa]
p_{atmos} = Atmospheric pressure [kPa]
n = Stress exponent, which is defined as:

$$n = 0.381\, I_c + 0.05\left(\frac{\sigma'_{v0}}{p_a}\right) - 0.15 \tag{2.25}$$

I_c is in this formula defined as:

$$I_c = [(3.47 - log\, Q_t)^2 + (log\, F_r + 1.22)^2]^{0.5} \tag{2.26}$$

With Q_{tn} and F_r as defined by Robertson (2009).

2.4 Q/P relations of direct push methods with water injection

In this chapter examples are given of several direct push methods and the existing *Q/P-k* relations related to the mentioned method. The methods mentioned in this part use water injection from the probe into the soil. Pressure transducers that are installed near the injection point measure the pressure distribution in the soil around the injection point and based on the measured pressure, the hydraulic conductivity can be derived.

2.4.1 Dipoolsonde

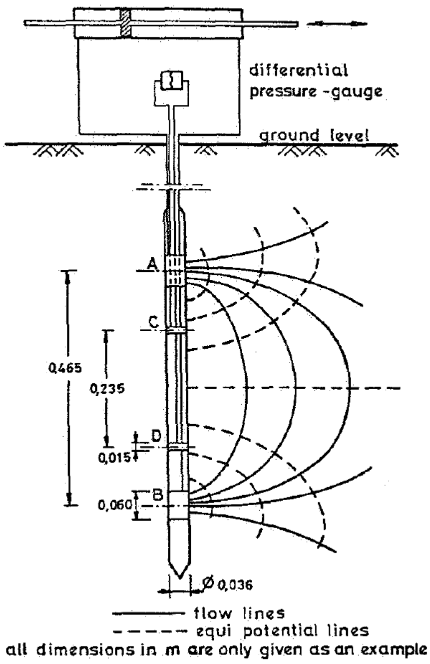

Figure 2.5: Dipoolsonde (Rietsema, 1983)

This probe is one of the first tools developed to determine the hydraulic conductivity in-situ through the use of a probe. When the depth is reached at which the hydraulic conductivity has to be determined, the water is injected through screen *A* and extracted through screen B at exactly the same rate. Two pressure transducers (*C* and *D* in figure

2.4) are present between the two injection filters (*A* and *B)* at a distance of 0.115 metre from each filter. According to Rietsema (1983) the dipool probe can't be used in clay type soils. One of the reasons mentioned being the injection filters could get clogged and affects the probes usability.

The hydraulic conductivity relation for this tool is based on the following equation:

$$h_{r,z} = \frac{Q}{4\pi\sqrt{k_h k_v}\sqrt{r^2 + \frac{k_h}{k_v}z^2}} \tag{2.27}$$

For $r=0$ and $k_h=k_v$, the following applies:

$$h_{r=0,z} = \frac{Q}{4\pi k_h z} \tag{2.28}$$

$$h_c = \frac{Q}{4\pi k_h(L_1 - L_2)} - \frac{Q}{4\pi k_h(L_1 + L_2)}, h_D = -h_c \tag{2.29}$$

$$h_c - h_D = \frac{Q}{2\pi k_h}\left(\frac{1}{L_1 - L_2} - \frac{1}{L_1 + L_2}\right) \; or \tag{2.30}$$

$$k_h = \frac{Q}{C(h_C - h_D)} = \frac{Q}{C\Delta h} \tag{2.31}$$

With:

$C = \frac{2\pi}{\frac{1}{L_1-L_2} - \frac{1}{L_1+L_2}}$ and $\Delta h = h_C - h_D$

h_i = Head at location *i*[m]

L_1 = Half of the length between the 2 injection filters *(0.465/2 = 0.2325 meter)*

L_2 = Half of the length between the 2 pressure transducers *(0.235/2 = 0.1175 meter)*

z = distance pressure measuring location on probe beneath or above injection point [m]

q = Injection flow rate [m^3/s]

k_h = horizontal hydraulic conductivity [m/s]

2.4.2 Monopoolsonde

The monopoolsonde is a tool developed by GeoDelft, now known as Deltares. It was developed in the early 90s, but has never become a commonly used tool.

The tool uses a cylindrical surface injection filter of centimetre length, through which the water is injected. Below the injection filter there are two strain gauges, giving the head difference over those two strain gauges.

The relation that was created for this method is (Lambert, 1996):

$$\Delta h = C\frac{Q}{k} \quad or \quad k = C\frac{Q}{\Delta h} \tag{2.32}$$

With:

Q = Injection flowrate [m^3/s]

Δh = Potential decay over the 2 measuring locations [m]
C = Constant [-], based on the geometry of the infiltration filter and potential measuring locations.

With a cylindrical filter with a height of 10 centimetre and probe diameter of 36 millimetres as shown in Figure 2.6, C = 0.943.

k = Hydraulic conductivity [m/s]

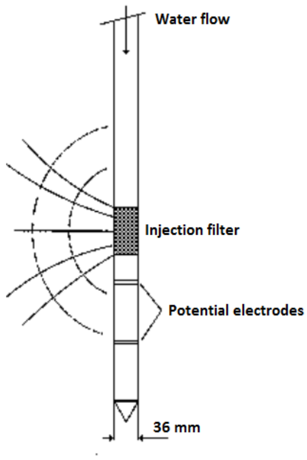

Figure 2.6: Monopoolsonde (van Ree, 2003)

Equation (2.32) gave higher values than expected during the first field tests, based on conventional tests done at the same location. Therefore, C was corrected to 0.74.

The relation that is given for the monopoolsonde by Lambert (1996), is also given by Zschornack et al. (2013). They define C as:

$$C = \frac{1}{4\pi r} \tag{2.33}$$

With r defined as the distance from the injection location to the pressure transducer.

2.4.3 The perméafor

The perméafor is a French probe designed for logging the hydraulic conductivity. Water is injected from a cylindrical screen which is smaller than the probe diameter. The probe performs 5 to 10 measurements per metre. The tests only take place for 10 seconds, meaning that a stable pressure head might not be reached. The relation between Q, P and h is (Barghava, 2012) :

$$Q = \frac{2\pi \frac{l}{D}}{log \frac{l}{D} + \sqrt{\frac{l^2}{D^2} + 1}} k\Delta h D \tag{2.34}$$

In which:
l = length of probe screen(PT1) [m]
D = diameter of probe screen [m]

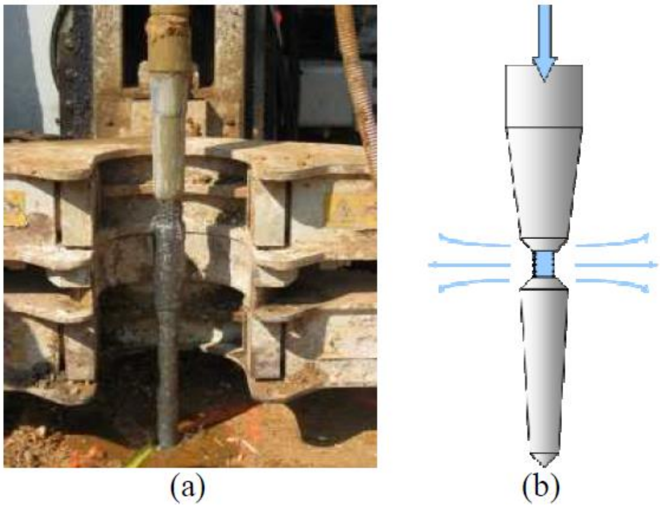

Figure 2.7: The perméafor probe, according to Fargier et al. (2013)

2.4.4 Direct push permeameter or DPP

Butler Jr. et al. (2007) give a relation for a probe called DPP (Direct Push Permeameter), where water is injected through the DPP screen and pressure is measured at the 2 pressure transducers in the rod as shown in Figure 2.8. This probe is almost the same as the monopoolsonde, the only differences are the length of the injection filter (0.025 m) and that the pressure transducers are not ring transducers, but circular transducers placed on the side of the probe.

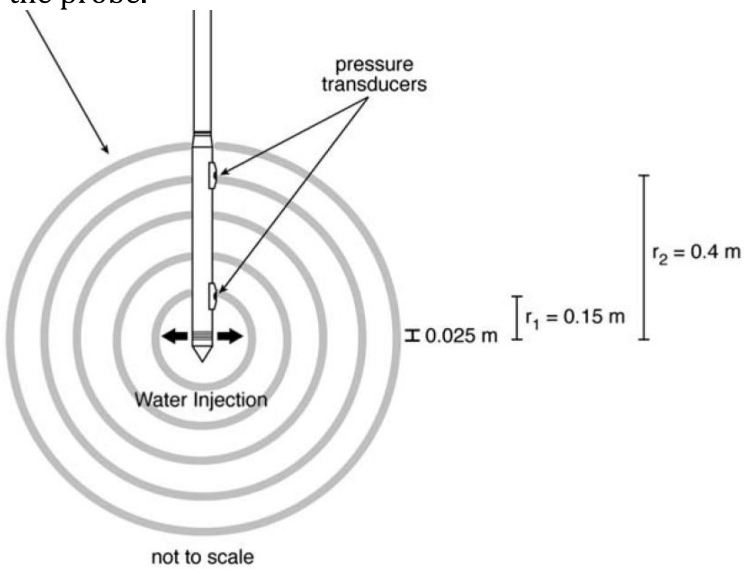

Figure 2.8: DPP according to Butler et al. Jr. (2007), note that at the pressure transducer no injection ports are present

The relation Butler et al. use to determine the hydraulic conductivity is:

$$k = \frac{Q}{4\pi\Delta h}\left(\frac{1}{r_1} - \frac{1}{r_2}\right) \qquad (2.35)$$

In which:
r_1 = distance from DPP injection screen of pressure transducer 1(PT1) [m]
r_2 = distance from DPP injection screen of pressure transducer 2(PT2) [m]
Δh = Head difference between pressure head at PT1 and PT2 [m]

r_1 and r_2 for the DPP are 0.15 meter and 0.4 meter.

2.4.5 Cone permeameter

The cone permeameter is a probe which injects water from a cylindrical screen near the tip and is only used in stationary conditions. The relation used to determine the hydraulic conductivity is exactly the same as used with the DPP. The large difference is the amount and location of the pressure transducers. Not 1 or 2, but 5 pressure transducers are installed near the injection point at 0.05, 0.075, 0.15, 0.40 and 0.80 metre.

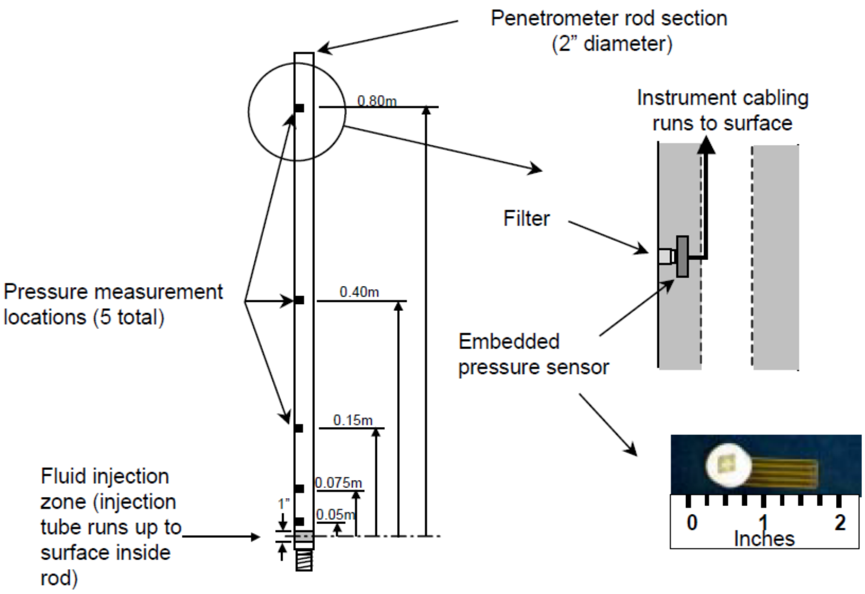

Figure 2.9: Cone permeameter according to Lowry et al. (1999)

2.4.6 In-situ permeameter

The in-situ permeameter (Lee et al., 2008) is a technique where water is injected in the soil around the probe through a screen above (Figure 2.10a) or in (Figure 2.10b) the tip of the probe. The hydraulic conductivity is determined in the following way:

$$k = \frac{Q}{4\pi \Delta h a_s} \tag{2.36}$$

In which:
k = hydraulic conductivity [m/s]
Q = measured volumetric flowrate [m^3/s]
Δh = applied pressure head [m]
a_s = effective radius of the spherical injection zone [m]

The effective radius (a_s) can be calculated by the following formula:

$$a_s = \sqrt{\frac{1}{2} a l} \tag{2.37}$$

In which:

a = radius of the screen[m]
l = length of the screen[m]

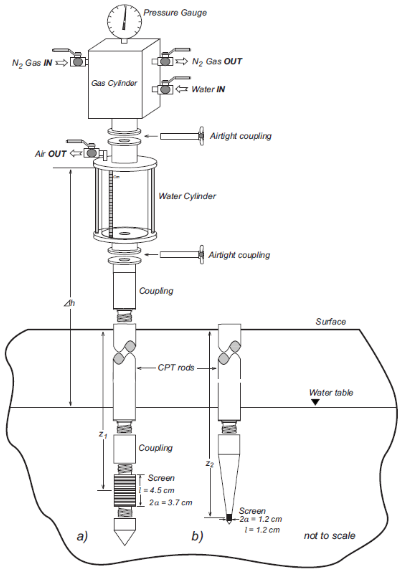

Figure 2.10: In-situ permeameter (Lee et al., 2008). In figure (a) the screen is placed above the tip. In figure (b) the injection screen is placed in the tip.

The pressure is measured at surface level and no correction are made for surface level to injection level, which is done with the DPIL (Dietrich et al., 2008).

2.4.7 Direct-push Injection Logger or DPIL

Dietrich et al. (2008) gives a probe that looks like the in-situ permeameter as illustrated in Figure 2.10a and the direct push permeameter. Though this probe does not measure in stationary mode, but in continuous advancement mode.

This method also uses an injection screen near the tip of the probe where water is injected into the ground. There are no pressure transducers near the injection point or on the rod. The injection pressure is measured at surface level and the resistance that is encountered is a measure for the hydraulic conductivity.

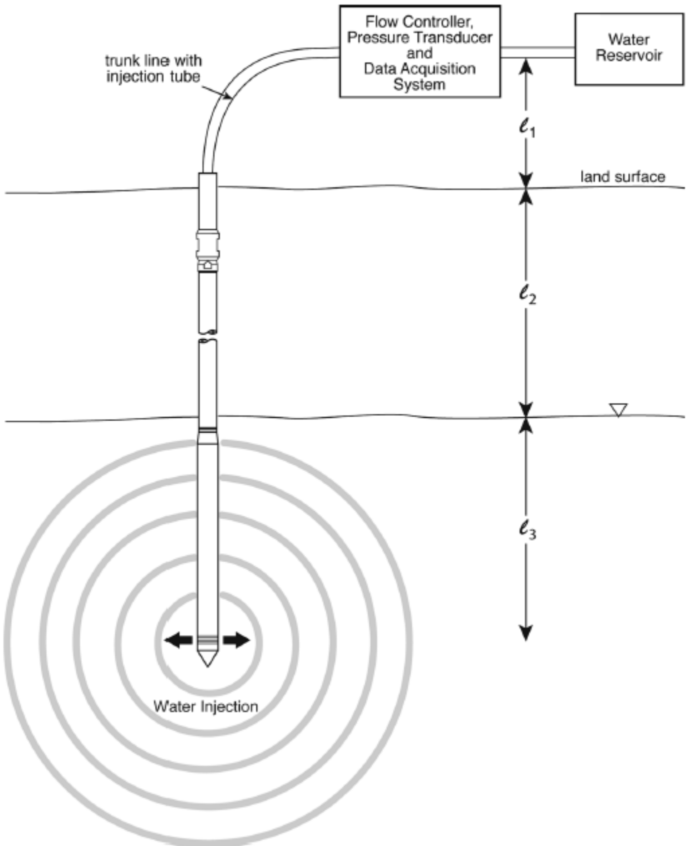

Figure 2.11: DPIL according to Dietrich et al., 2008. Note that the it is not to scale.

The proposed calculation method of the hydraulic conductivity given by Dietrich et al. (2008) is:

$$k_{DPIL} = \frac{1}{R_{total} - R_{tube}} \tag{2.38}$$

In which:
K_{DPIL} = relative hydraulic conductivity, which can be correlated to absolute values by conventional methods done around the same location.
R_{total} = resistance to water injection or the ratio of injection pressure(p_{inj}) to the injected water flow rate (Q), p_{inj}/Q. p_{inj} is defined as:

$$p_{inj} = p_{trans} + p_{l_1+l_2} \tag{2.39}$$

With:
P_{trans} = the pressure measured at the transducer on the surface [kPa]
p_{li} = the pressure exerted by a water column of length l_i (see Figure 2.11)

The resistance of the tube that transfers water from the pump to the injection point is also taken into account. This is the R_{tube} term in the formula.

The resistance R_{tube} can be determined by using, according to Dietrich et al. (2008), the Hagen-Poiseuille law:

$$R_{tube} = \frac{8Lv}{\pi r^4} \tag{2.40}$$

In which:
L = the length of the tube between the pressure transducer and the screen [m]

r = the radius of the tube [m]
v = the kinematic viscosity of the injected fluid [m^2/s]

In case turbulent flow is present within the tube, the resistance R_{tube} also becomes dependent on the flow rate and the roughness of the tube inner wall. When turbulent flow occurs, the following formula can be used:

$$R_{tube} = aQ + b \tag{2.41}$$

In which a and b are parameters that can be determined using regression analysis of flow and pressure data from the DPIL equipment.

To determine whether or not there is turbulent flow within the tube, the Reynolds number[Re] can be used to determine this. At $Re=2100$ the boundary between laminar and turbulent flow within a tube is assumed. Reynolds number, for flow in a tube, is given as:

$$Re = \frac{2Q}{r\pi\upsilon} \tag{2.42}$$

In which:
Q = flowrate [m^3/s]
r = radius of the tube [m]
υ = kinematic viscosity [m^2/s]

With $Re=2100$, this means that the critical flow rate for a certain tube is:

$$Q_r = 1050r\pi\upsilon \tag{2.43}$$

This resistivity of the tube should only be taken into account when the pressure is measured at surface level. This can be ignored, when the pressure is measured at injection level, like most other mentioned probes do. Pressure measurement at injection level is preferred, as errors in the determination of the tube resistance can be eliminated.

2.4.8 High-Resolution K or HRK probe

The HRK probe (Liu et al. 2009) combines the direct push permeameter(DPP) with water injection from openings at the side of the probe. Behind the injection screens are pressure transducers installed. The water is injected continuously during advancement into the ground through all the screens. The injection through the DPP injection screen (Figure 2.12) is to prevent it from getting clogged. Because of the combination of the DPP screen and the 2 smaller injection points, the probe can be used in 2 modes:

- Pressure measurement during movement, based on pressures at the smaller injection ports.
- Stationary measurement, only injection from the DPP screen.

The pressures measured at Pressure Transducers PT1 and PT2 can be transformed to hydraulic conductivity by equation (2.44). In practice only the results of PT2 are analysed, because PT1 is influence by the injection of water of the DPP screen and the pore pressure increase around the tip, caused by the movement of the probe.

The DPP injection screen is used in stationary conditions. After reaching a certain depth, water injection through the screen at PT1 and PT2 stops and only injection through the DPP screen takes place. The pressure transducers at PT1 and PT2 can then be used as pressure transducers and equation (2.44) gives the hydraulic conductivity. This unique combination of continuous advancement measuring and stationary measuring gives the opportunity to compare the results of both methods.

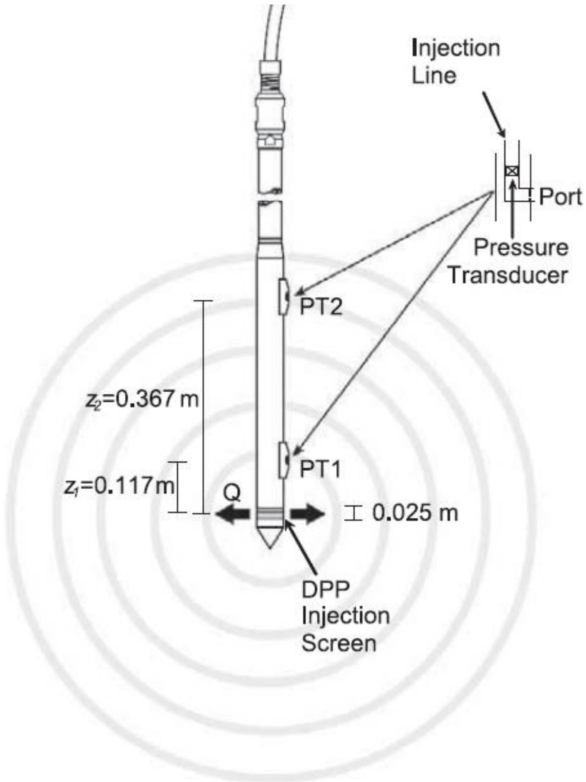

Figure 2.12:In-situ permeameter with DPIL according to Liu et al., 2009

The hydraulic conductivity for this tool is determined by the following relation:

$$k = 10^b(DPIL)^a \text{ or} \quad (2.44)$$

$$log_{10}(k) = a\ log_{10}(DPIL) + b \quad (2.45)$$

Where a and b are parameters which have to be determined through calibration and the variable *DPIL* at PT2 (*DPIL = injection flowrate / induced pressure head at PT2 [ml/min/m]*). The values for a and b were determined to be a = 2.5 and b = -9.0 (Liu et al, 2009). Note that for this relation k is in metre per day.

2.4.9 Hydraulic Profiling Tool or HPT

The Geoprobe HPT is used in a similar way as shown by Liu et al. (2009). The HPT probe however only has 1 injection point and the pressure transducer is installed inside the probe at injection level (See Figure 2.13).

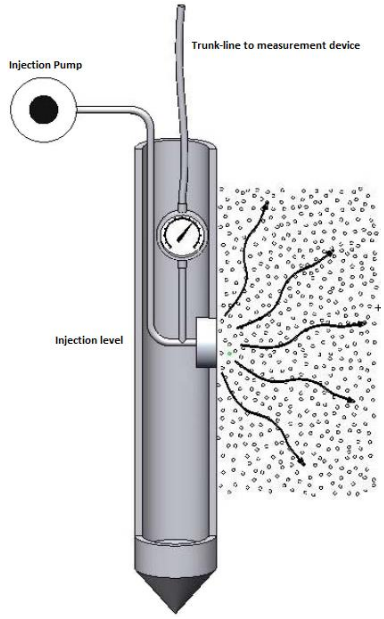

Figure 2.13: Geoprobe HPT schematic illustration (McCall, 2011)

The hydraulic conductivity relation proposed by Geoprobe, in SI Units is:

$$k = 0.3048 * (21.14 * ln(\frac{Q}{p} 6.894) - 41.71) \qquad (2.46)$$

With:
k = hydraulic conductivity [m/day]
Q= injection flowrate [ml/min]
p= injection pressure, defined as total pressure minus the hydrostatic and atmospheric pressure [kPa]

This empirical relation was developed based on field data from one location in the US, with k-values varying from 0.2 to 20 meter per day. This solution is quite different from the other methods, containing a logarithmic factor.

The HPT system can be combined with a normal CPT cone. The CPT data helps gain a better understanding of the lithology encountered and enables a better determination of the hydraulic conductivity than conventional methods.

2.4.10 Fugro HPT

Fugro (Fugro, 2015) uses an in-house designed and manufactured version of the HPT (Figure 2.14). The big difference is the design of the tip of the probe. The Fugro HPT can be equipped with standard CPT cones, which means more soil parameters are obtained and the for the situation necessary CPT cone can be used. If this cone is fitted with pressure transducers (u1, u2, u3), a steady state analysis can be conducted. Darcy's law for spherical flow can be used to analyse this data. This gives the possibility to compare the *k*-values derived from the pressure transducer at the HPT screen and the one(s) in the CPT cone.

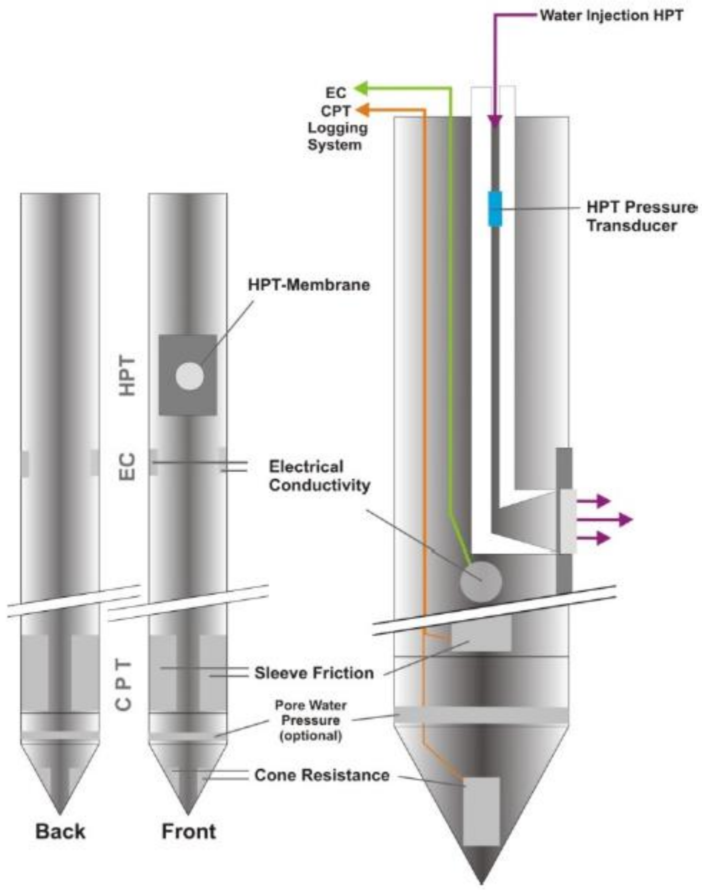

Figure 2.14: Fugro HPT schematic illustration. Note that the CPT cone is exchangeable, meaning that a specific CPT cone can be equipped with the probe

2.5 Literature on the injection zone

2.5.1 Anisotropy theory

In the scope of this research, the hydraulic conductivity is the property that can be anisotropic. From practice it is known that ratio of the horizontal to vertical hydraulic conductivity is often found to be about 10:1. Direct push methods for hydraulic conductivity estimation can only measure pressure and this measured pressure is independent of any direction. However, when the injection location and pressure transducer are spatially separated, something can be said about the hydraulic conductivity between these locations (Bruggeman, 1994). Research on anisotropy is already done by Liu et al. (2008) on the Direct Push Permeameter (DPP) probe. The hydraulic conductivity estimations based on the numerical calculations were promising.

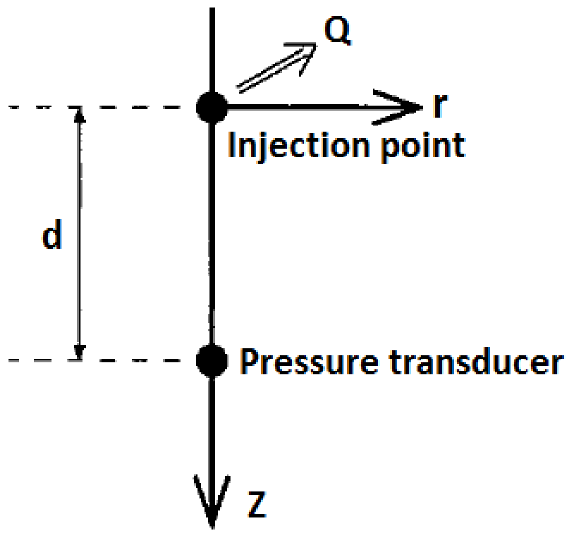

Figure 2.15: Schematic view of injection location and pressure transducer (Bruggeman, 1994)

Hydraulic conductivity in isotropic soils is spherically symmetric, meaning the only variable defining the location is the radius. As presented in paragraph 2.2 the hydraulic conductivity can be defined by the following relation:

$$k = \frac{Q}{4\pi \Delta h r} \tag{2.47}$$

And the pressure drop over a certain radius:

$$\Delta h = \frac{Q}{4\pi k r} \tag{2.48}$$

In anisotropic soils, a difference in horizontal (k_h) to vertical (k_v) hydraulic permeability is assumed. Flow is no longer spherical in symmetry but becomes axial in symmetry. In the horizontal plane it is symmetric, but differs from the vertical direction.

The radius becomes $\rho = \sqrt{r^2 + z^2}$ (Pythagoras) with *r* as the radius in horizontal direction and *z* the distance in vertical direction. Anisotropy can be incorporated in Darcy's law for spherical flow by multiplying *z* with a coefficient of anisotropy λ and replacing k by $k_{average}$. These are defined as:

$$k_{average} = \sqrt{k_h k_v}$$

$$\lambda k_v = k_{average} \rightarrow \lambda = \frac{k_{average}}{k_v} = \frac{\sqrt{k_h k_v}}{k_v} \rightarrow \lambda^2 = \frac{k_h k_v}{{k_v}^2} = \frac{k_h}{k_v} \rightarrow \lambda = \sqrt{\frac{k_h}{k_v}}$$

This results then in the following equation:

$$\Delta h = \frac{Q}{4\pi \sqrt{k_h k_v} \sqrt{r^2 + \frac{k_h}{k_v} z^2}} = \frac{Q}{4\pi \sqrt{k_h k_v r^2 + {k_h}^2 z^2}} \tag{2.49}$$

The location of the pressure transducer is directly beneath or above the injection point, meaning *r=0* and *z* is the distance between the injection point and the pressure transducer *d* as shown in Figure 2.15. When both are implemented in equation (2.49), it becomes:

$$\Delta h = \frac{Q}{4\pi K_h d} \quad \rightarrow \quad K_h = \frac{Q}{4\pi \Delta h d} \tag{2.50}$$

The result is quite surprising. When measuring a hydraulic pressure difference over a vertical distance a horizontal conductivity is calculated. This result was also obtained by Hantush (1961) and Moran and Finklea (1962).

2.5.2 Multiple layers in the injection zone

The zone of pore pressure increase around the injection point depends on the hydraulic conductivity, which varies for every soil type. Low hydraulic conductivities lead to higher pressure increases around the injection point and a greater zone of pore pressure increase compared to higher hydraulic conductivities. But what happens if the probe encounters a small embedded layer or a boundary between 2 layers?

Zschornack (2013) gives an approach to analyse which pressure transducer configuration is best for absolute hydraulic conductivity determination in a heterogeneous subsurface using the direct push permeameter (paragraph 2.4.4). The spatial distribution of the pressure transducers along the probe is numerically analysed. From the analysis it can be concluded that the ratio of the distance between the pressure transducer and the injection point and to the thickness of the small embedded layers is very important in the determination of relative changes in hydraulic conductivity. The lower this ratio is (<<1), the better the changes in hydraulic conductivity are noticed in the resulting conductivity estimations. This means that the probe that is best able to notice embedded layers, is the HPT probe. The distance of the pressure transducer to the injection point of the HPT is in theory zero, but results in chapter 5 show that this values is approximately the radius of the screen. Probes with pressure transducer(s) close the injection point are also better estimating the boundary between layers.

Probes with pressure transducers at greater distance from the injection point have a greater zone of detection, and therefore will be less sensitive to noticing small embedded layers and boundaries between layers. This can be seen in Figure 2.16, where the zone of detection intersects with a thin embedded layer. This figure comes from Liu et al. (2008), in which an analysis is done with different scenarios of thin high-k and low-k embedded layers around the DPP. The results, based on different locations of embedded layer close to the pressure transducers and injection point, vary a lot and show that when using the DPP small embedded layers are not very likely be noticed in the final result.

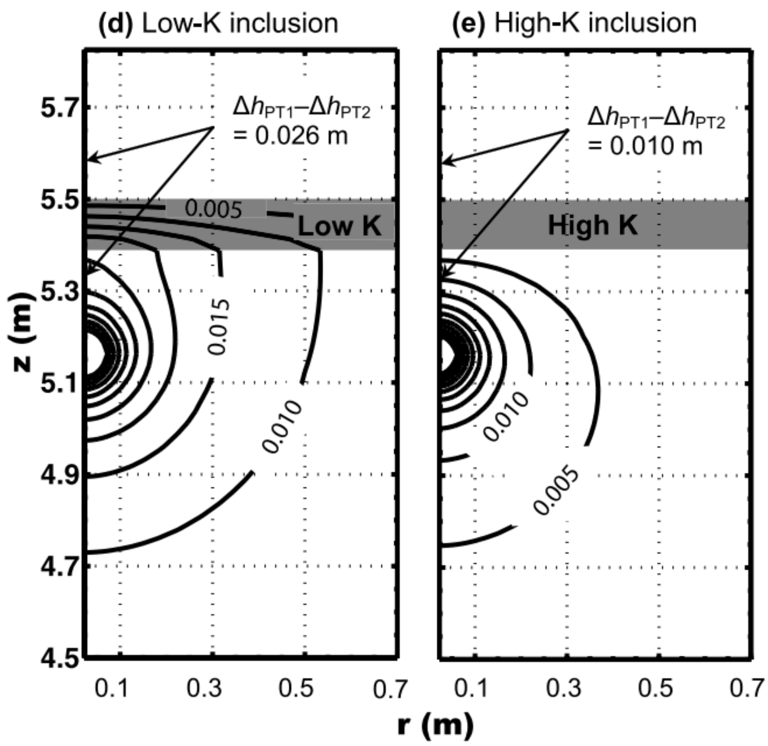

Figure 2.16: Thin embedded low- and high-k layer and the effect it has on the pressure distribution (Liu et al., 2008)

Köber et al. (2009) make a comparison between the Geoprobe HPT and DPIL and test both at a contaminated refinery site in Germany and conclude that the HPT has a better resolution of distinctive permeability differences but a lower sensitivity for smaller variations in *k*. This is only based on the results shown in Figure 2.17. Köber et al. give as a possible reason for the different observations may be a limited sensitivity of the devices and the small *k* range at the site of investigations. The low correlation could also be a consequence of measurement errors of DPIL investigations at individual positions.

It should be noted that the HPT probe is continuously injecting and measuring during advancement into the subsurface, whereas the DPIL only measures in steps of 30 centimetres.

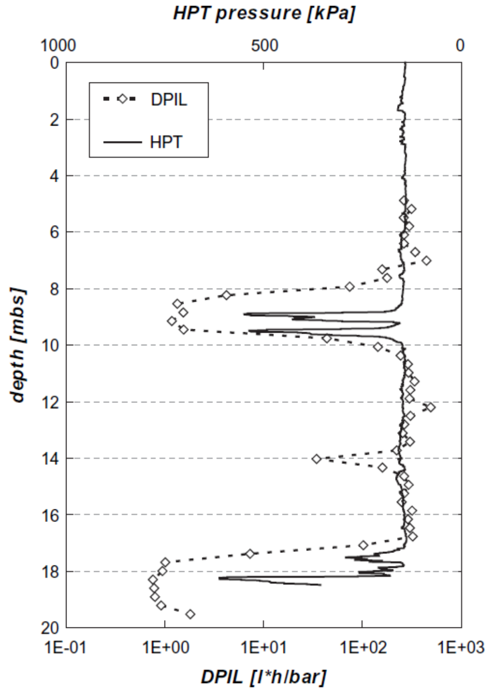

Figure 2.17: Comparison of results obtained by DPIL and HPT at same location (Köber et al., 2009)

2.5.3 Disturbed zone

The cone penetration causes deformation of the soil around the probe, creating a disturbed zone or 'skin'. The question is how this zone affects the hydraulic permeability of the soil determination with direct push methods. Liu et al. (2008) and Robertson (2010) describe the effect of the cone penetration on the soil.

Liu et al. (2008) describe it as compaction in relation to the direct push permeameter (paragraph 4.2.2). A numerical model is made where a low-*k* skin is modelled along the probe. In Figure 2.18(a) the hydraulic conductivity of the low-*k* skin is varied and in Figure 2.18(b) the thickness is varied. The base hydraulic conductivity is 1.5E-3 m/s. From the analysis is concluded that compaction does not play a significant role for hydraulic conductivity estimation with the DPP. A reason for this is the configuration of the pressure transducers.

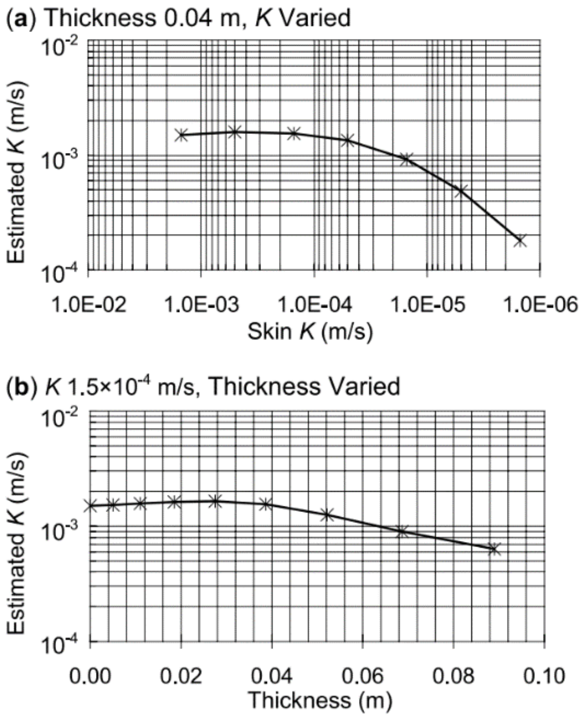

Figure 2.18: (a) Variation of hydraulic conductivity of the 4 centimetre k-skin, (b) thickness variation of skin with 10x smaller hydraulic conductivity of the skin (k of skin is 1.5E-4 m/s) (Liu et al., 2008)

Robertson (2010) gives the following relation for horizontal hydraulic conductivity:

$$k_h = (c_h \gamma_w)/M \qquad (2.51)$$

With:
k_h= Horizontal hydraulic conductivity [m/s]
c_h= Coefficient of consolidation in the horizontal direction [-]
γ_w= unit weight of water [kN/m^3]
M= 1-D constrained compressibility modulus

Equation (2.51) proves that the hydraulic conductivity is dependent on the coefficient of consolidation and compressibility of the soil. These are variables, meaning that the effect of the surrounding soil isn't constant and a specific zone of disturbance can't be drawn.

2.5.4 Clogging

Clogging of the injection screen leads to a pressure increase, resulting in a faulty measurement. Probes that perform pumping tests at certain depths are extra vulnerable to clogged screens compared to probes that perform continuous analysis. This is because water is not injected during movement into the subsurface. While proceeding into the subsurface the chance of encountering fine soil particles that clog the screen is quite high. Therefore, an injection flowrate during advancement can be used to prevent the filter from getting clogged with fine soil (Butler et al., 2002).

Liu et al. (2008) numerically analyse the effect of clogging for the DPP by applying a thin layer to the screen with a hydraulic conductivity of 1.5E-4 m/s and the surrounding soil set to a value of 1.5E-3 m/s, or a factor 10 difference. The results of the analysis show that for the DPP probe clogging has a minimal influence on hydraulic conductivity estimation with the DPP. This is because the effect is comparable to a disturbed zone around the cone. The low-*k* skin does affect the pressure distribution. But at greater distance, where the pressure transducers are located, the effect of the clogged screen is very small on the pressure transducer. Probes with pressure transducers closer to the injection point will be more influenced,

The smaller screen compared to other probes of the HPT (radius of 0.007 m) causes the injection flowrate of 500 ml/min to reach a velocity of 0.217 m/s. This is a big advantage compared to others methods, because this high injection velocity will remove fine particles from the screen and therefore reduce the chance of clogging. For the DPP injection rates are used 3.6 l/min, but this screen is much bigger. This bigger injection screen causes the injection velocity through the DPP screen of only 0.02 m/s.

2.5.5 Short-circuiting

Short-circuiting or channelling along the probe is a process which can take place during hydraulic profiling. The pressure increase causes the injected water searching for the path of least resistance. The smooth surface of the probe or an annulus along the side of the probe can be/create this path of least resistance. This annulus is created by the probe itself. This happens with probes which have parts of the injection trajectory just sticking out of the probe. An example is the HPT, which can be seen in Figure 2.19.

Figure 2.19: Injection screen of HPT

Water accumulation between the probe and soil near the injection point is something that must take place. The HPT probe has an injection flowrate of 500 ml/min. The soils next to the injection point have a hydraulic conductivity that is a factor 10-1000000 smaller than the velocity of the injected water. This means the water can't dissipate into the soil and must go somewhere.

Measures to prevent channelling are proposed by Butler et al. (2007). First is to decrease the injection rate, keeping it as low as possible. High injection rates increase the chance of short-circuiting. Second, doing 2 tests at same depth with different injection rates. By doing this the 2 results can be compared and if there is a large deviation in the obtained hydraulic conductivity, short-circuiting could be taking place. And third: Injection rate determination on the basis of expected hydraulic conductivity over that depth interval. Particular care should be given to low hydraulic conductivity intervals.

A numerical analysis on channelling is done by Zschornack et al. (2013). A high hydraulic conductivity skin was modelled along the probe and this skin is surrounded by a homogeneous aquifer with a hydraulic conductivity of 5E-5 m/s. From that analysis was concluded that channelling could have significant impact on the hydraulic conductivity estimation.

2.5.6 Generated pore pressures around cone

Fitzgerald and Elsworth (2010) and Elsworth (2013) did a numerical analysis on the generated pore pressures caused by the movement of a CPT probe. Based on their results a better understanding of what takes place can be made. The calculation results are given in Figure 2.20 and Figure 2.21.

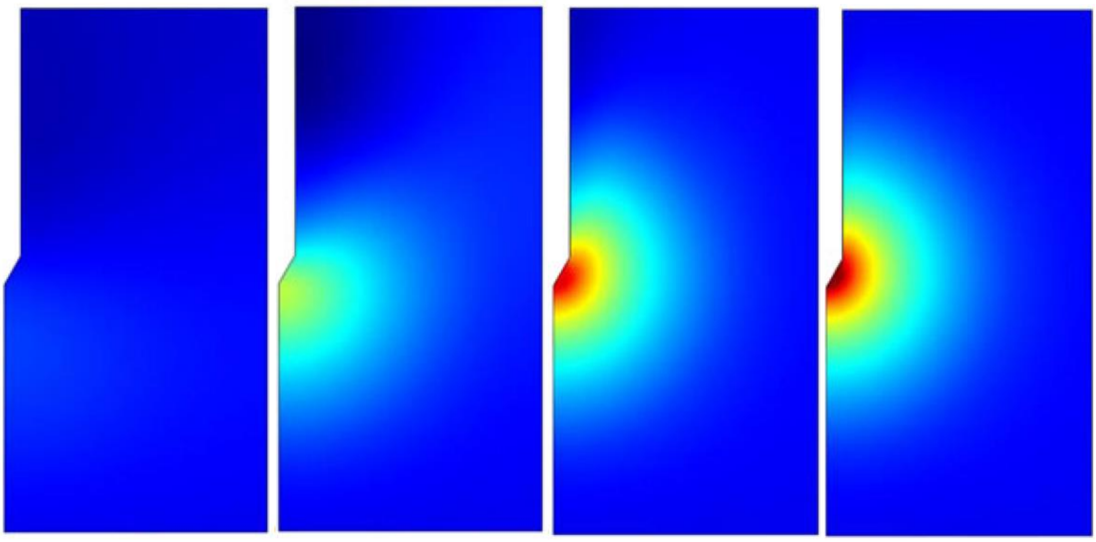

Figure 2.20: Pore-pressure generation around probe tip, for different dimensionless penetration rates (Elsworth, 2013)

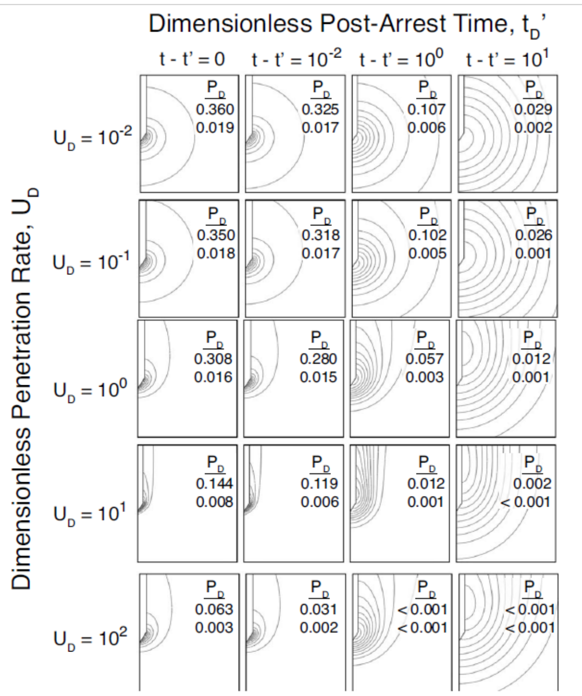

Figure 2.21: Pore-pressure generation around probe tip, for different dimensionless penetration rates(U_D) (Fitzgerald and Elsworth, 2010)

These result show that the pore pressure generation around the tip is the largest and decreases with further advancement of the probe into the subsurface. Also these results are dimensionless. From these results can be concluded that, as expected, the penetration rate plays an important role in the generated pore pressures by movement of the probe. Because it is hard to predict the development of the excess pore pressures generated by movement, empirical formulas are developed or Darcy's law is used with a reduction term. The difficulty in the prediction of the pressure distribution lies in the fact that the soil can vary in soil type, anisotropy, heterogeneity and the soil in deformed by movement of the probe, all affecting the hydraulic conductivity.

2.5.7 Available solutions for moving HPT Q/P analysis

The empirical relation given by the Geoprobe for the HPT is given as:

$$k = 0.3048 * (21.14 * ln(\frac{Q}{p} 6.894) - 41.71) \tag{2.52}$$

Fugro suggested to use the relation given by Bruggeman (1999):

$$k = \frac{Q}{4\pi \Delta h r} erfc(\frac{\beta r}{2\sqrt{t}}) \tag{2.53}$$

Liu et al. (2009) suggest to use a power-law relation of the form:

$$k = 10^b (\frac{Q}{\Delta h})^a \tag{2.54}$$

According to Liu et al. (2009), the factors are: a =2.5 and b = -9.0. According to Rogiers et al. (2013), the factors are a = 0.32 and b = -3.91.

Bohling et al. (2012) suggest a comparable power transform:

$$k = e^b (\frac{Q}{\Delta h})^a \tag{2.55}$$

Unfortunately, Bohling et al. (2012) do not give values for a and b.

Fugro also came up with a fixed value, assuming the relation to be linear.

$$k = 1.15 * \frac{Q}{\Delta h} \tag{2.56}$$

3 Numerical Modelling

3.1 Introduction model

In chapter 2 multiple methods for hydraulic conductivity estimation with direct push methods were described. Several of these methods were verified with numerical calculations and at maximum two types were compared. The model is made in software program Comsol Multiphysics version 5.1. Comsol is a finite element based program, able to analyse and solve complex problems involving multiple kinds of physics. Multiphysics will initially not be used for the current study. As Darcy's law is already defined in Comsol and the fact that the program has a good GUI, in which models can be created quite easily, Comsol is used as a basis to analyse the direct push methods given in chapter 2. This analysis helps in understanding these tools and how their different approach to relate the injection rate and measured pressure head works out in practice.

The first range of models is set up simple as possible, modelling a homogeneous and isotropic soil. In a later stage anisotropy of the hydraulic conductivity can be included an analysed. By creating one model and adapting it if necessary to other kinds of techniques, makes the whole process easier and the methods can be compared more easily.

3.2 Model Setup

3.2.1 Model domain and mesh

The models are built following the basic steps in Comsol. The chosen space dimension is 3D, because for the DPIL/HPT injection, the injection direction is in one direction so the whole model is non-symmetric.

The first model will be made out of 1 component. Later on this can be divided into multiple parts to model two 2 types of aquifer with different parameters in contact with each other. The model domain consists of one block where the injection point can be placed in the middle of the block.

The hydraulic conductivity of the model is defined by Darcy's law. To define the size of the model, Darcy's law for spherical flow can be used:

$$k = \frac{Q}{4\pi\Delta hr} \quad \rightarrow \quad radius\ of\ model = \frac{Q}{4\pi\Delta hk}$$

By defining k with a fixed value, the radius at which a certain head increase takes place can be calculated.

The following assumptions are made/criteria are set:

- a maximum head increase at the edge of the model of 0.001 metre
- maximum injection rate of 6000 ml/min, or 1E-4 m^3/s.
- and hydraulic conductivity (k) of 9E-5 m/s (approx. 7.77 m/day)

This value of k is chosen because this values is a good average value. Not too high, which would lead to a very low pore pressure meaning the error in the final result will increase and not too low, resulting in a very high pore pressure increase and bigger influenced area. Because the pore pressure increase extends further than in high permeable soils, the model becomes bigger meaning that the model becomes more complex to calculate.

To meet the criteria set above, the minimum radius r of the model domain should be:

$$r = \frac{Q}{4\pi\Delta hk} = \frac{1 * 10^{-4}}{4\pi * 0.001 * 0.00009} \approx 30\ m$$

Two times the radius is the diameter, so the model must have a size of 60 x 60 metre on the horizontal direction and the thickness is set to 30 metre below the injection point/screen. This means that if the injection location is modelled at 2.5 metre, the total thickness of the model is 32.5 metre.
The mesh is made with the *user-controlled mesh* option in Comsol. Using the *standard physics-controlled mesh* results in an unnecessary complex mesh and complications of the mesh formation around the injection point. The mesh is automatically refined to allow the circular shape of the cone. This is also preferred for the calculation, because detail around the injection point is important.
The following settings are used to create the mesh:

Calibrate for:	*General physics, custom*	
	Value	**Unit**
Maximum element size	10	m
Minimum element size	0.003	m
Maximum element growth rate	1.3	[-]
Curvature factor	0.6	[-]
Resolution of narrow regions	1	[-]

Table 3.1: Comsol mesh generation settings

The resulting mesh is shown in Figure 3.1.

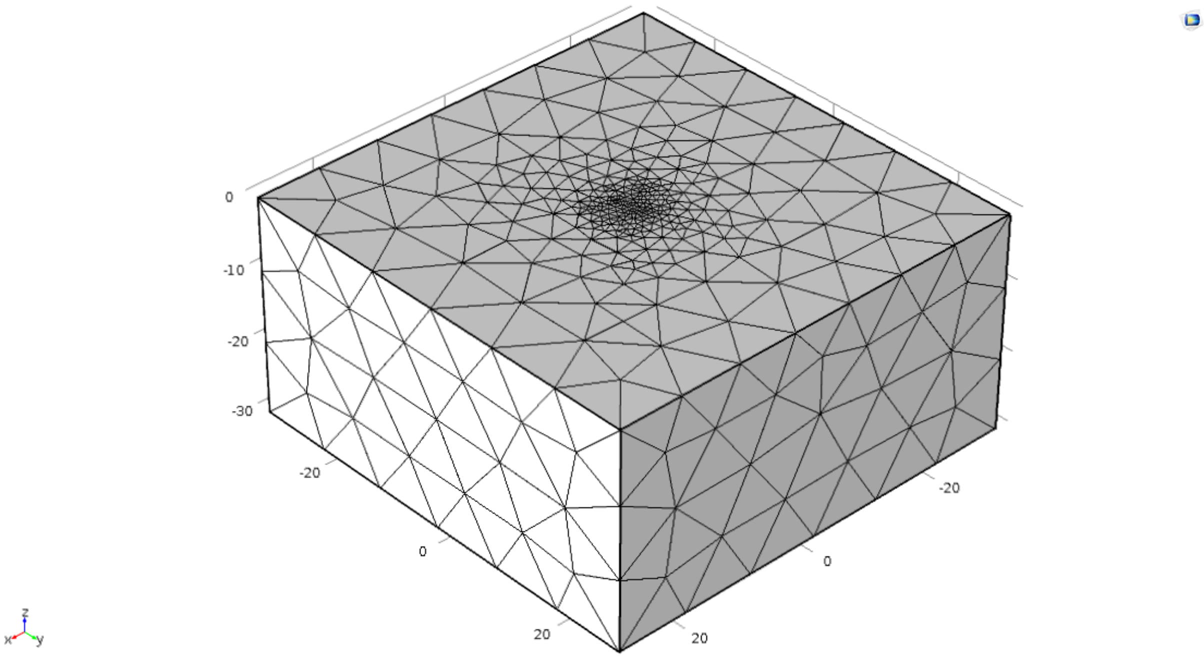

Figure 3.1: Mesh of full model domain, around the cone the mesh is automatically refined to allow circular shape

3.2.2 Material properties of Fluid and matrix properties

There is only one type of physics used in the first model, which is Darcy's law. Two materials are selected, soil and water. Both can be picked from the available materials library as:

- Soil [solid]

The only variable for the soil is the hydraulic conductivity. It is defined in the *Fluid and Matrix Properties* (Figure *3.2*).

- Water [liquid]

Comsol includes empirical relations used to determine the density and dynamic viscosity for the fluid properties based on the temperature. These equations are given in Appendix A. In these equations *T* is temperature in Kelvin as defined in the *Fluid and Matrix Properties.* In Comsol this value is set standard to T = 293.15 Kelvin.

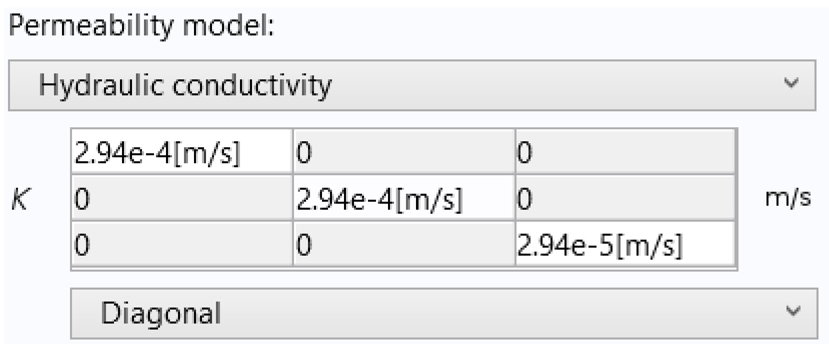

Figure 3.2: Defining permeability anisotropy. X and Y direction are assumed the same and Z-value is a lot smaller (factor 10 in this case)

3.2.3 Boundary conditions

The initial values are set to hydrostatic conditions, with ground water level or saturated zone starting at ground surface level. This is created by setting the initial conditions in the Darcy's law tab in Comsol to Hydraulic head and setting H to 0. This creates a hydrostatic pressure profile in the soil block. The head is defined as:

$$p = p_{atmos} + \rho_w * g * -z \tag{3.1}$$

There are 3 boundary conditions applied to the after initial conditions:

- Hydraulic head boundary
- No flow boundary
- Inlet boundary

The hydraulic head boundary is applied to all the outer boundaries of the block. The no flow boundary is applied to boundaries at which no flow can take place. In this case this is the rod of the probe. The inlet is applied at the boundary which model the injection screen of the probes.

3.2.4 Verification of the model

In order to verify the results that will be acquired from the model, a verification is done on the model and on Darcy's law for spherical flow or equation (2.8). At first the hydrostatic pressure distribution is verified. The result is shown in Figure 3.3. A line is plotted from surface level to 5 metre of depth and over that length the pressure head is plotted. Because the pressure head is given in metre, the line should follow the length of the line 1:1. As can be seen in Figure 3.3, this is the case, so this boundary conditions works correct.

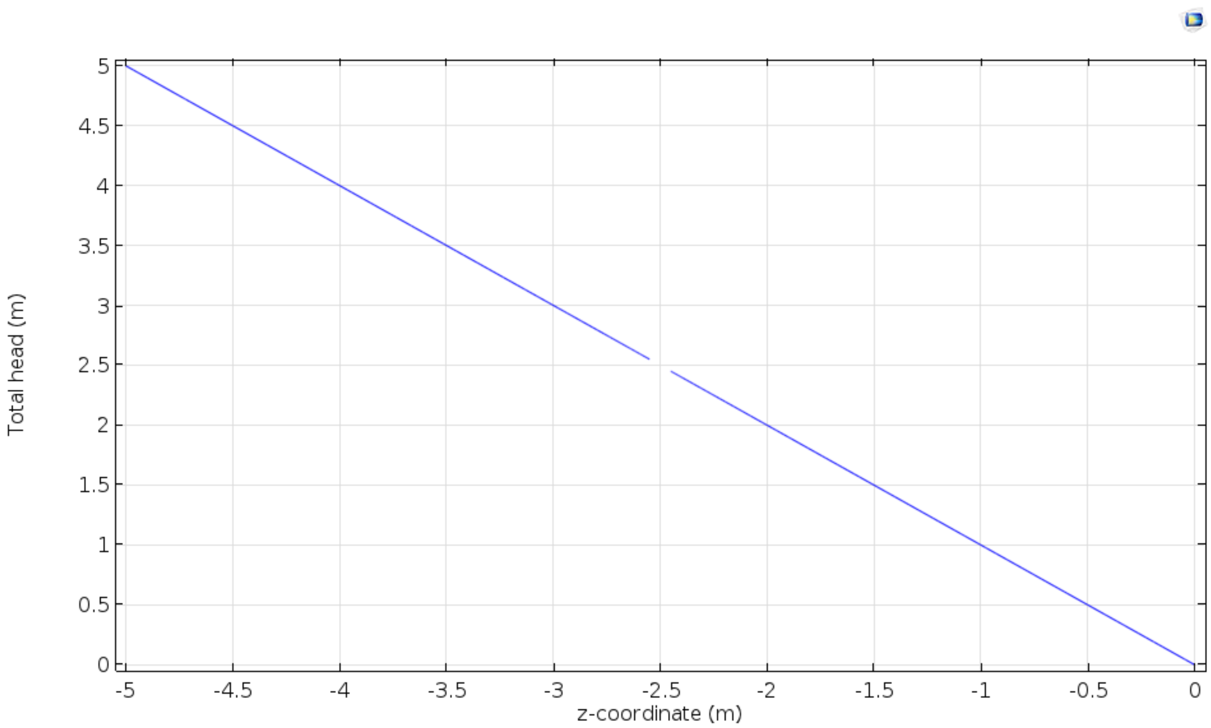

Figure 3.3: Hydrostatic head distribution

To verify the flow in the model, a mass balance is done. The model is analysed by a sphere with a radius of 5 centimetres (Figure 3.4). From this sphere water is injected into the soil to create perfect spherical injection. The sphere is placed at 2.5 metre depth. The amount of injected water is 1000 ml/min.

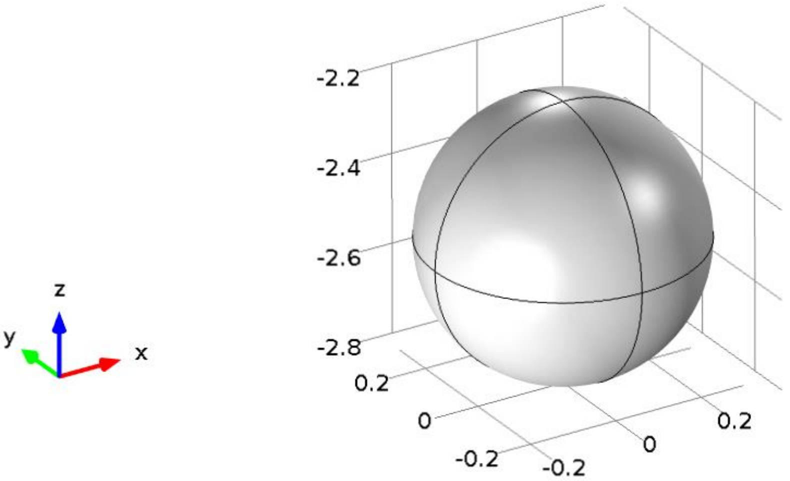

Figure 3.4: Sphere as it is modelled for analytical verification of model

The mass balance is done by creating a second sphere around the small sphere. This sphere is also placed at 2.5 metre depth and the radius is 2 metre. The mass balance becomes:

$$Q_{inlet} = \int_S Q_{out}\, dS \tag{3.2}$$

The injection rate is 1000 ml/min, or 1.6667E-05 m^3/s. The surface integral over the sphere gives a value of 1.6647 m^3/s. This means that at 2 metre radius, the error is 0.001%.

3.2.5 Verification of Darcy's law for spherical flow

As most of the methods given in chapter 2.4 use Darcy's law for spherical flow, it is good to validate this method. The numerical results obtained by Liu et al. (2008) show that the result from the Darcy law for spherical flow can result in some error.

The model used in paragraph 3.2.4 is calculated with a smaller sphere of 0.5 centimetre and an injection rate of 500 ml/min. When a cross-section line is drawn from surface level through the injecting sphere down to 5 metre depth, this results in the graph of Figure 3.5. When zooming in on the area around the sphere, it results in

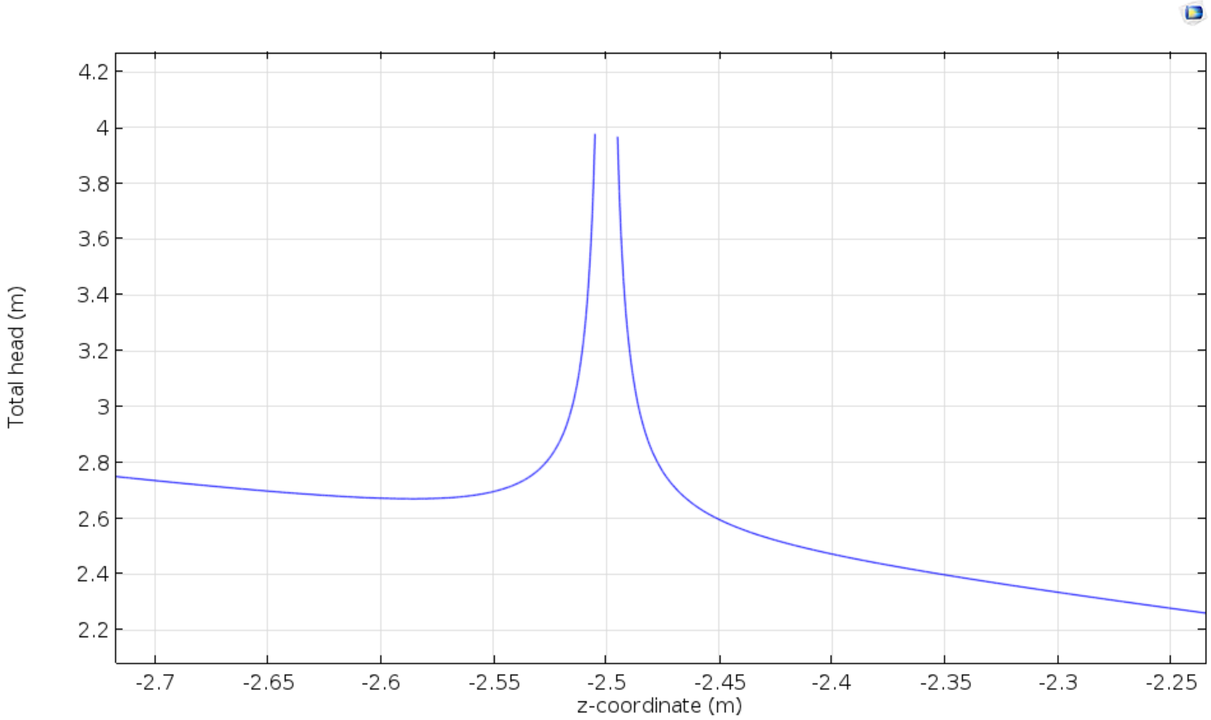

Figure 3.6.

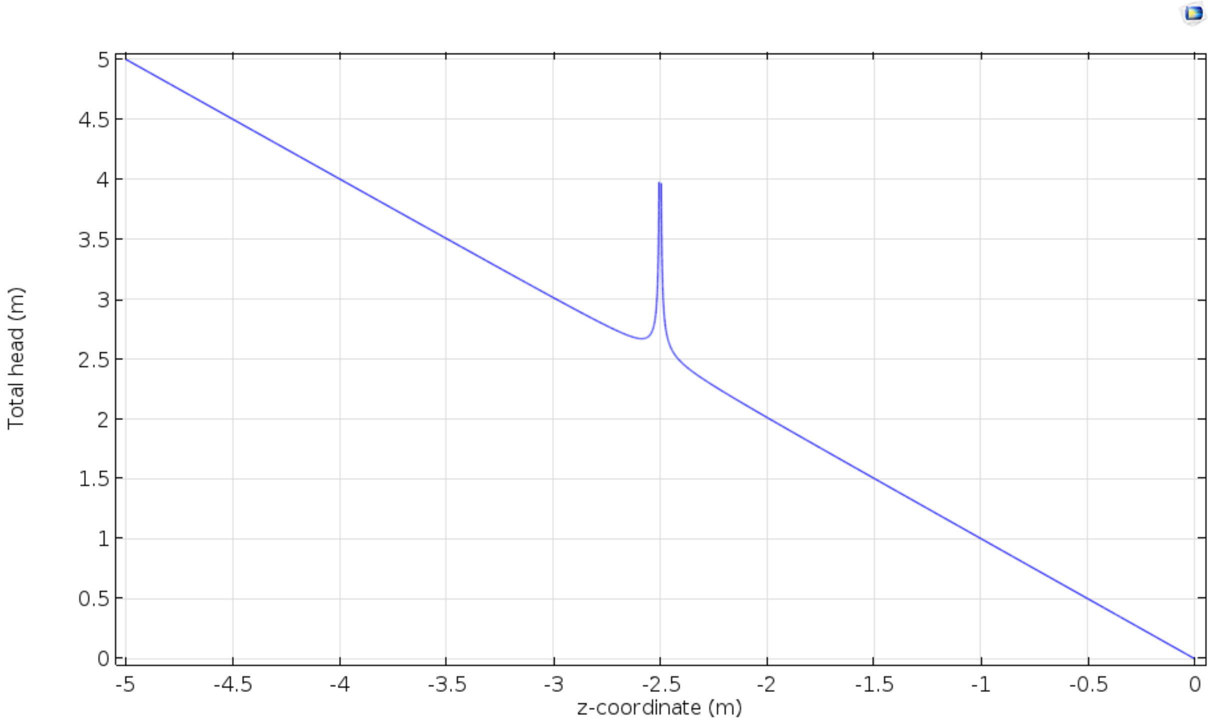

Figure 3.5: Pressure head as is results from injecting 500 ml/min from sphere at 2.5 metre depth

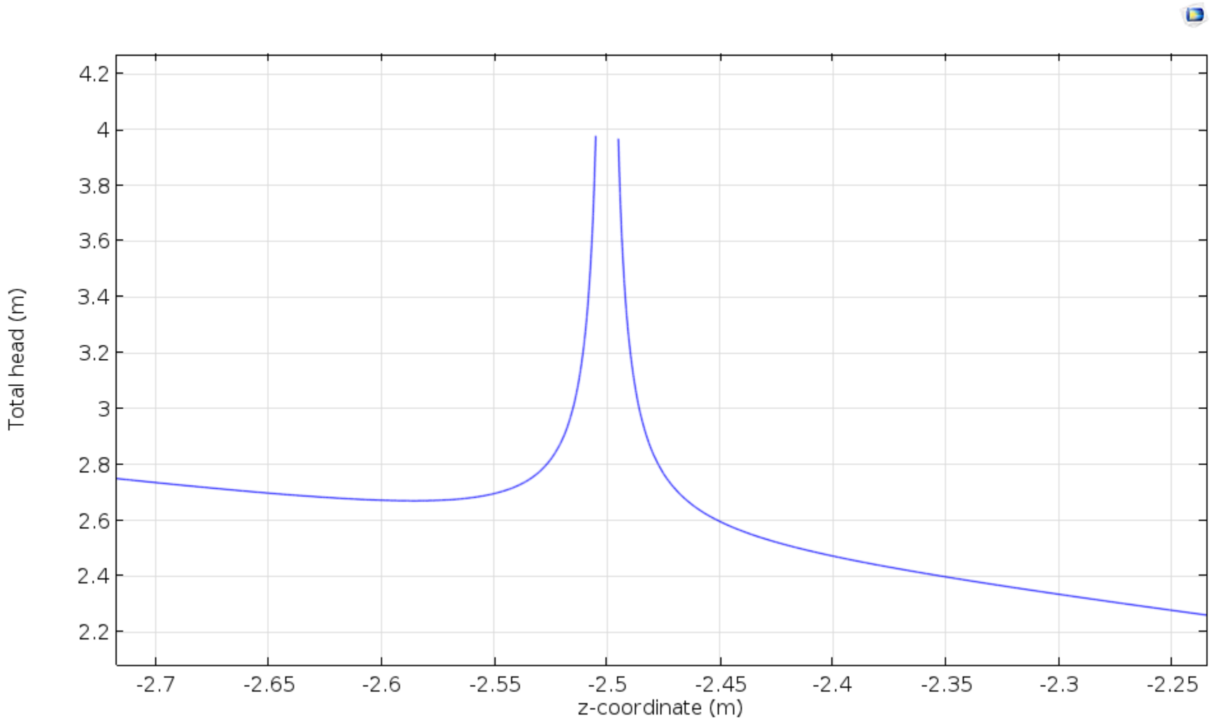

Figure 3.6: Pressure head as it results from injection from sphere at 2.5 metre depth, zoomed at injection zone

When applying Darcy's law for spherical flow to calculation results, the result becomes:

	Value	***Unit***
Radius PT1	0.020	m
Radius PT2	0.10	m
Total Head 1	2.8460	m
Total Head 2	2.4721	m
ΔH1	0.366	m
ΔH2	0.0721	m
k1 =	9.05E-05	m/s
k2 =	9.19E-05	m/s
k1,2 =	9.03E-05	m/s

Table 3.2: Results of application of Darcy's law on spherical point source

The virtual pressure transducers no. 1 and no. 2 are placed respectively at 2 and 10 centimetres above the injection point. The calculated head at pressure transducer 1 is 2.8460 metre and at pressure transducer 2 it is 2.4721 metre. This means that the pressure head increase due to injection at both locations is 0.366 metre and 0.0721 metre, respectively. Based on Darcy's law the following hydraulic conductivity is calculated based from the model results at the closest pressure transducer, no. 1:

$$k1 = \frac{Q}{4\pi\Delta hr} = \frac{8.333 * 10^{-6}}{4\pi * 0.366 * 0.020} = 9.05 * 10^{-5}\ m/s$$

The same can be done at virtual pressure transducer 2:

$$k2 = \frac{Q}{4\pi \Delta hr} = \frac{8.333 * 10^{-6}}{4\pi * 0.0721 * 0.10} = 9.19 * 10^{-5}\ m/s$$

Both results show that with increasing radius the hydraulic conductivity overestimation increases.

And based on 2 pressure transducers:

$$k1,2 = \frac{Q}{4\pi(\Delta h_1 - \Delta h_2)}(\frac{1}{r_1} - \frac{1}{r_2}) = \frac{8.33 * 10^{-6}}{4\pi * 0.29}(\frac{1}{0.02} - \frac{1}{0.1}) = 9.03 * 10^{-5}\ m/s$$

The result of calculation with 2 pressure transducers is the best approximation of both methods. When creating a cross-section line from the middle of the probe and taking the pressure head from that line and applying both forms (keeping 5 centimetre distance between the two measurement points) of the Darcy's law for spherical flow equation, the conclusion from the equation above is confirmed (Figure 3.8).

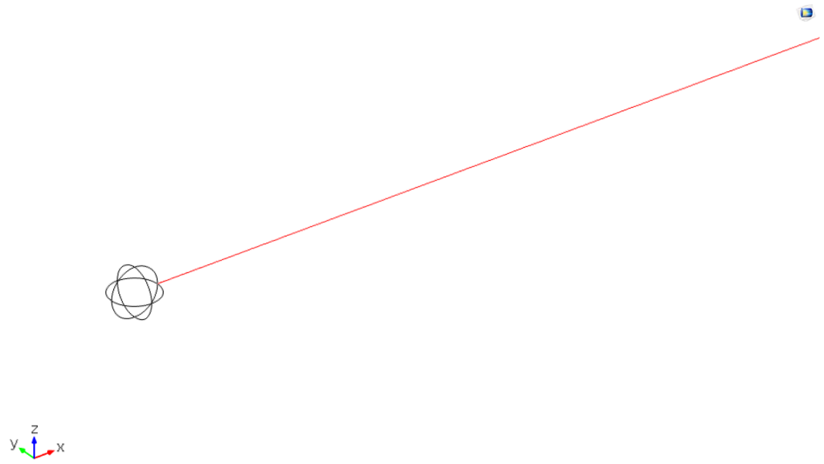

Figure 3.7: On the left the sphere is shown by circular contours. The red line is the so-called cutline, along which the pressure distribution is taken. This pressure distribution is used to determine the hydraulic conductivity shown in Figure 3.8. The 2 virtual pressure transducers as given in Figure 3.8 are separated 5 centimetres from each other and moved from the sphere, keeping a constant distance of 5 centimetres between them.

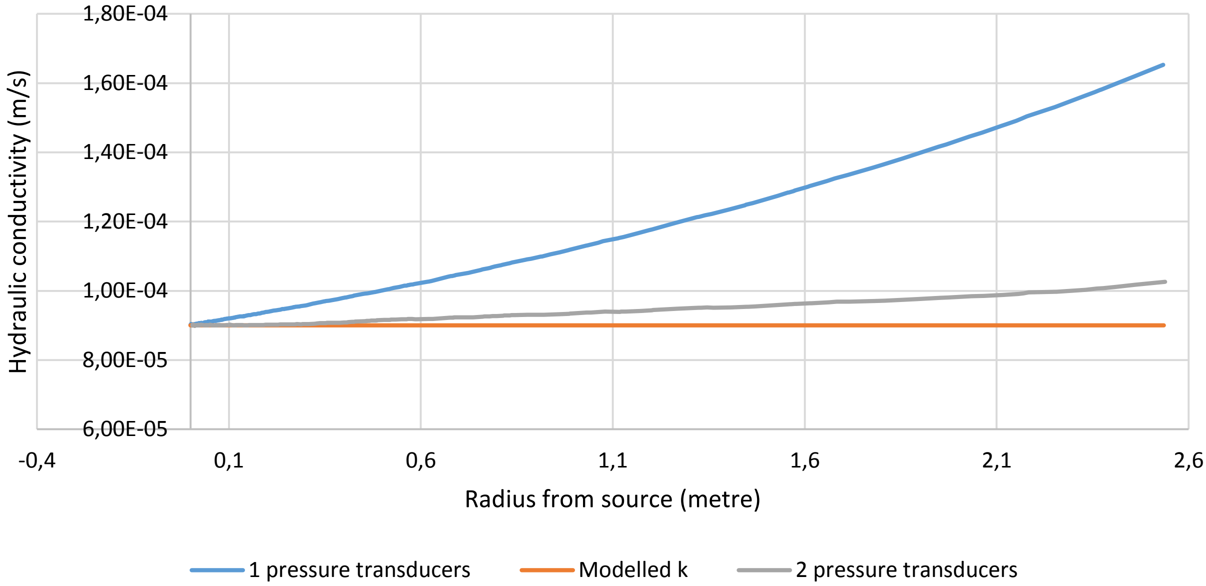

Figure 3.8: Comparison of analysis with 1 and 2 virtual pressure transducer

This overestimation is the result from the fact that equation (2.1) is that the pressure head decreases with a very high rate because the water dissipates fast with increasing radius. The pressure head will then reach values close to zero. Therefore the hydraulic conductivity estimation will increase, because the pressure head is decreasing faster than the increasing radius *r*. In the end, the equation becomes a fraction with in the denominator a value of almost zero, causing the hydraulic conductivity to increase.

To analyse what takes place around the probe, and the effect of gravity on the pressure distribution, the sphere is moved towards 10 metres depth and 3 cut lines are created, all starting from the sphere. These cut lines are shown in Figure 3.9.

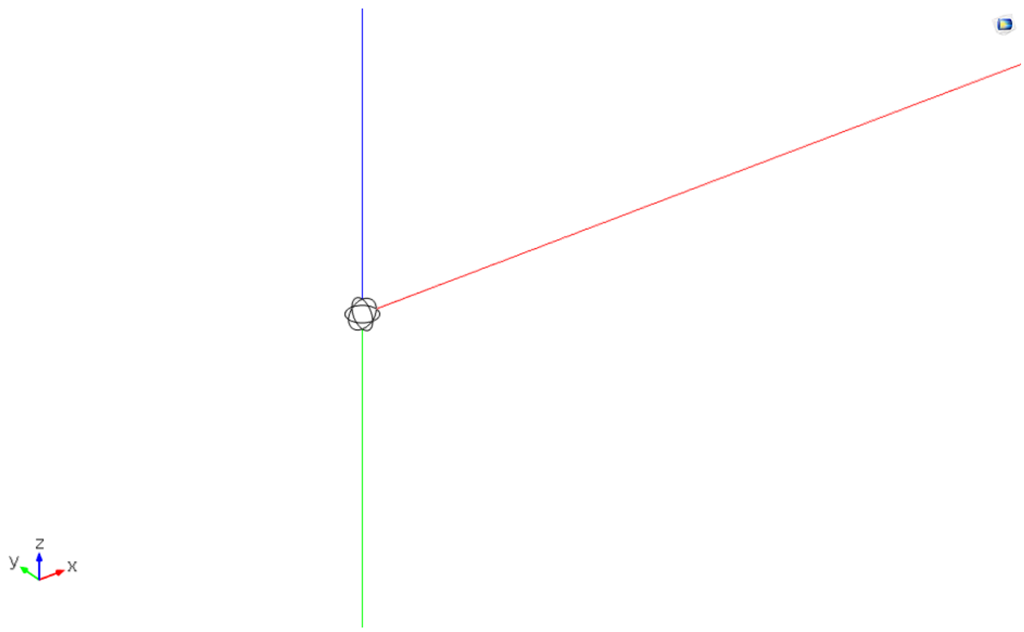

Figure 3.9: 3 Cut lines along which pressure is plotted. The sphere from which water is injected is shown by circular contours. Along the blue, green and red line is the pressure distribution plotted, given in Figure 3.10

Along these cut lines the pressure the total head is plotted, as shown in Figure 3.10.

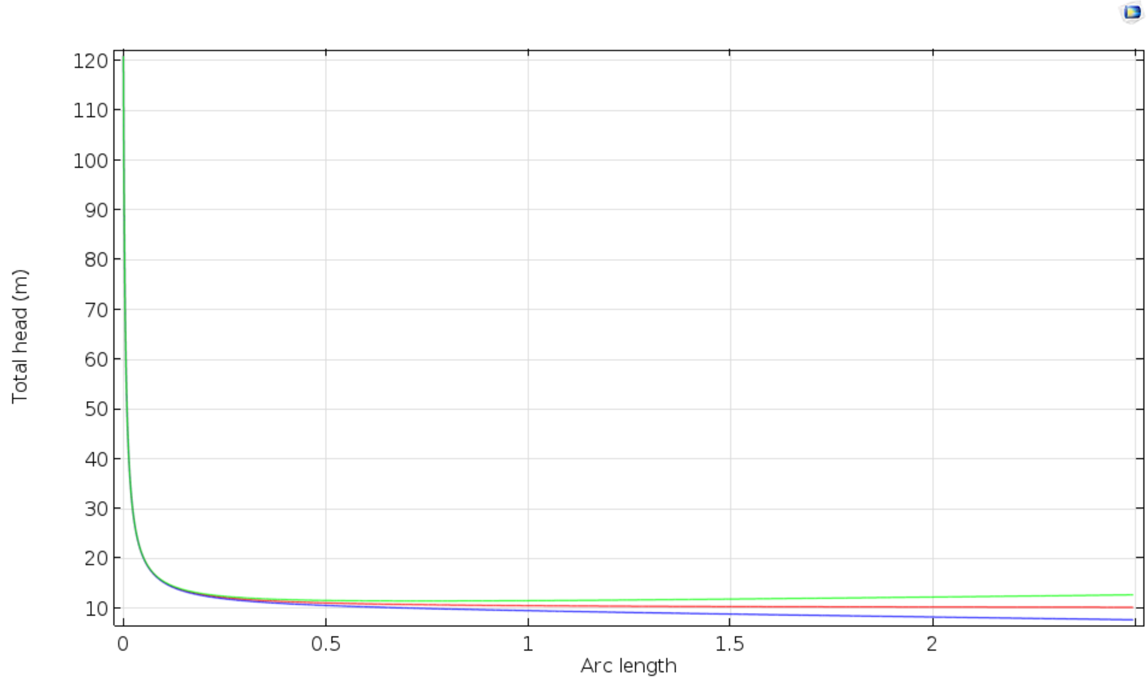

Figure 3.10: Total head along these cut lines, 10 metres depth

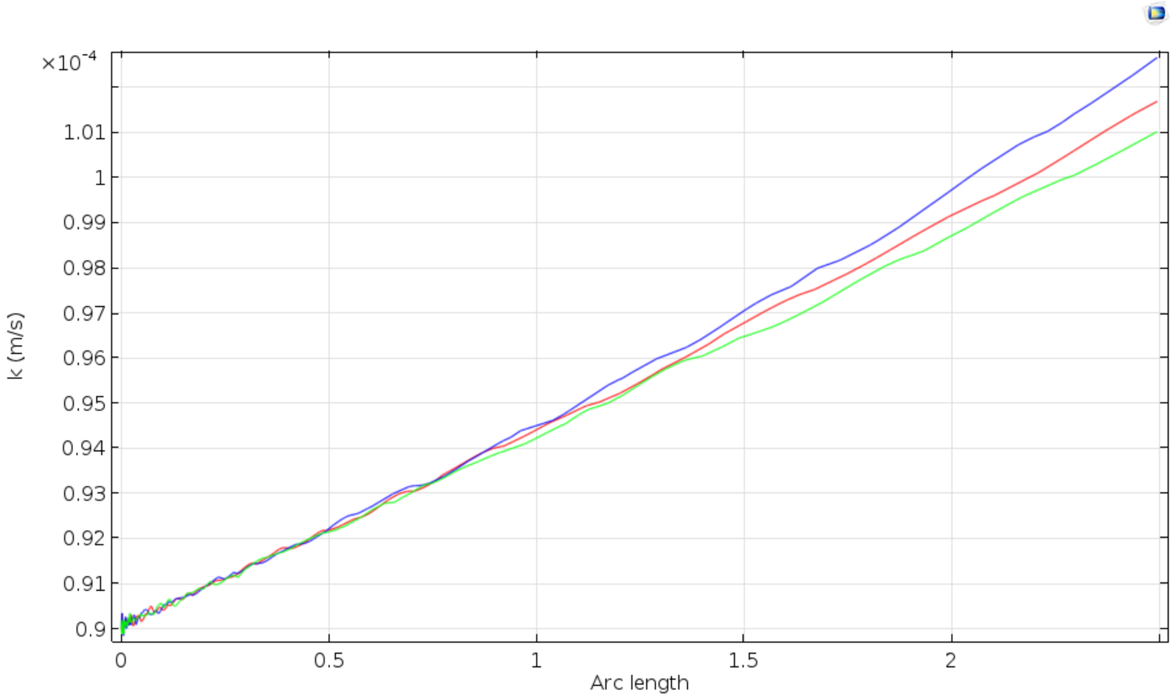

Figure 3.11: Hydraulic conductivity along the 3 cut lines, arc length in metre

This result shows that the within 0.5 metre range the results are comparable. What is interesting is the deviation in the signal in the beginning. This deviation increases with depth, meaning that it is rounding error in Comsol.

With the gravity turned off, this results in the pressure head shown in Figure 3.13. The resulting hydraulic conductivity is based on this pressure head and the result is exactly the same as with the gravity turned on. This proves that gravity doesn't have any effect on the result.

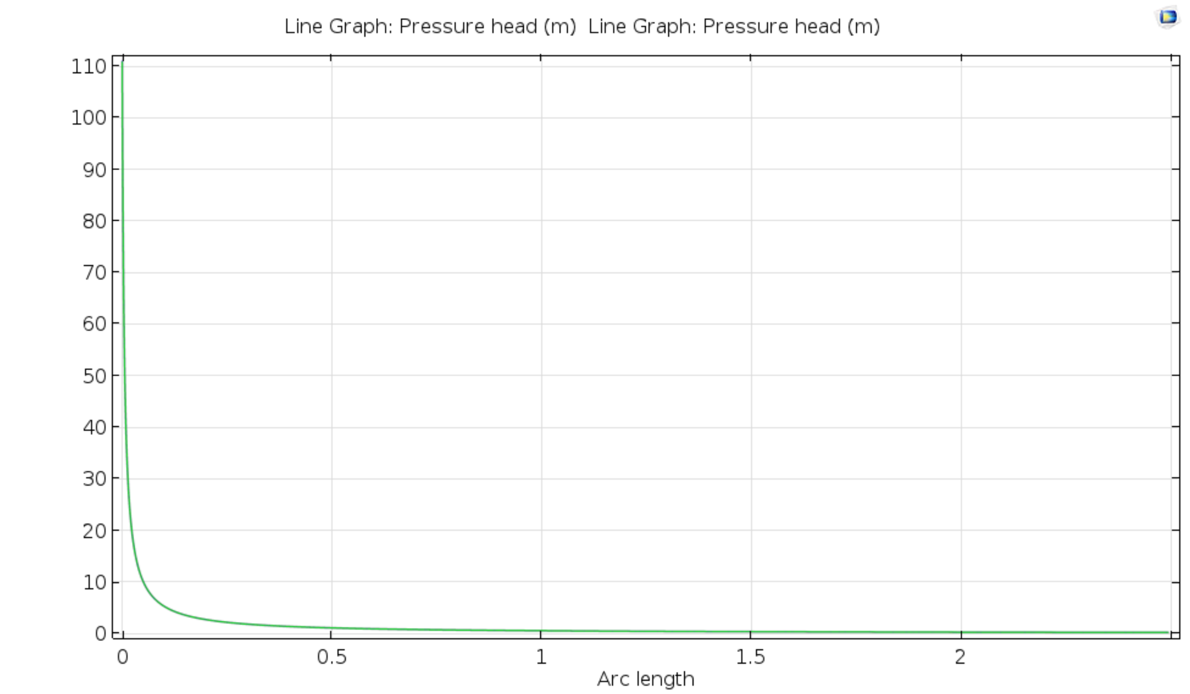

Figure 3.12: Pressure head along the 3 cut lines. Because the lines fall over each other only one line is visible, arc length in metre and on the y-axis total pressure head in metre

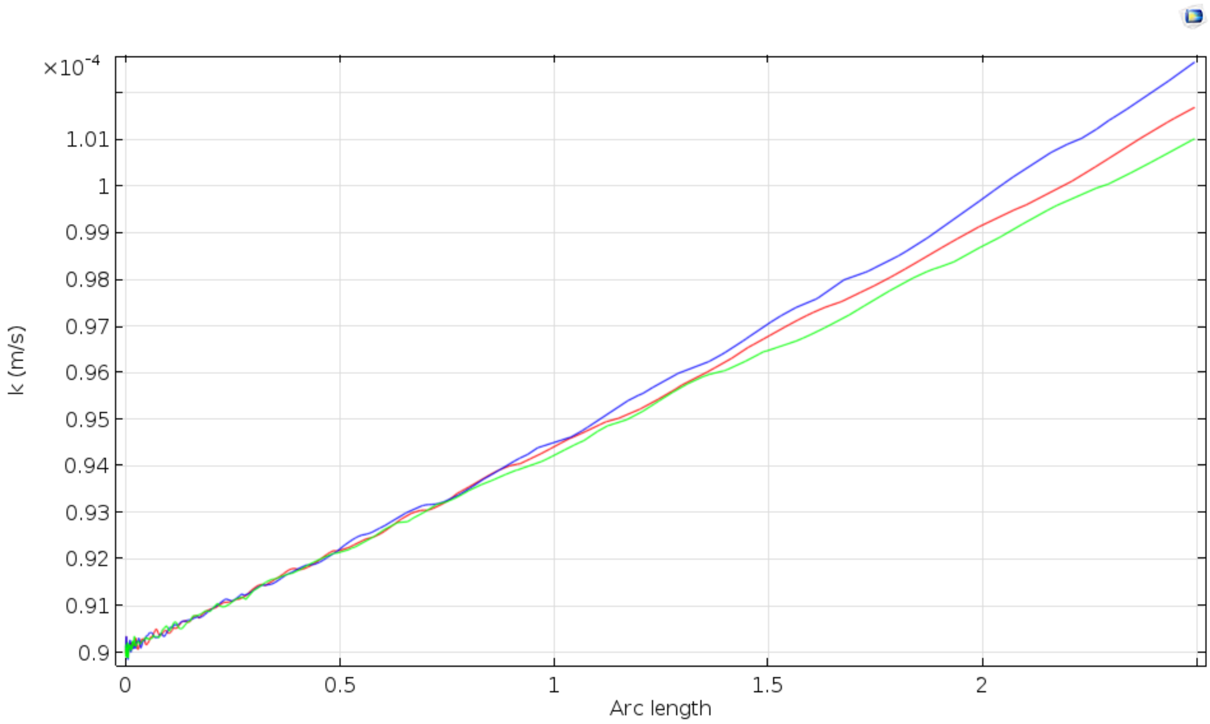

Figure 3.13: Hydraulic conductivity along the 3 cut lines, without any gravity effects, arc length in metre

3.2.6 Modelling probes

The probes mentioned in the introduction are added to the working model. All probes are modelled at a depth of 2.5 metre below the surface. A rod is modelled as a cylinder with a radius of 2 centimetres (4 centimetre diameter) and at the end a cone (2cm height) is modelled with a 45-degree angle. For the HPT and HRK probes an extra cylinder is added perpendicular at the side of the rod of the probe to create the injection screen. The cylinder (rod), the cone (tip) and the injection screen cylinder (injection point) are combined as a union and subtracted from the block by using the geometry difference option in COMSOL. This will result in the model shown in the Figure 3.14 - Figure 3.17.

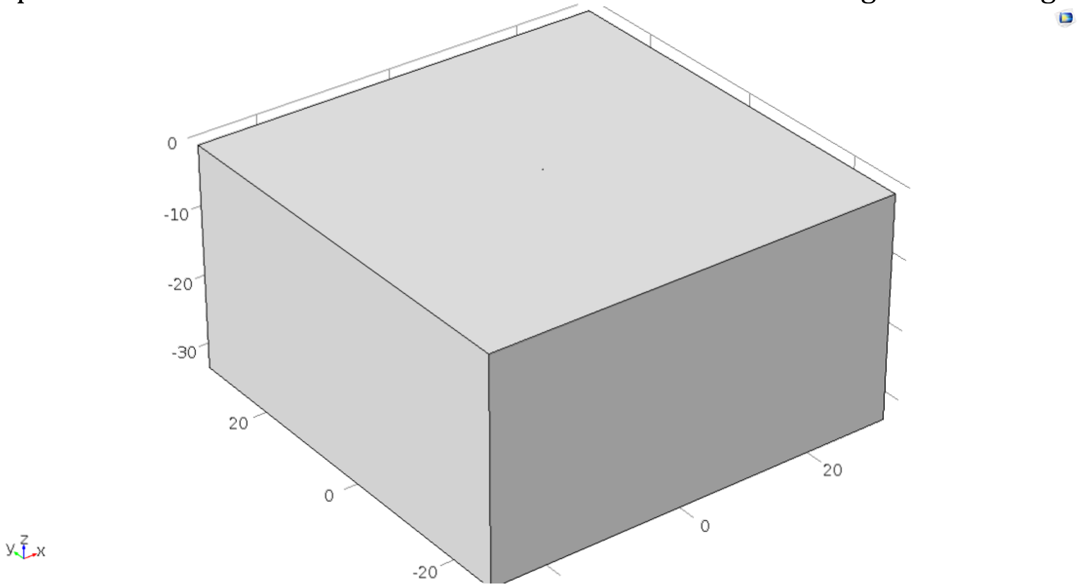

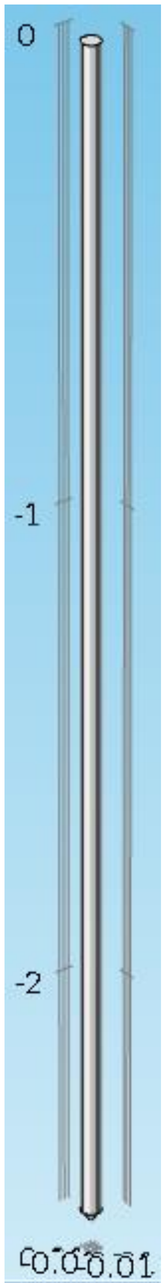

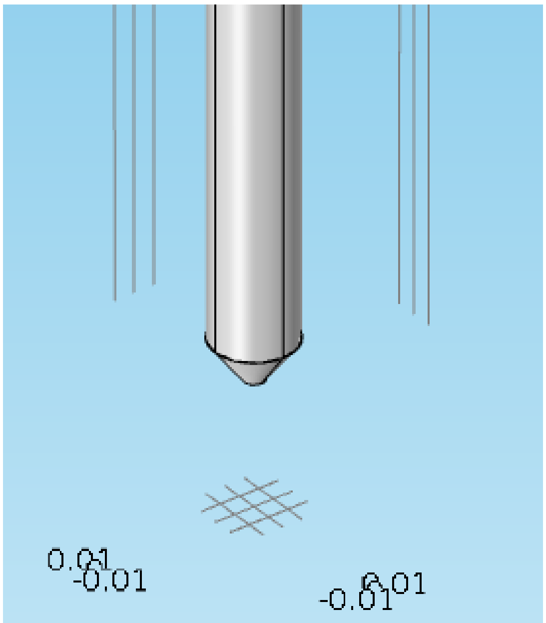

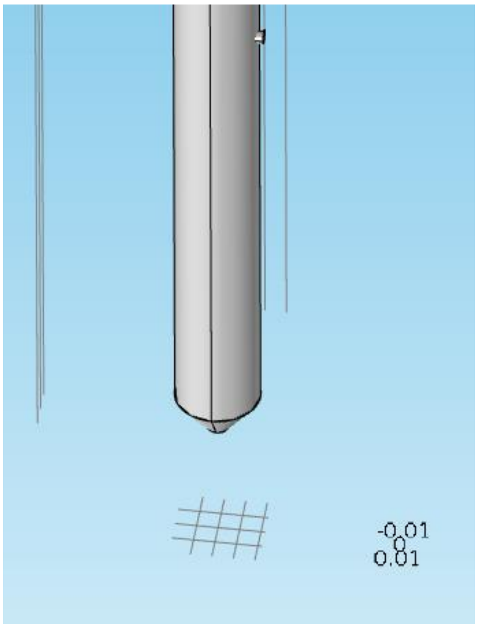

Figure 3.14: The whole model domain 60 m x 60 m x 32.50 m soil block

Figure 3.15: The probe as modelled, 2,5 m length and radius of 2cm

Figure 3.16: Detail of the probe cone (tip, at an angle of 45degrees) and rod

Figure 3.17: Detail of the HPT probe incl. injection screen (screen diameter of 7 mm, top of the

The pressure transducer of the HRK and HPT probe is placed in the injection trajectory. This differs from the other methods where the pressure transducers are placed at certain radius from the injection location. To know what takes place inside the injection trajectory, a small part of this trajectory is modelled. The inside is given an extremely high value for the hydraulic conductivity to resemble an open flow. The result is shown in Figure 3.18.

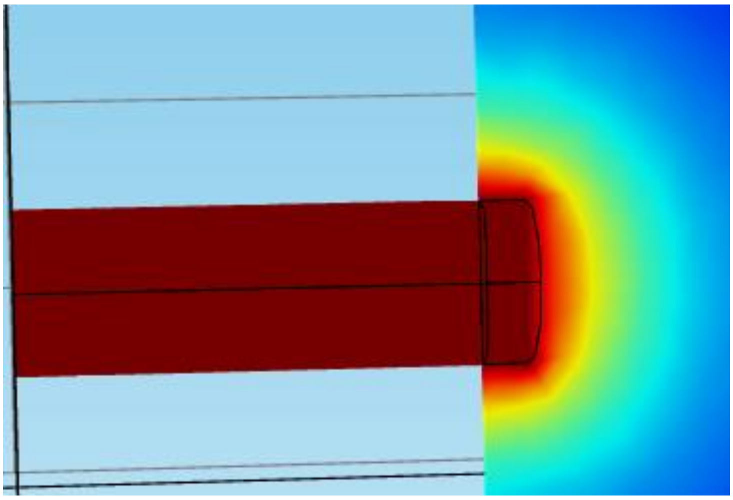

Figure 3.18: Injection trajectory. showing uniform pressure distribution inside the trajectory

This is important because it means that the pressure encountered in the middle of the injection screen is the same as the pressure inside the injection trajectory. Based on the given relation multiple injection rates and hydraulic conductivities were tested.

For the calculation of non-continuous probes, stationary settings are used. This means Comsol will calculate to a stationary situation. In practice this would mean that injection is started and continued until there is no change in the measured pressure head. This is necessary because Darcy's law for spherical flow is based on this stationary situation. For probes that measure with advancement of the probe, require a more difficult analysis because a moving probe has to be modelled. This case will not be analysed in this thesis. Two examples of final pore pressure distribution around the injection point are given in Figure 3.19 and Figure 3.20.

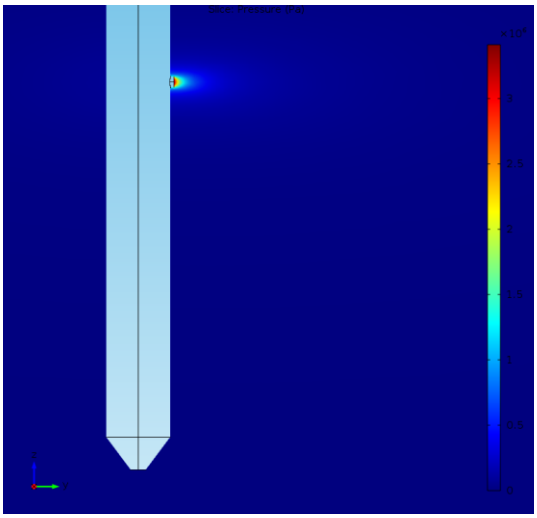

Figure 3.19: HPT injection into the soil, anisotropic conditions

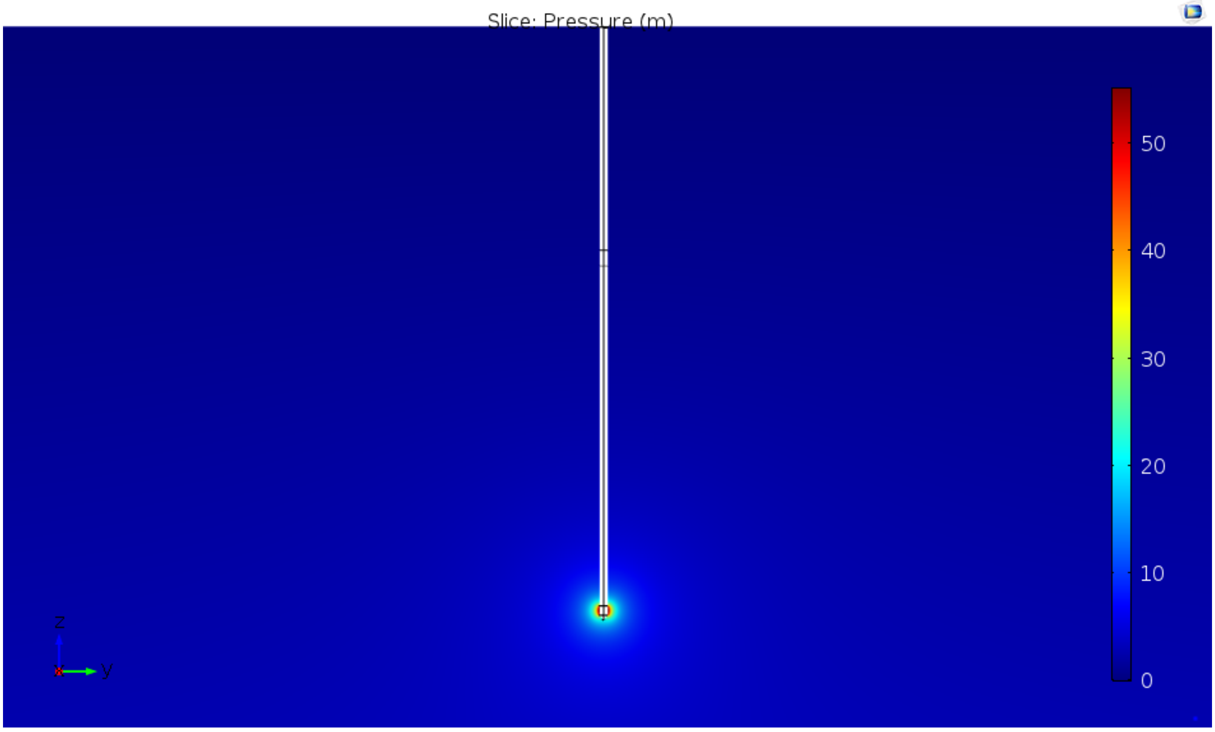

Figure 3.20: In-situ permeameter injection with uniform hydraulic conductivity

4 Validation of the direct push methods

4.1 Introduction

As described in chapter 2, there are several methods that have a been developed over time under different names and slightly different geometry/setup. Each system having their own relation to determine the hydraulic conductivity. The probes however are almost the same, the major difference being the location of the pressure transducers and the shape of the injection filter. These methods are:

- Dipoolsonde
- Monopoolsonde
- Direct push permeameter or DPP
- In-situ permeameter
- HPT
- HRK
- DPIL

Most of the mentioned methods can be simulated using one basic model with slight alterations, as already described in chapter 3. Unfortunately, the Monopoolsonde and DPIL (Dietrich et al., 2008) cannot be modelled. The relation proposed for the Monopoolsonde is based on the 2 pressure transducers at specific locations beneath the injection screen. Because no documentation can be found on the distance of these 2 locations from the injection screen, no model can be made. For the DPIL (Dietrich et al. ,2008) the relation only gives a relative hydraulic conductivity, meaning that no comparison can be made with the analytical approach.

4.2 Q/P-k relation verification

4.2.1 Dipoolsonde

The probe is adapted to create the dipoolsonde. 2 cylindrical screens are modelled exactly as illustrated in Figure 2.5. The radius of the probe 1.8 centimetre. The hydraulic conductivity for the Dipoolsonde is analysed with equation (2.31). The injection rate is applied to the upper filter. To the lower extraction filter the same flowrate is applied.

According to Rietsema (1983) the injection rate was around 1.75E-3 m^3/s for 2 injection filters.

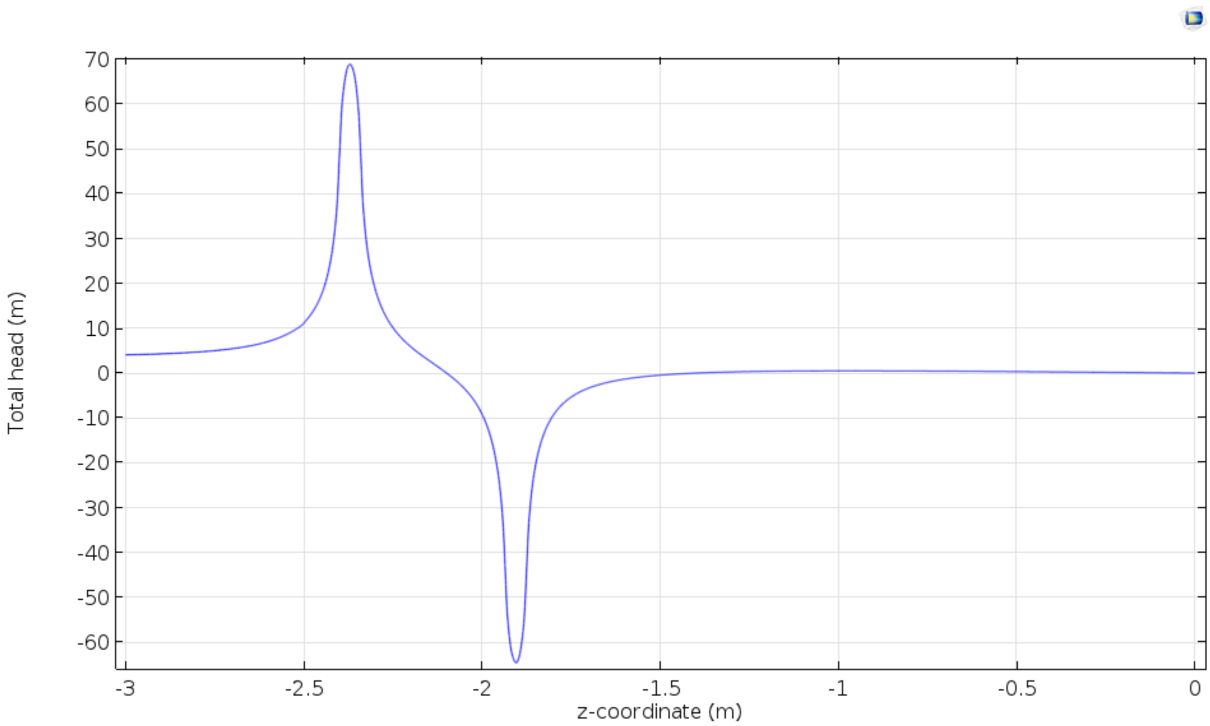

Figure 4.1: Total head distribution along the Dipool probe

	Value	*Unit*	*Value*	*Unit*
Injection flowrate(Q)	*500*	*ml/min*	*105000*	*ml/min*
Total head at PT C	*1.9498*	*m*	*23.3180*	*m*
Total head at PT D	*2.1009*	*m*	*4.8948*	*m*
Hydrost. head at PT C	*1.8475*	*m*	*1.8475*	*m*
Hydrost. head at PT D	*2.0875*	*m*	*2.0875*	*m*
Pressure head C	*0.1023*	*m*	*21.4705*	*m*
Pressure head D	*0.0134*	*m*	*2.8073*	*m*
Total Δhead	*0.0889*	*m*	*18.6632*	*m*
Length 1	*0.2325*	*m*	*0.2325*	*m*
Length 2	*0.1175*	*m*	*0.1175*	*m*
C	*1.07616259*	*[-]*	*1.076163*	*[-]*
Hydraulic cond. (k)	*8.71E-05*	*m/s*	*8.71E-05*	*m/s*

Table 4.1: Results from Dipoolsonde Comsol analysis

Note the difference in pressure head at pressure transducers *C* and *D* when comparing both injection rates. For a low injection rate of 500 ml/min the head is dominated by the hydrostatic head, concluding from *D>C*. When the injection rate increases to the in practice used value (105 l/min), the pressure head is dominated by the injection of water from screen A.

4.2.2 Direct Push Permeameter(DPP)

For the DPP probe an injection screen must be created with a height of 2.5 centimetre and situated at the end of the probe.

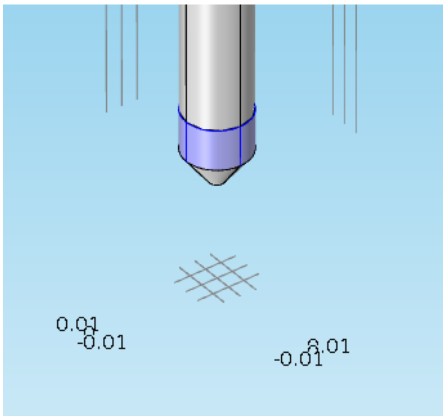

Figure 4.2: DPP injection filter with an adjusted filter length of 2.5 cm

The DPP has two pressure transducers located above the injection screen. The relation to determine the hydraulic conductivity with the DPP is:

$$k = \frac{Q}{4\pi\Delta h}\left(\frac{1}{r_1} - \frac{1}{r_2}\right) \quad (4.1)$$

r_1 = distance from DPP injection screen of pressure transducer 1(PT1) [0.15 m]
r_2 = distance from DPP injection screen of pressure transducer 2(PT2) [0.40 m]

r_1 and r_2 for the DPP are 0.15 meter and 0.4 meter.

The pressure transducer does not have to be integrated in the Comsol model. A *cut line* is used to create a line intersecting the model directly next to the probe. Two *cut point* can be created at the location of the two pressure transducers to resemble the pressure transducers. The resulting data from these two *cut points* can be plotted.

The results of the numerical calculation of this probe are the following:

	Value	***Unit***	***Value***	***Unit***	***Value***	***Unit***
Injection flowrate(Q)	500	ml/min	1000	ml/min	2000	ml/min
Total head PT1	2.3821	m	2.4266	m	2.5158	m
Total head PT2	2.104	m	2.1204	m	2.1534	m
Distance PT1	0.15	m	0.15	m	0.15	m
Distance PT2	0.40	m	0.40	m	0.40	m
Depth Inj. Point	2.4875	m	2.4875	m	2.4875	m
Hydrostatic head PT1	2.3375	m	2.3375	m	2.3375	m
Hydrostatic head PT2	2.0875	m	2.0875	m	2.0875	m
Pressure head at PT1	0.0446	m	0.0891	m	0.1783	m
Pressure head at PT2	0.0165	m	0.0329	m	0.0659	m
ΔHead	0.0281	m	0.0562	m	0.1124	m

Hydraulic cond. (k)	9.83E-05 m/s	9.83E-05 m/s	9.83E-05 m/s

Table 4.2: Results from DPP Comsol analysis

Based on paragraph 3.2.5, an overestimation is expected. The distance from injection screen to pressure transducers is large and the distance between the 2 pressure transducers is quite high. Next to that is the source not a perfect point source. The screen injects the water from a cylindrical screen, creating a donut-shape pressure distribution (Figure 4.3). Because the water is injected more in the horizontal than into the vertical direction, the measured pressure head at the pressure transducers will be lower than expected. Therefore, an overestimation of the hydraulic conductivity is the result.

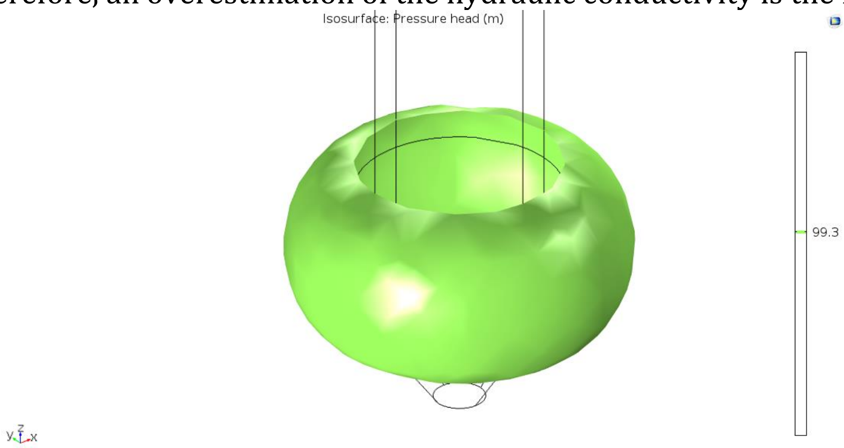

Figure 4.3: Donut shape injection pressure distribution

4.2.3 In-situ permeameter

The radius *r* in Darcy's law for spherical flow is replaced with a_s. From paragraph 2.4.6 is known that the equation for this probe then becomes:

$$k = \frac{Q}{4\pi \Delta h a_s} \qquad (4.2)$$

In which:
k = Hydraulic conductivity[m/s]
Q = Measured volumetric flowrate[m^3/s]
Δh = applied pressure head[m]
$a_s = \sqrt{\frac{1}{2}al}$ = effective radius of the spherical injection zone [m]
a = radius of the screen[m]
l = length of the screen[m]

The filter has the same radius as the rod of the probe, 2 centimetres and a height of 4 centimetres. In the article of Lee et al. 2008 no injection rates are defined/mentioned therefore an assumption is made for the standard injection rate. Based on the HPT probe an injection rate of 500, 1000 and 2000 millilitre/minute is assumed.

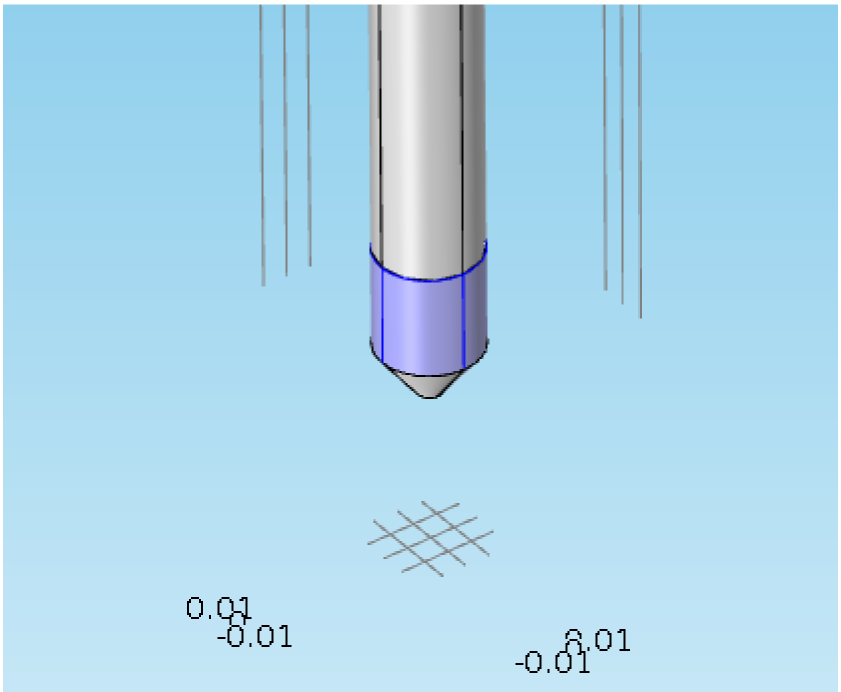

Figure 4.4: In-situ permeameter injection filter, with a filter length of 4 cm, as modelled in Comsol

The results from the model analysis are given in Table 4.3.

	Value	***Unit***	***Value***	***Unit***	***Value***	***Unit***
Injection Flowrate (Q)	500	*ml/min*	1000	*ml/min*	2000	*ml/min*
Total Head	2.8834	*m*	3.2867	*m*	4.0935	*m*
Hydrostatic head	2.48	*m*	2.48	*m*	2.48	*m*
Pressure head	0.4034	*m*	0.8067	*m*	1.6135	*m*
Radius probe	0.02	*m*	0.02	*m*	0.02	*m*
Length of screen	0.04	*m*	0.04	*m*	0.04	*m*
a_s	0.02	*m*	0.02	*m*	0.02	*m*
Hydraulic cond. (k)	8.22E-05	*m/s*	8.22E-05	*m/s*	8.22E-05	*m/s*

Table 4.3: Results from Comsol analysis on in-situ permeameter

Three different injection rates result in the same value of k = 8,22E-5 m/s. The soils hydraulic conductivity is set to a value of 9E-5 m/s, so there is a small deviation. This small deviation is not as expected. The proposed correction from r to a_s seemed to be good, but in the model this leads to an underestimation.

4.2.4 HRK probe

The HRK probe is a combination of the Direct Push Permeameter(DPP) and the HPT. The DPP is already analysed in paragraph 4.2.2, and the given hydraulic conductivity estimation is the same as given by Butler et al. (2007). This means that no further analysis is necessary for the lower injection filter.

The other 2 injection filters, PT1 and PT2, inject water during advancement into the soil. Data from PT1 and PT2 is retrieved in the form of *Q/P* (ml/min/m) and measured pressure (Total head). The hydraulic conductivity for this tool is determined by the following relation:

$$k = 10^b (DPIL)^a \qquad (4.3)$$

With a =2.5 and b=-9.0 (Liu et al, 2009) and *DPIL = injection flowrate / induced pressure head at PT2[ml/min/m]* and k in meter per day. The values of a and b were found by calibration using slug-test data and are based on continuous measurement during advancement.

The model that is used is exactly the same as with the HPT, which is shown Figure 3.17. The measured pressure is determined by creating a plot of the pressure directly pointing out of the injection point. Note that the pressure transducer is located behind the injection screen. In Figure 4.5 the exact line from which the data is taken is plotted. The injection location is placed at a depth of 2.26 metre. and the injection surface is placed 2 millimetres from the probe and has a diameter 7 millimetre, exactly the same diameter as in practice. The result along the red line is shown in Figure 4.6.

Figure 4.5: Red line indicates the arc along which the pressure is plotted

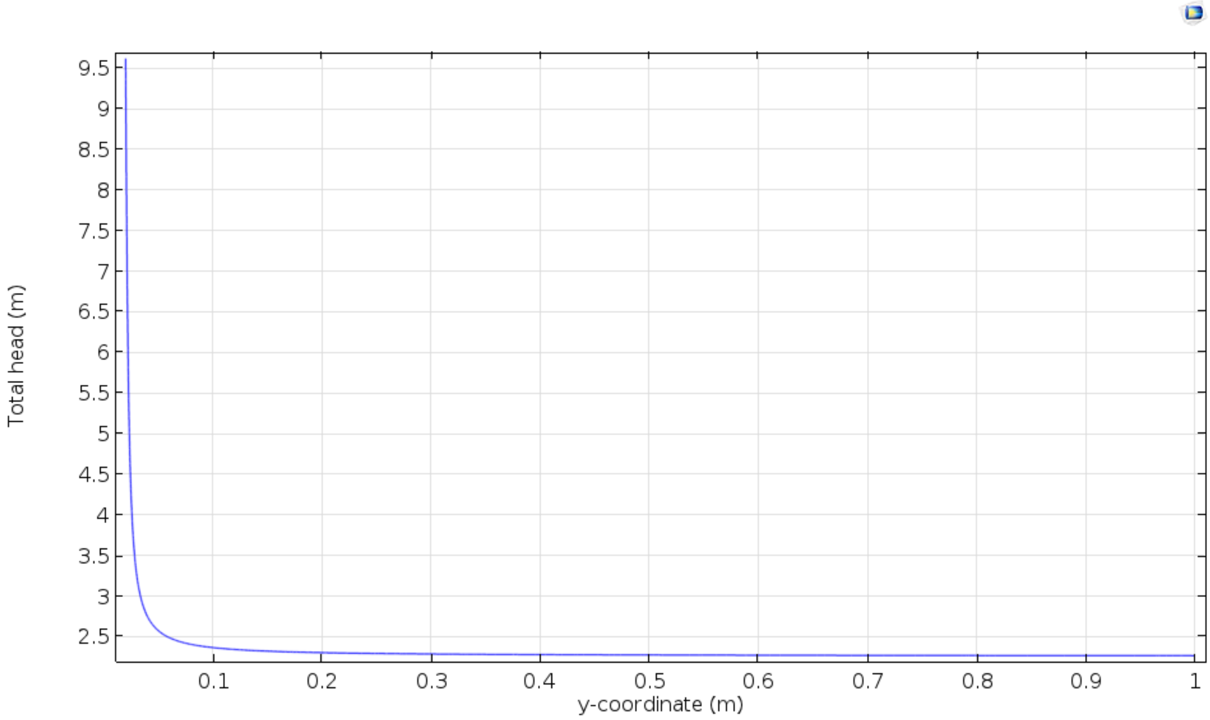

Figure 4.6: Result of plot along red line for injection of 500 ml/min and k = 9E-5 m/s

	Value	***Unit***	***Value***	***Unit***	***Value***	***Unit***
Injection flowrate (Q)	*500*	*ml/min*	*1000*	*ml/min*	*2000*	*ml/min*
Total head	*9.4*	*m*	*16.7*	*m*	*31.1*	*m*
Hydrostatic head	*2.26*	*m*	*2.26*	*m*	*2.26*	*m*
Pressure head	*7.2*	*m*	*14.4*	*m*	*28.9*	*m*
k (m/s)	*4.04E-05*	*m/s*	*4.01E-05*	*m/s*	*3.99E-05*	*m/s*
k (m/day)	*3.49*	*m/day*	*3.46*	*m/day*	*3.45*	*m/day*

Table 4.4: Results from HRK analysis is Comsol

The signal of measurement during advancement is made up out of 2 parts. The pressure head induced by the injection of water from the screen and the pressure head induced by the movement of the cone. The cavity expansion as a result of movement of the probe leads to displacement of soil and water and as a result the pore pressure around the tip of the probe will increase. The cone will move downward and the pressure transducer will then move through the area where the cavity expansion took place. As a result, the total head will increase. But because the probe is moving, a stationary pore pressure distribution will not be reached. The induced head by the injection from the screen will be lower compared to a stationary situation. The analysis done in this chapter is stationary, so higher total head caused by injection will be reached. But the exact effect on the total head by cavity expansion caused by the movement of the probe is unknown. Therefore, an exact conclusion on the result can't be made. What can be seen is that the hydraulic conductivity is underestimated. As a conclusion on that, the empirical relation given by Liu et al. (2009) to estimate the hydraulic conductivity is in this case dominated by the pressure head induced by the injected water and not by the movement of the probe.

4.2.5 Geoprobe HPT

The relation proposed by Geoprobe. in SI units is:

$$k = 0.3048 * (21.14 * \ln(\frac{Q}{p}6.894) - 41.71) \quad (4.4)$$

With:
k = Hydraulic conductivity(m/day)
Q = Injection flowrate(ml/min)
p = Injection pressure, defined as total pressure minus the hydrostatic and atmospheric pressure(kPa)

	Value	***Unit***	***Value***	***Unit***	***Value***	***Unit***
Injection flowrate (Q)	*500*	*ml/min*	*1000*	*ml/min*	*2000*	*ml/min*
Total head	*94.5*	*kPa*	*166.8*	*kPa*	*311.4*	*kPa*
Hydrostatic head	*22.6*	*kPa*	*22.6*	*kPa*	*22.6*	*kPa*
Pressure head	*71.9*	*kPa*	*144.2*	*kPa*	*288.8*	*kPa*
k (m/s)	*1.42E-04*	*m/s*	*1.41E-04*	*m/s*	*1.41E-04*	*m/s*
k (m/day)	*12.23*	*m/day*	*12.21*	*m/day*	*12.20*	*m/day*

Table 4.5: Results from HPT analysis in Comsol

Also this *Q/p-k* relation leads to an overestimation of the hydraulic conductivity. More analysis might be interesting, to see what takes place when the permeability is increased and decreased. Based on the assumption that the relation should result in an overestimation, one could also say something about the rate of overestimation. If the hydraulic conductivity is relatively high, the induced excess pore pressure around the probe is relatively low. This is because the pore water can dissipate faster and therefore a smaller pressure increase will take place. If this excess pore pressure increase is smaller, the result gets closer to stationary conditions and therefore to Darcy's law. Also analysing the HPT with Darcy's law at stationary conditions, would interesting.

4.3 Conclusion

There is a clear distinction between the direct push methods and stationary direct push methods to be used for hydraulic conductivity estimation. Methods that analyse during movement of the probe are empirically based and show some small to large overestimation of the hydraulic conductivity, while Darcy's law based relations show results close to Darcy's law solution. This is visualised in Figure 4.7. This overestimation is something that is expected. Both methods relate the pressure increase around the cone to the hydraulic conductivity. The methods that analyse during movement of the probe must also incorporate the excess pore pressures that are induced by the probe movement. The proposed relations don't describe this pressure increase analytically, but create an empirical relation. Because the excess pore pressure that is induced by the probe are taken into account in the empirical relations, and the Comsol analysis in the part is stationary, the pore pressures are smaller in the Comsol analysis than these would be with on-the-fly results. Smaller values mean that the hydraulic conductivity is higher. Concluding from that, the hydraulic value of these methods should overestimate the value of the real value. This is in fact the case. In Table 4.6 the generated pressure head of the probes is given. What can be noticed is that the pressure head varies enormously. This is important to know, because it affects the effects taking place in the injection zone, mentioned in chapter 6.

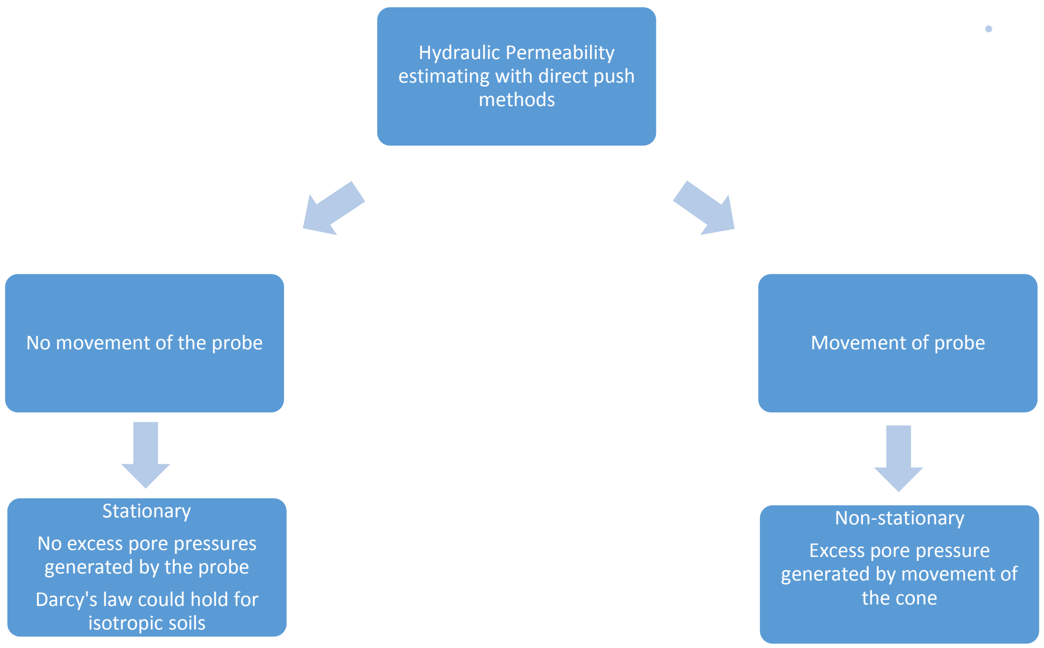

Figure 4.7: Schematic scheme of direct push methods

	Generated pressure head
Dipoolsonde	21.34 m
Direct push permeameter or DPP	0.0446 m
In-situ permeameter	0.4034 m
HPT /HRK	7.2 m

Table 4.6: Generated pressure head by the injection of water from the probe

5 Applying Darcy's law to HPT/HRK

5.1 Introduction

The hydraulic profiling tool, or HPT, and the HRK probe currently follow an empirical relation to translate the measured relative hydraulic conductivity (Q/P) to an absolute hydraulic conductivity (k) for results obtained from a moving probe. This empirical relation was determined by tests performed in a test field with the HPT and compared to slug tests performed at the same location and depth.

The HPT tool measures the flowrate (Q) in millilitre per minute and the downhole pressure in psi or kPa, continuous when advancing into the soil. The Fugro HPT measures the pressure also at a pressure transducer 40 centimetre below the injection screen. The ratio of the flow rate and downhole pressure result in a relative hydraulic conductivity given in millilitre/minute/kPa or millilitre/minute/psi. With the use of the slug testing in boreholes/piezometers, absolute hydraulic conductivity values were determined. By plotting the HPT *Q/P* data against the slug tests data, a trend line was fitted as shown in Figure 5.1. This trend line was defined as an empirical relation that is now proposed by the manufacturer of the tool as an accurate relation to determine the hydraulic conductivity with the HPT.

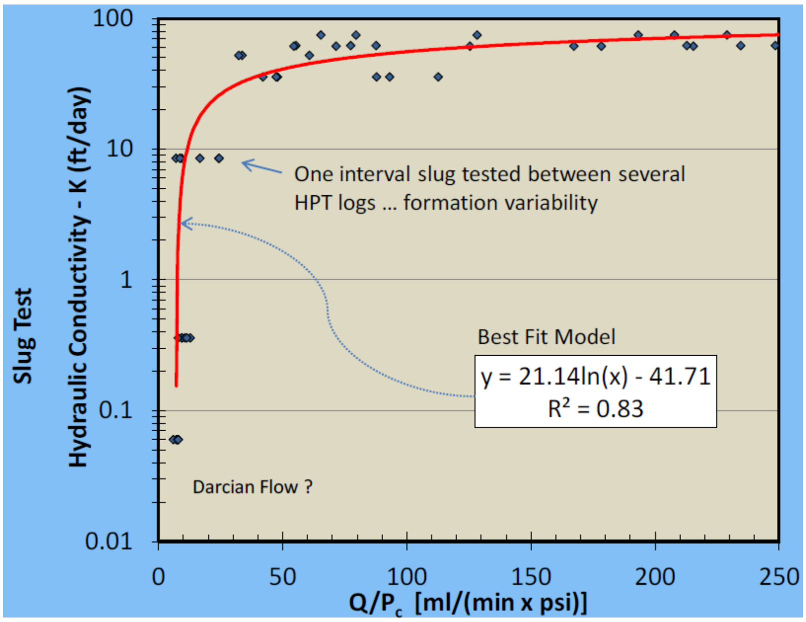

Figure 5.1: Slug test and HPT data taken at the same depth plotted as one data point, in red the trend line (McCall, 2013)

The resulting trend line as shown in Figure 5.1 looks like it is accurate, but experience in practice have shown some deviation from results that were acquired with slug tests. The logarithmic factor in the equation is the factor that creates large deviation in the final result. That's why the question arises: *can the hydraulic conductivity be determined by the HPT with the use of the spherical representation of Darcy's law under stationary conditions?*

The fact is that Darcy's law is based on spherical flow from a point source that emits water in a spherical direction. The HPT injects water sideways and therefore the injection shape is different from spherical flow. How different this shape is, will be shown in this chapter. What is also different for the Geoprobe HPT is that use of Darcy's law with other tools is based on the pressure drop over a certain radius. The radius is in practice the distance between the water injection point and the pressure transducer above or below the point source or between two pressure transducers. But the Geoprobe HPT does not have a pressure transducer above or below the injection point, it is at the same location as the point source.

In this chapter the previous made model for the HPT is used to see how the pressure develops around the probe and an analysis is made with the use of Darcy's law for spherical flow with the Geoprobe HPT. Note that same model is used, meaning that this analysis is in stationary conditions. Further analysis in non-stationary is recommended.

5.2 Pressure development around HPT probe

The pressure development around the HPT probe is an important factor, because if the pressure development shape can be determined, the surface area can be described. This surface area can then, with the use of Darcy's law, give an estimation of the hydraulic conductivity using HPT data.

The model used is exactly the same as used in chapter 4. An isotropic soil is assumed with a hydraulic conductivity of 9e-5 m/s and an injection rate of 0.217 m/s or 500 ml/min. A contour plot is created in the pressure distribution of the model of the HPT, used in paragraph 4.2.5. This contour plot is made along the *xy*-plane, at the same depth as the HPT injection point. The *xy*-plane is chosen because the hydrostatic head does not change, because the depth is constant. The results are shown in Figure 5.2 and Figure 5.3.

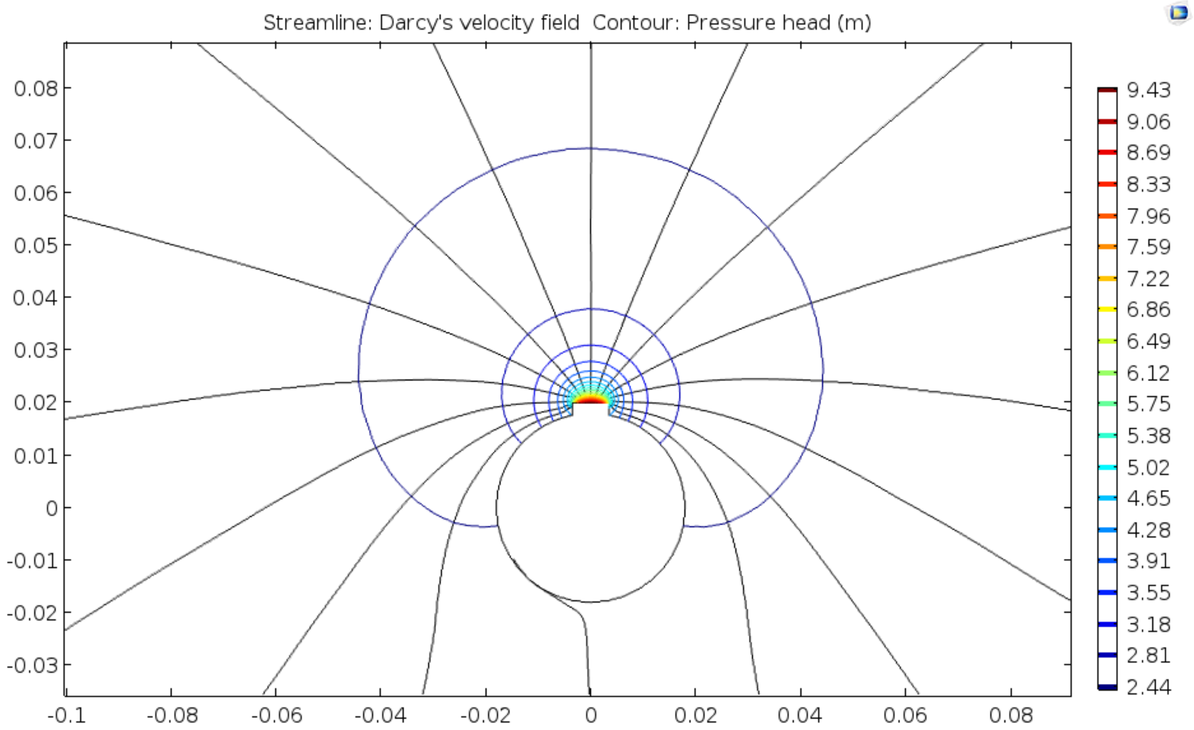

Figure 5.2: Pressure head distribution (in m H2O) of the HPT probe, water injection in the y-direction (zoomed in). Units in metre. Black lines indicate the flowlines

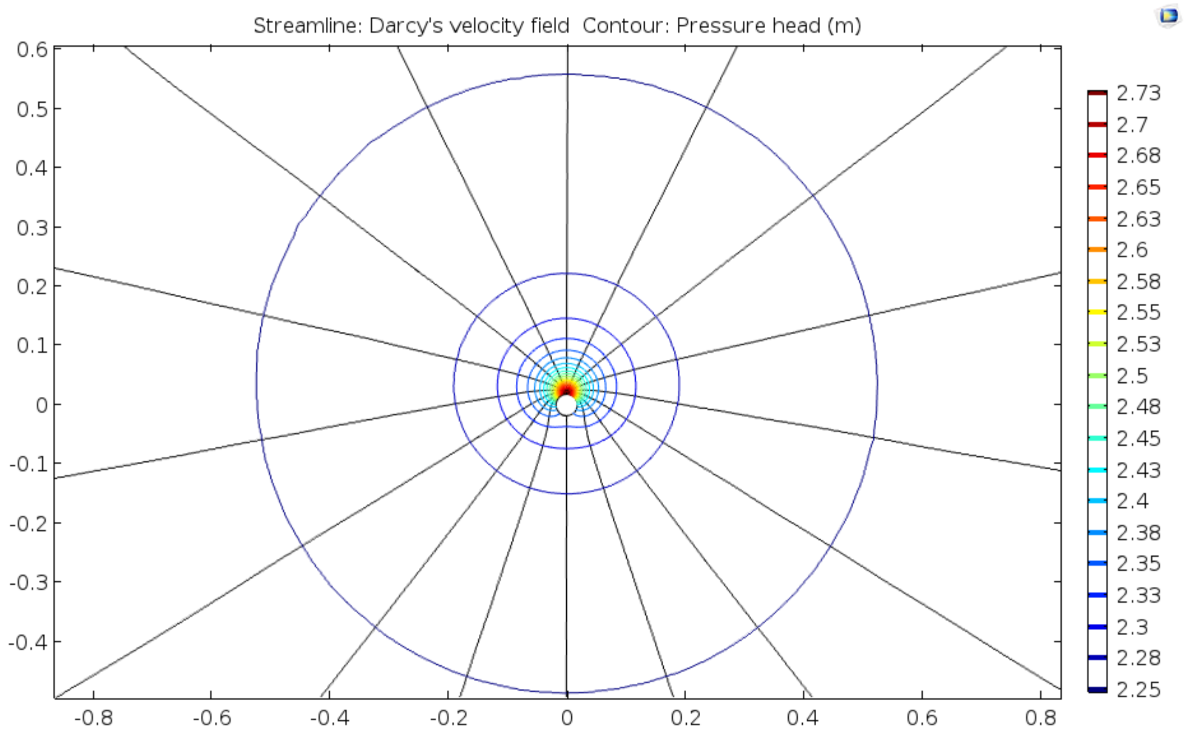

Figure 5.3: Pressure head distribution of the HPT probe, water injection in the y-direction. Units in metre. Black lines indicate the flowlines

Figure 5.2 and Figure 5.3 both show the same result, Figure 5.2 is zoomed in on the higher pressures around the probe. The shape goes from a half circle to a cardioid type shape (Figure 5.4). In Figure 5.3 can be seen that the shape becomes more spherical with increasing radius.

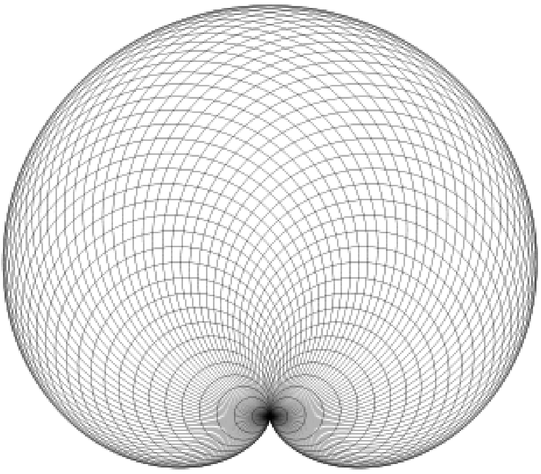

Figure 5.4: Cardioid shape

Comsol has also the possibility to create isosurfaces. Isosurfaces are 3D surfaces that have exactly the same value of the variable, in this case pressure. This function is used to create pressure surfaces in 3D. These surfaces are shown in Figure 5.5-Figure 5.8.

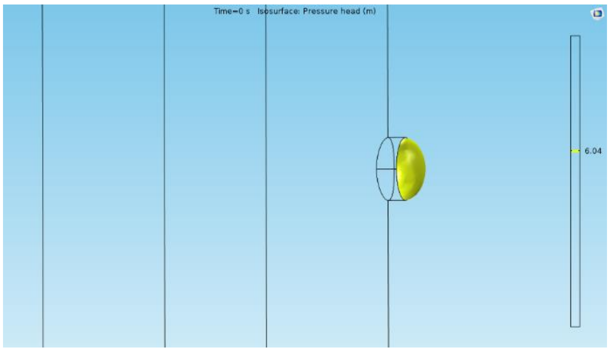

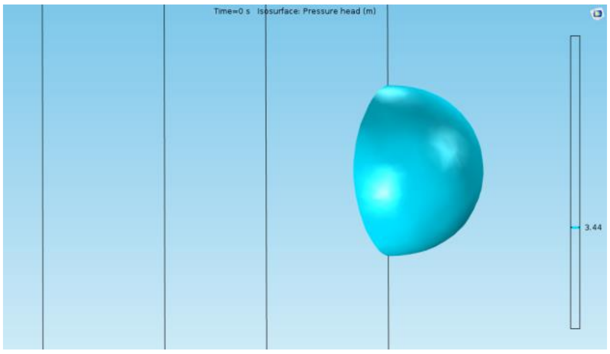

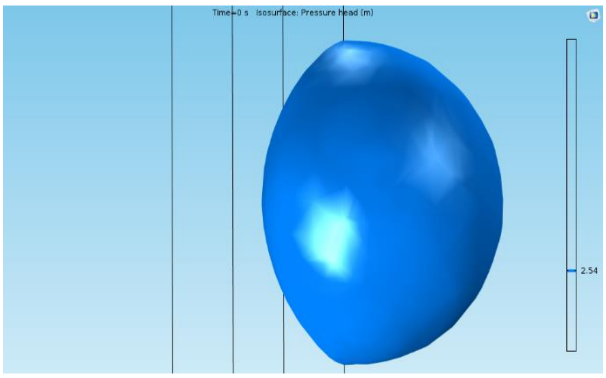

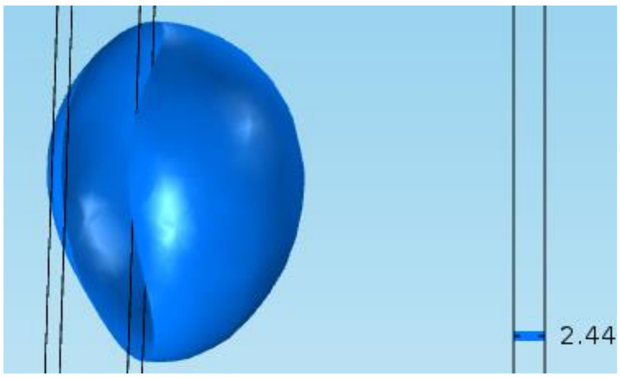

Figure 5.5: Isosurface of total head = 6.04 metre for injection from HPT

Figure 5.6: Isosurface of total head = 3.44 metre for injection from HPT

Figure 5.7: Isosurface of total head = 2.54 metre for injection from HPT

Figure 5.8: Isosurface of total head = 2.44 metre for injection from HPT

Based on the results as shown in Figure 5.8 can be concluded that the pressure distribution is clearly not spherical close to the injection point but becomes more spherical when the radius stating from the screen increases.

5.3 Applying Darcy's law

From the previous paragraph was concluded that the flow is not spherical. Though an attempt is made to apply Darcy's law to the results from the HPT analysis in Comsol. The pressure head is taken at the middle of the filter, just as in paragraph 2.4.9. The result is given in Table 5.1.

	Value	***Unit***
Injection rate(Q)	500	ml/min
Injection rate(Q)	3.34E-05	m3/s
Injection screen radius	0.0035	m
Total head at screen	9.8015	m
Depth	2.26	m
pressure head	7.5415	m
Hydraulic conductivity (k)	1.007E-04	m/s
real k	9.00E-05	m/s

Table 5.1: Calculating k by using Darcy's law for spherical on HPT data from Comsol model

As expected the resulting analytically calculated conductivity doesn't correspond to the absolute hydraulic conductivity value. Even though the value does not deviate much from the real value a possible correction is analysed.

5.4 Correction factor

The radius of the injection screen is set at 3.5 millimetres. This is debatable whether or not we can use this as the distance between the injection point and pressure transducer. The pressure transducer is not at 3.5 millimetres from the injection point and therefore the chosen diameter of 3.5 millimetres might have to be changed. The shape of injection flow is not spherical (Figure 5.5-Figure 5.8), but the calculation with Darcy's law for spherical flow in paragraph 5.3 showed that the deviation from the modelled hydraulic conductivity is not that large. Figure 5.3 also shows that the pressure distribution at greater radius from the injection point is more spherical.

That is why a correction factor is proposed. This correction factor can be added to the equation for spherical flow to correct for the non-spherical shape and correct for the distance between injection point and pressure transducer. *Pi* (π) and radius r can be included in the correction factor, but in this report they will be kept out of the correction factor to avert any unclearness of this factor. The equation with C included becomes:

$$k = \frac{Q}{4\pi C \Delta h r} \tag{5.1}$$

In which C is the dimensionless correction factor for a non-spherical form of the pressure field. This factor is determined by analysis in Comsol with the HPT model. The test done in the paragraph 5.3 gives the modelled value and the calculated value. By dividing the calculated k with the modelled k value this factor is acquired. The first estimation of C is then:

$$\frac{calculated\ K}{modelled\ k} = C = \frac{1.007 * 10^{-4}}{9.00 * 10^{-5}} = 1.119$$

To test whether or not this correction factor is appropriate to use, an analysis with higher injection rates and lower hydraulic conductivity is done. The results of the analysis with lower permeability is shown in Table 5.2. The permeability is reduced with a factor 100 to 9E-7 m/s.

	Value	***Unit***
Injection rate(Q)	500	ml/min
Injection rate(Q)	3.34E-05	m3/s
Injection screen radius	0.0035	m
Total head	756.41	m
depth	2.26	m
pressure head	754.15	m
Hydraulic conductivity (K)	1.007E-06	m/s
real k	9.00E-07	m/s

Table 5.2: Comsol analysis of HPT with k reduced 9E-7 m/s

If the correction factor C is applied to the result from Table 5.2, this results in:

$$\frac{Calculated\ K}{C} = \frac{1.007*10^{-6}}{C} = 9.00 * 10^{-7} m/s$$

Which is exactly the same value as the absolute hydraulic conductivity modelled in Comsol.

In Table 5.2 the results are shown of an analysis in Comsol with doubled injection rate, so 1000 ml/min and the hydraulic conductivity is 9E-5 m/s.

	Value	***Unit***
Injection rate(Q)	1000	ml/min
Injection rate(Q)	6.68E-05	m3/s
Injection screen radius	0.0035	m
Total head	17.343	m
depth	2.26	m
Pressure head	15.0830	m
Hydraulic conductivity (k)	1.007E-04	m/s
real k	9.00E-05	m/s

Table 5.3: HPT analysis in Comsol with doubled injection rate to 1000 ml/min

The results from the analysis with doubled injection rate show that *C* is also correct for changing injection flow rates, as the results are exactly the same as the one with 500 ml/min as injection rate.

C can be described as a geometrical correction factor and therefore it should change if the geometry is changed. The diameter of the probe is modelled as 4 centimetres, while in practice this can also be 3.6 centimetre or another value close to it. This is tested in a new model. The geometry is changed by decreasing the diameter of the probe to allow a new determination of the correction factor *C.* The radius of the probe is set to 1.8 centimetre (3.6 centimetre diameter is the diameter of HPT probe), and the other variables are not changed, unless these are mentioned in Table 5.4.

	Value	***Unit***	***Value***	***Unit***	***Value***	***Unit***
Injection rate(Q)	500	ml/min	500	ml/min	1000	ml/min
Injection rate(Q)	3.34E-05	m3/s	3.34E-05	m3/s	6.68E-05	m3/s
Injection screen radius	0.0035	m	0.0035	m	0.0035	m
Total head	9.6189	m	738.15	m	16.978	m
depth	2.26	m	2.26	m	2.26	m
pressure head	7.3589	m	735.89	m	14.7180	m
Hydraulic cond. (k)	1.032E-04	m/s	1.032E-06	m/s	1.032E-04	m/s
real k	9.00E-05	m/s	9.00E-07	m/s	9.00E-05	m/s
Factor C	1.1468		1.1468		1.1467	

Table 5.4: Factor C determination for probe with 1.8 centimetre

The factor C for a HPT probe with a diameter of 4.0 centimetre results in a value of *C* of 1.119. For a diameter of 3.6 centimetre the value of *C* is 1.147. Conclusion: With increasing probe diameter the correction factor decreases.

5.5 HPT Anisotropy

Chapter 6.2 proves that the hydraulic conductivity can be determined when the soil in anisotropic. Paragraph 5.4 proves that the HPT probe can be used to determine the hydraulic conductivity by using Darcy's Law for spherical flow with a correction factor. Based on both the question rises if the hydraulic conductivity derived from HPT results can be used in an anisotropic case ($k_h \neq k_v$).

To analyse if anisotropy changes the approach from paragraph 5.4 and if the correction factor *C* does not change, an analysis is done in Comsol. The Comsol model from paragraph 2.4.9 is used. Anisotropy is created in the soil with a $k_v/k_h = 1/10$, or $k_h = 9E\text{-}5\ m/s$ and $k_v = 9E\text{-}6\ m/s$. The diameter of the probe is 3.6 centimetre, because this is the real diameter of the HPT probe. All the other properties are not changed or are mentioned in Table 5.5: Anisotropy analysis with HPT.

	Value	Unit
Injection rate(Q) ml/min	500	ml/min
Injection rate(Q)m3/s	3.34E-05	m3/s
Pi	3.1416	[-]
Injection screen radius	0.0035	m
Total head	9.6189	m
depth	2.26	m
pressure head	7.3589	m
Hydraulic conductivity	1.032E-04	m/s
real k	9.00E-05	m/s

Table 5.5: Anisotropy analysis with HPT

$$\frac{calculated\ K}{real\ k} = C = \frac{1.032 * 10^{-4}}{9.00 * 10^{-5}} = 1.147$$

5.6 Conclusion

The Hydraulic profiling tool injects water in only one direction. This causes that the basic Darcy's law for spherical flow is not applicable for the HPT probe Q/P-k conversion, because the pressure distribution development is different from a point source that emits spherically. But the differences in the calculated k-values and the set k-value value. That is why a correction factor is proposed and tested. This factor is based on the real value of the hydraulic conductivity as given to the soil in Comsol and the results that is based on the analysis in Comsol. The factor C has proven during multiple analysis with changing injection rates and hydraulic conductivity to be correct for a certain geometry of the HPT probe. If the geometry changes, the factor C also changes. The factor C is also not influenced by anisotropy.

The resulting factor C will be a little different in practice. Though testing this factor on data from the field is something that could be done and give some insight on how accurate this factor really is.

6 Injection zone

6.1 Introduction

The determination of hydraulic conductivity with the Comsol model has assumptions for the conditions. The soil in not disturbed, water enters the soil perfectly, no turbulence, the soil is isotropic. But in practice this is not the case. That is why in this chapter important factors will be elaborated that can play a role in the final hydraulic conductivity estimation. The following processes/effects are analysed:

- Anisotropy
- Disturbed zone around the cone
- Depth effect
- Short-circuiting
- Liquefaction
- Clogging

6.2 Anisotropy

The models that will be used are the same as described in the chapter 3. The models can be adapted to the specific needs for the analysis that will be done. The theory that is used is given in paragraph 2.5.1. The result shows that theoretically k_h could be determined by:

$$\Delta h = \frac{Q}{4\pi K_h d} \quad \rightarrow \quad K_h = \frac{Q}{4\pi \Delta h d} \tag{6.1}$$

The given methods are analysed and verified by simulation of the model. The results of the analysis are presented in the next paragraph.

6.2.1 Modelling anisotropy

The effects of anisotropy are analysed with the model in which the injection source is modelled as a sphere. For the first run an anisotropy ratio of $k_v : k_h = 1{:}10$ is assumed. A horizontal hydraulic conductivity of *9e-5 m/s* is assumed resulting in a vertical hydraulic conductivity of *9e-6 m/s*.

The injection rate is set to a value of 1.5 m/s, to generate high values of pore pressures around the sphere to make sure the signal to noise ratio is good. Figure 6.1 shows the result assuming an isotropic soil, Figure 6.2 shows the result of the anisotropic model.

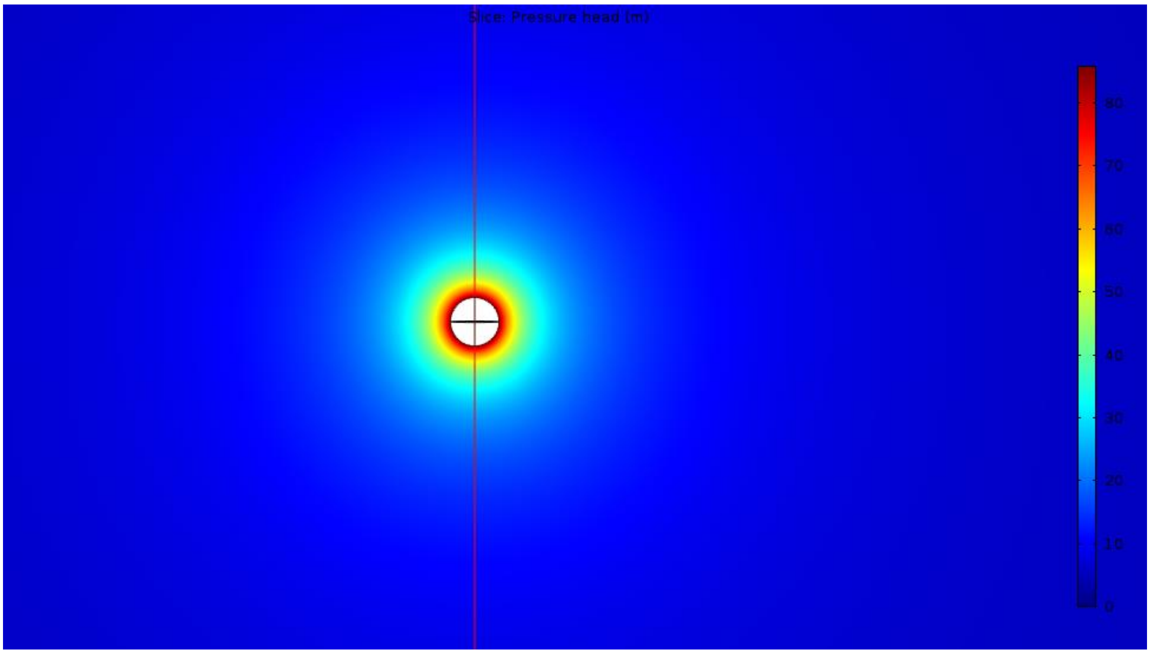

Figure 6.1: Isotropic pressure distribution of isotropic hydraulic conductivity, displayed in total head [m]

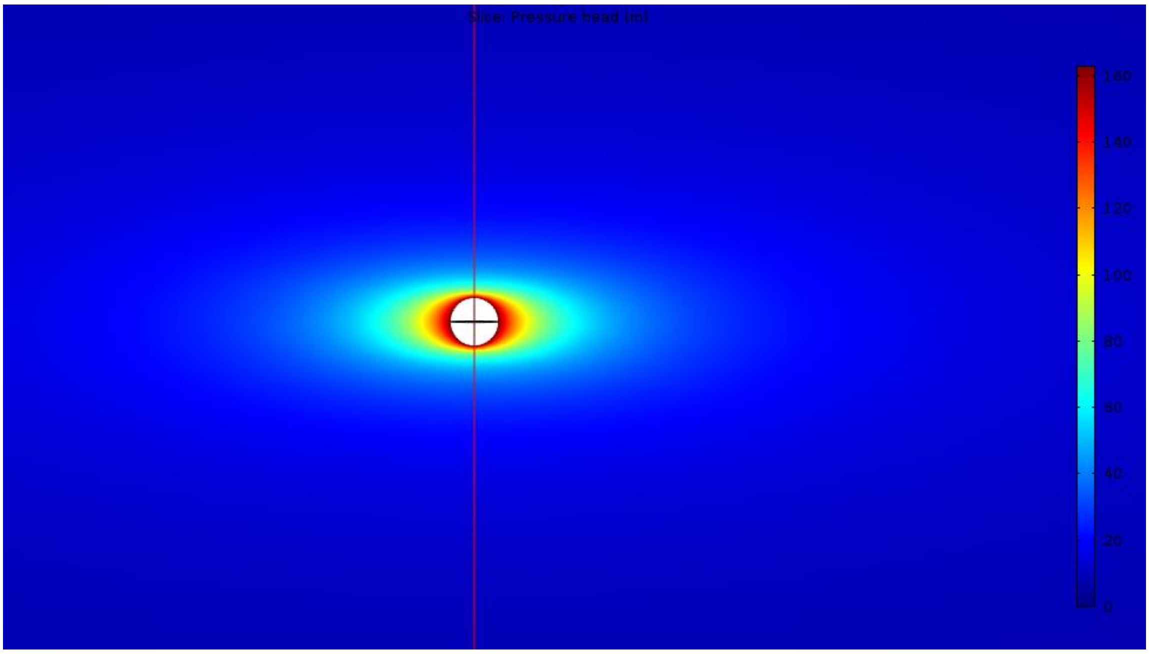

Figure 6.2: Anisotropic pressure distribution of isotropic hydraulic conductivity, displayed in total head [m]

To analyse the pressure distribution around the injection point, multiple pressure transducers are modelled, at 10 cm, 20 cm and 30 cm above the injection location. This gave the following results:

	Value	**Unit**	**Value**	**Unit**	**Value**	**Unit**
Injection rate(Q)	1.5	m/s	1.5	m/s	1.5	m/s
Injection rate(Q)	4.71E-04	m^3/s	4.71E-04	m^3/s	4.71E-04	m^3/s
Radius PT	0.1	m	0.2	m	0.3	m
Total head	6.4598	m	4.2887	m	3.4948	m

Hydrost. head	2.40	m	2.30	m	2.20	m
Δ Head	4.0598	m	1.9887	m	1.2948	m
Horizontal hydr. cond. (k_h)	9.24E-05	m/s	9.43E-05	m/s	9.65E-05	m/s

Table 6.1:Results Comsol analysis with anisotropy, k_v:k_h=1:10

The results are close to the exact value of *9e-5 m/s*, equation (6.1) seems to give a good approximation of the horizontal hydraulic conductivity.

To analyse the effect of the anisotropy ratio on the hydraulic conductivity, in positive and negative perspective, 2 additional calculation series were done. In the first series the anisotropy ratio is decrease to $k_v: k_h = 1{:}2$, or $k_h = 9e\text{-}5\ m/s$ and $k_v = 4.5e\text{-}5\ m/s$. This gave the result in Table 6.2.

	Value	***Unit***	***Value***	***Unit***	***Value***	***Unit***
Injection rate(Q)	1.5	m/s	1.5	m/s	1.5	m/s
Injection rate(Q)	4.71E-04	m³/s	4.71E-04	m³/s	4.71E-04	m³/s
Radius PT	0.10	m	0.20	m	0.30	m
Total head	6.4598	m	4.2904	m	3.4961	m
Hydrost. head	2.40	m	2.30	m	2.20	m
Δ Head	4.0598	m	1.9904	m	1.2961	m
Horizontal hydr. cond. (k_h)	9.2E-05	m/s	9.42E-05	m/s	9.64E-05	m/s

Table 6.2: Results Comsol analysis with anisotropy, k_v:k_h=1:2

These results are almost similar to the ones shown in Table 6.1. The values at 20 and 30 centimetres are a little closer to the real value, but it's only a marginal difference.

When the anisotropy ratio is increased to more extreme values of $k_v: k_h = 1{:}100$ or $k_v = 9e\text{-}7\ m/s$ and $k_h = 9e\text{-}5\ m/s$, the results in *Table 6.3* are found.

	Value	***Unit***	***Value***	***Unit***	***Value***	***Unit***
Injection rate(Q)	1.5	m/s	1.5	m/s	1.5	m/s
Injection rate(Q)	4.71E-04	m3/s	4.71E-04	m3/s	4.71E-04	m3/s
Radius PT	0.10	m	0.20	m	0.30	m
Total head	6.4598	m	4.2904	m	3.4961	m
Hydrost. head	2.40	m	2.30	m	2.20	m
ΔHead	4.0598	m	1.9904	m	1.2961	m
Horizontal hydr. cond. (k_h)	9.38E-05	m/s	9.52E-05	m/s	9.84E-05	m/s

Table 6.3: Results Comsol analysis with anisotropy, k_v:k_h=1:100

The resulting hydraulic conductivity has the same order of magnitude however deviated from the real value of *9e-5 m/s*. The reason for that is explained in paragraph 3.2.5.

The previous results are simulated with pressure transducers above the injection point. In order to analyse the effect of the location of the measurement points a simulation was run with pressure transducers modelled beneath the injection point at the same distances to the injection point. An anisotropy ratio of 1:10 is used. The results are shown in Table 6.4: Virtual pressure transducers placed beneath the injection location.

	Value	***Unit***	***Value***	***Unit***	***Value***	***Unit***
Injection rate(Q)	1.5	m/s	1.5	m/s	1.5	m/s
Injection rate(Q)	4.71E-04	m3/s	4.71E-04	m3/s	4.71E-04	m3/s
Radius PT	0.1	m	0.2	m	0.3	m
Total head	6.4902	m	4.6546	m	4.0898	m
Hydrost. head	2.60	m	2.70	m	2.80	m
ΔHead	3.9902	m	1.9546	m	1.2898	m
Horizontal hydr. conductivity (k)	9.34E-05	m/s	9.59E-05	m/s	9.69E-05	m/s

Table 6.4: Virtual pressure transducers placed beneath the injection location

The pressure transducers beneath the injection point show some higher overestimation of the hydraulic conductivity compared to the results with the virtual pressure transducers above the injection point.

As a final check, the anisotropy is changed to a ratio of k_v:k_h = 10:1 or just the opposite of what normal is. The result is comparable to the previous results.

	Value	***Unit***	***Value***	***Unit***	***Value***	***Unit***
Injection rate(Q)	1.5	m/s	1.5	m/s	1.5	m/s
Injection rate(Q)	4.71E-04	m3/s	4.71E-04	m3/s	4.71E-04	m3/s
Radius PT	0.1	m	0.2	M	0.3	m
Total head	6.4435	m	4.6365	M	4.077	m
Hydrost. head	2.50	m	2.70	M	2.80	m
ΔHead	3.9435	m	1.9365	M	1.277	m
Horizontal hydr. conductivity (k)	9.51E-05	m/s	9.68E-05	m/s	9.79E-05	m/s

Table 6.5: Opposite anisotropy, with k_h modelled as 9.0E-5 m/s.

6.2.2 Conclusion

The relation proposed by Bruggeman (1994) seems to be accurate to determine the hydraulic conductivity in the horizontal direction using vertical hydraulic pressure differences. By using Darcy's law for spherical flow to estimate the hydraulic conductivity with direct push methods, the resulting k that is estimated is k_h.

6.3 Disturbed zone

Based on the research done given in paragraph 2.5.3, an analysis done on the HPT probe to compare the results.

6.3.1 Modelling HPT with disturbed zone

To see which effect compaction has on the HPT, a model is made in Comsol in which the impact of the disturbed zone is analysed. The model of Lui et al. (2008) is chosen, to get a good comparison with the HPT and DPP and what is better in relation to the disturbed zone: measuring the pressure at the injection point or at pressure transducer above the injection point. A compacted zone around the probe is simulated by modelling a soil layer with a thickness of 0.04 m around the probe over its full length. A hydraulic conductivity 10 times lower than the matrix conductivity is assumed. The hydraulic conductivity of the skin is set to 9E-6 m/s and the surrounding soil is set to 9E-5 m/s. The injection flow rate is kept at 500 ml/min. All the other model settings remain the same as the previous simulations described in chapter 3.2. Running the low-*k* skin simulation results in an increase in hydraulic head pressure of 71.96 meter at the injection port. The resulting pressure head profile is shown in Figure 6.4.

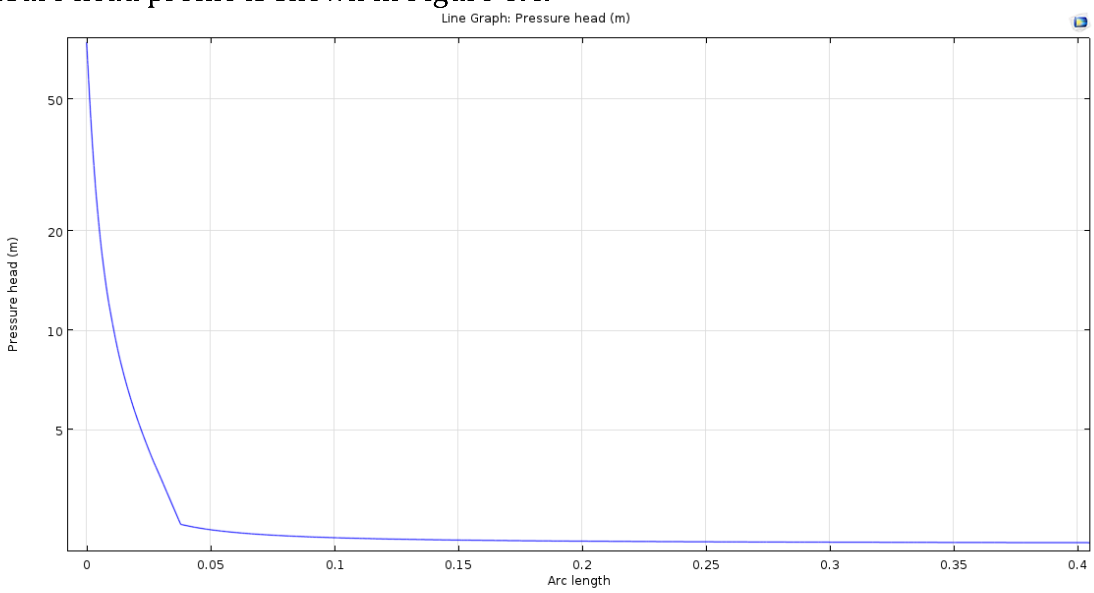

Figure 6.3: Pressure head along line, plotted from injection point 40 centimetre in horizontal direction

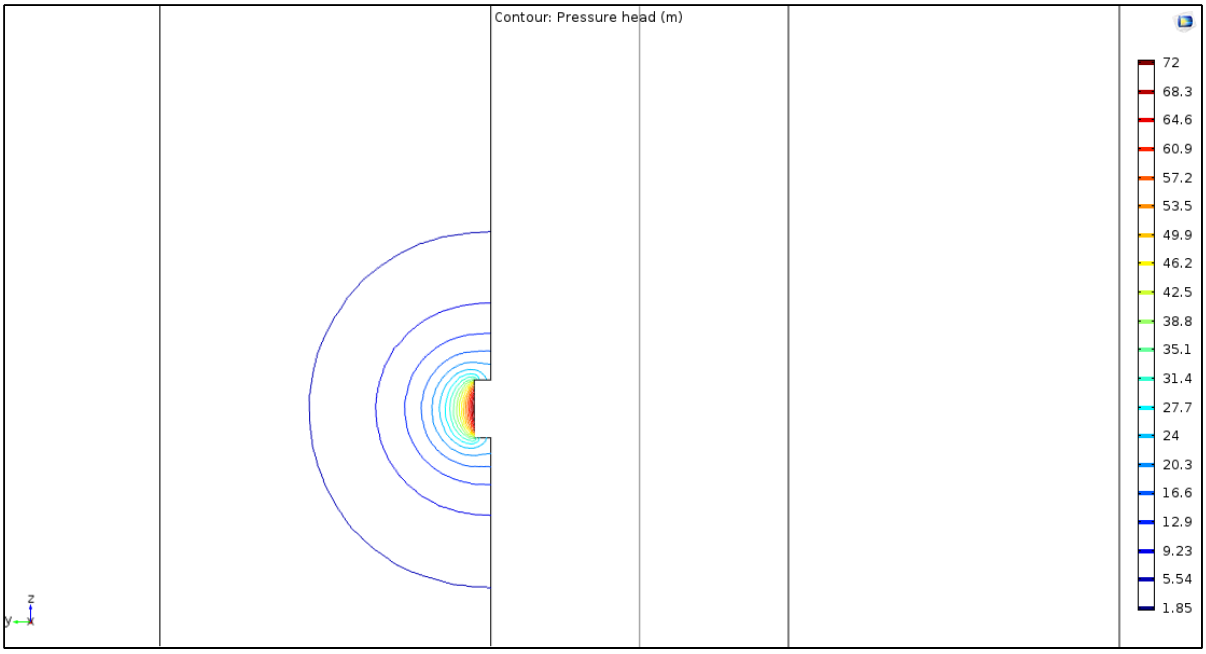

Figure 6.4: Comsol model with HPT injection point and low-k skin of 4 centimetre

When taking the correction factor as presented in chapter 5 into account, the following hydraulic conductivity is calculated based on the simulation results:

$$k = \frac{Q}{4\pi C \Delta h r} = \frac{3.348 * 10^{-5}}{4\pi * 1.1498 * 71.96 * 0.0035} = 9.17 * 10^{-6} m/s$$

The results of the simulation of the injection incl. skin /compaction around the probe are shown in Figure 6.4. The pressure build-up as shown in the profile of Figure 6.4 next to the probe is almost fully situated in the skin.

By decreasing the thickness of the skin, the calculated hydraulic conductivity should approach the *k*-value of the surrounding soil. This approach is performed and the results are given in

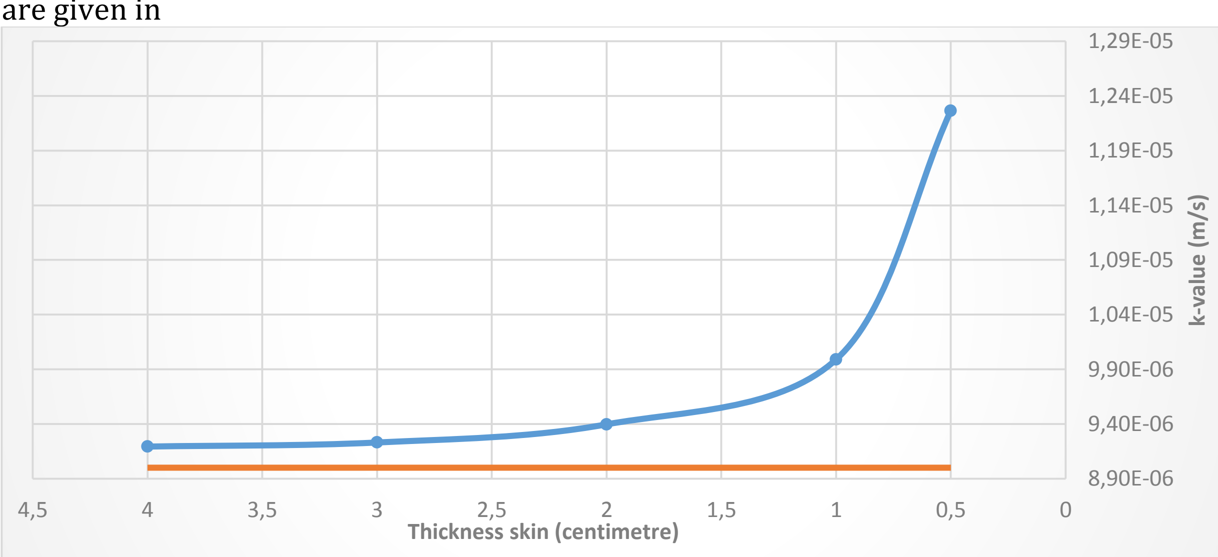

Figure 6.5: The x-axis is the thickness of the low-k skin surrounding the probe, on the y-axis the calculated k-value. The orange line is the modelled value of the skin, and the blue line is the k-value as calculated. As the skin becomes thinner, it approaches slowly the value of the surrounding soil

This result is completely in accordance with the result obtained by Liu et al. (2008). The result from Liu et al. (2008) is given in Figure 6.6, and there can be seen that close to the injection point the pressure distribution is disturbed, but at greater radius from the injection point the distribution becomes almost the same as the base scenario.

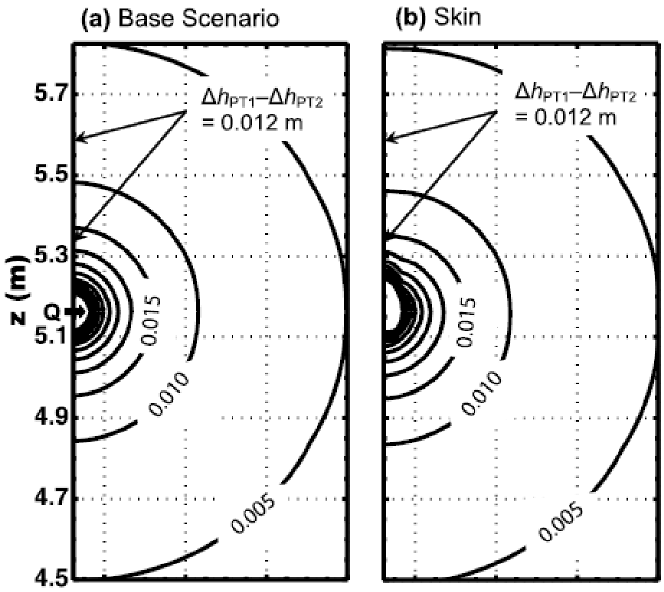

Figure 6.6: Pressure distribution along DPP probe, (a) is base scenario and (b) is with a 4 centimetre skin (Liu et al., 2008)

The conclusion from this analysis is that the HPT probe can be highly influenced by the formation of a skin around the probe. The result obtained by Liu et al. (2008) shows that the DPP is almost not affected by the skin. The real size of this skin and the hydraulic conductivity deviation in the skin are taken here as fixed values, but in practice will be different based on soil type and size of the probe.

Extra research (laboratory testing) on this topic is recommended.

6.4 Depth effect

The signal that is measured by the pressure transducers during stationary injection can be divided into two parts, the hydrostatic pressure which is present in the soil and the pressure head induced by water injection at the injection point. The pressure head induced by injection depends on two factors, the hydraulic conductivity of the soil and the injection flowrate. The pressure head induced by the advancement of the probe into the soil is added when measurement during advancement into the soil is taking place.

What is important for the HPT probe in relation to the injection rate (Q) is the size of the injection screen (r). By decreasing the size of the injection screen (r), the pressure head next to the screen will increase, according to Darcy's law. Because of the increase of pressure head next to the screen, the signal to noise ratio will improve. This signal to noise ratio is defined as:

$$signal\ to\ noise\ ratio = \frac{Pressure\ head\ induced\ by\ injection}{Hydrostatic\ head + pressure\ head\ induced\ by\ injection}$$

The hydrostatic head increases with depth and resulting from that the total head increases as well. The ratio of pressure head to total head therefore decreases. This process is displayed in Figure 6.7. In this figure the HPT probe (paragraph 2.4.9) is assumed with a 7 mm screen, with an injection rate of 500 ml/min. Darcy's law for spherical flow is applied and the hydraulic conductivity is varied.

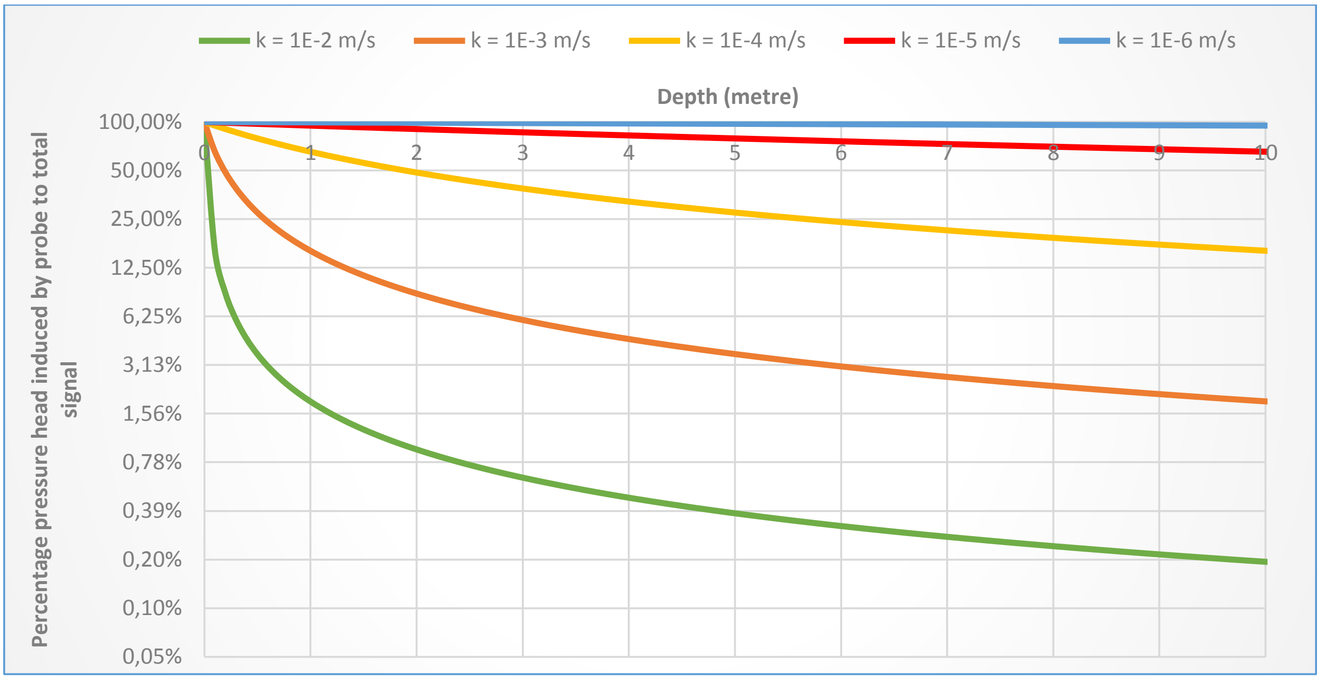

Figure 6.7: Signal to noise ratio of pore pressure increase induced by 500 ml/min injection from HPT

Whether or not a probe still can be used at a certain depth depends on the accuracy of the pressure transducer. Movement of the probe also has influence. The movement causes variations in the hydraulic head. When these variants become larger than the induced pressure head by injection of water, the error in the hydraulic conductivity estimation becomes larger. Note: The pressure increase by the movement of the probe is not taken into account, which would even reduce the percentage.

6.5 Liquefaction

Liquefaction is the process when pore pressures exceed the vertical stress, causing the soil to liquefy. This can be defined as (Fitts, 2002):

$$\text{Stable:} \quad h_{total} \leq \sigma_{vt}\ , \quad \sigma_{ve} \geq 0$$

$$\text{Unstable:} \quad h_{total} > \sigma_{vt}\ , \quad \sigma_{ve} = 0$$

With:
P = Total pore pressure at certain depth

σ_v = Total vertical stress on soil particles at certain depth
σ'_v = Effective vertical stress on soil particles, also defined as: $\sigma'_v = \sigma_v - P$

By injecting water into the soil, an increase of the total pore pressure is generated, Δh.

$$At\ Q = 0,\ h_{total} = h_{hydrostatic}$$
$$At\ Q > 0,\ h_{total} = h_{hydrostatic} + \Delta h$$

Liquefaction occurs when $\Delta h = \sigma'_v$ or $\sigma_v = h_{hydrostatic} + \Delta h + \sigma'_v$

This water is forced into the surrounding of the probe, as can be concluded from continuous injection rates of the probe. Because this injection rate is kept constant, the amount of pore pressure increase depends on the soil type. The maximum pressure which can be generated with the HPT is 100 Psi or 690 kPa (Geoprobe, 2013). Also the depth is important, as σ_{vt} is defined as $\sigma_{vt} = \rho g b$, with b = thickness of soil column above and ρ = unit weight of soil column above. Of course if there are multiple types of layers these can be divided into multiple equations and summed.

To find out if liquefaction occurs, the earlier created Comsol models can be used. The model used in chapter 5 can be used to generate a horizontal cross section to see whether or not the pore pressure head exceeds the vertical stress for the HPT probe. The model is not changed, so the depth of injection is 2.26 metre. The unit weight of the soil column above is assumed to be 2200 kg/m^3. The total vertical stress then becomes:

$$\sigma_v = 2200 * 9.81 * 2.26 = 48.8\ kPa$$

Assuming an injection rate of 500 ml/min and a horizontal hydraulic conductivity of 9E-5 m/s, the zone in which liquefaction occurs is indicated by a red line in Figure 6.8 and Figure 6.9. The red line indicates the boundary of the zone at which liquefaction can occur or where the total pore pressure equals the total vertical stress. This line is the hydrostatic pressure head + injection induced pressure head.

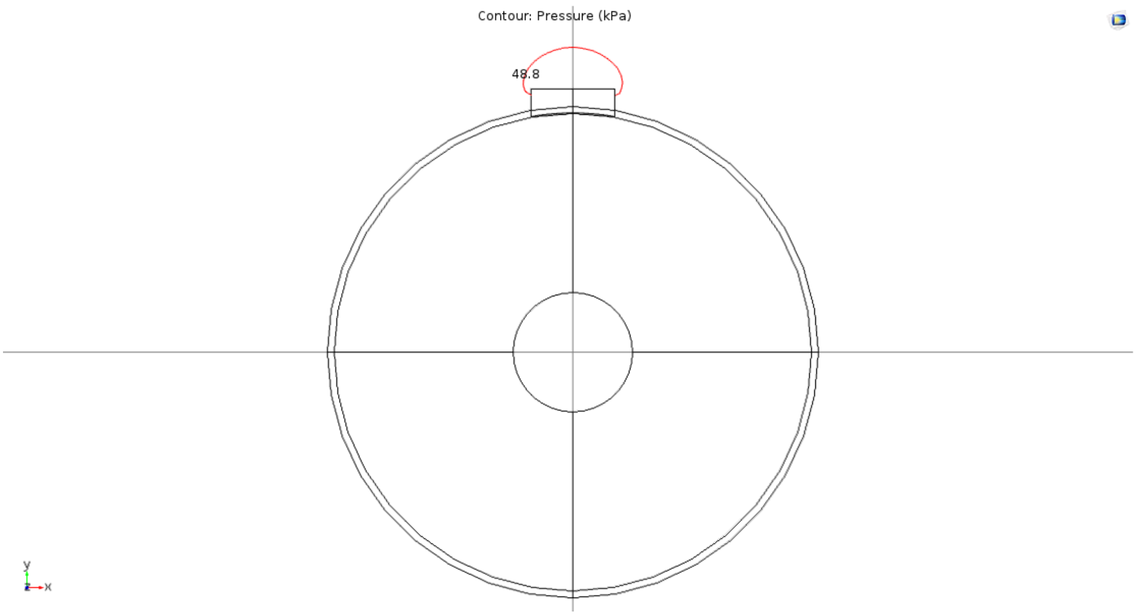

Figure 6.8: Red line indicates Boundary of liquefied zone or where pore pressure exceeds the vertical stress at a depth of 2.26 meter in a soil with k = 9E-5 m/s

When assuming a hydraulic conductivity of 9E-6 m/s and an injection flow rate of 500 ml/min, the area in which the pore pressure increases around the injection point increases. Therefore, the zone where liquefaction can take place increases, as displayed in Figure 6.9.

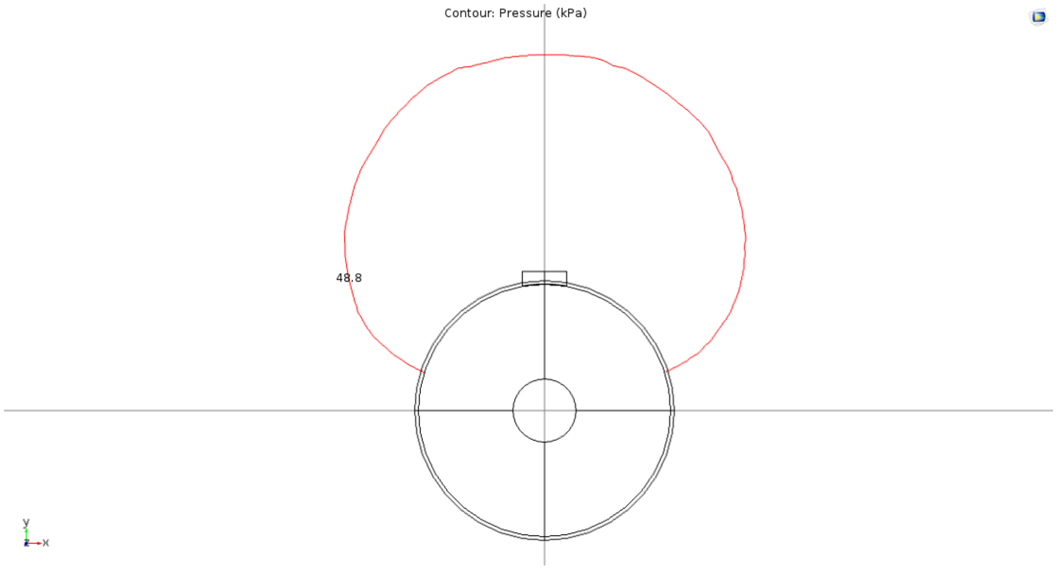

Figure 6.9: Red line indicates Boundary of liquefied zone or where pore pressure exceeds the vertical stress at a depth of 2.26 meter in a soil with k = 9E-6 m/s

6.5.1 Conclusion

Creating one figure in which the size of the liquefaction zone is created for all soil types and all depths is impossible. But one could say for each depth if liquefaction could occur or not. Figure 6.8 and Figure 6.9 show that liquefaction can take place. Liquefaction leads to deformation of the soil and as a result gives a wrong hydraulic conductivity estimation.

The zone in which liquefaction can take place decreases with depth in a continuous soil (as the overburden will increase) and increases in size/distance from the injection point in soil with lower hydraulic conductivity. The injection rate has a large influence on the zone in which liquefaction occurs, as high injection rates induce higher pore pressures. Keeping the injection rate as low as possible prevents from liquefaction taking place. The injection could also be altered when a sudden rise of pressure is taking place. Also note that in this analysis the horizontal stress increases due to cavity expansion of the probe are not taken in to account.

6.6 Reynolds number in relation to direct push injection methods

As water is injected through a small filter into the soil, non-laminar flow around the injection filter can occur. In Figure 2.1 it is shown that Darcy's law starts to diverge from the real solution when Reynolds number gets higher than *Re=1.* The HPT probe from paragraph 2.4.9 is analysed whether or not non-laminar flow by the injection of the water occurs and which effect this has on the collected data. Non-laminar flow could take place, but if it is only of small influence, it could be neglected. Because the focus of most of these tools is determining the hydraulic conductivity of aquifers, the focus is mainly on sandy soil types.

The Reynolds number in porous media can be calculated with the following relation (Fitts, 2002):

$$Re = \frac{\rho v d}{\mu} \tag{6.2}$$

In which:
Re = the Reynolds number [-]
ρ = unit weight of water [kg/m^3]
v = velocity of fluid [m/s]
d = D_{50}, median of soil particles size [m]
μ = dynamic viscosity of water [0.001002 kg/ms at 20^{o}Celsius]

The injection flowrate of the HPT probe is standard set to *500 ml/minute*, which corresponds to *500/60 = 8,333 ml/second*, or *0,008333 litre/second* which corresponds to *8.3333*10^-6 m^3/second* of injected water. The diameter of the smallest opening of a DPIL/HPT probe is *7.0 millimetres*, which means the radius of the screen is *0.0035 metre*. The surface area of the screen can be calculated from the radius: $\pi * r^2 = 3.85*10^{-5}\ m^2$. This means that the length of a cylinder to transfer this amount of water is: *Volume/surface area = 8,33*10^-6/3,85*10^-5=0.217 m*. Every second this length is transferred out of the injection point with a velocity of *0.217 metre/second* and is equivalent to 500 millilitres/minute.

As the surface area doesn't change, the Reynolds number can be calculated for different injection rates. This results in Figure 6.10.

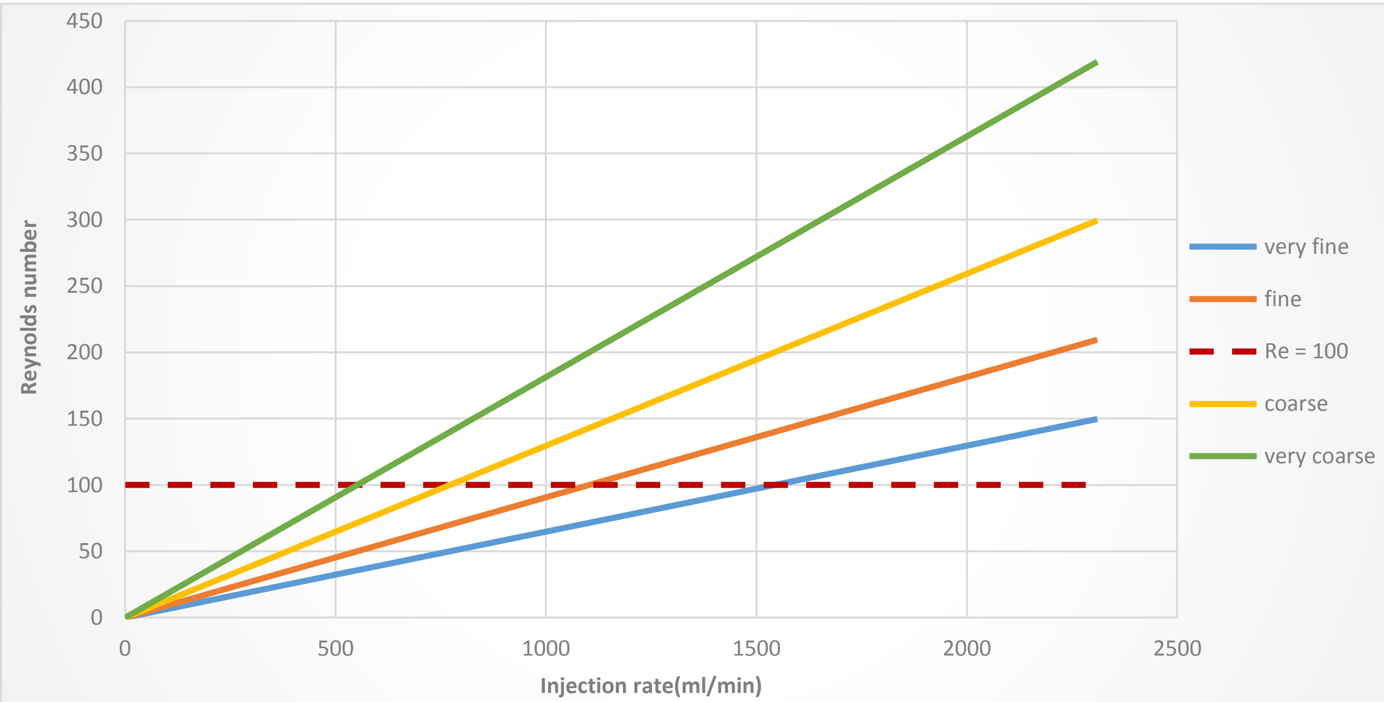

Figure 6.10: Reynolds number for given injection rates through 7 mm screen for 4 types of soil particle diameter(D_{50})

According to Dutch NEN-5104 code, the boundaries for types of sand are:

	Lower boundary	***Upper boundary***
Extremely coarse	0,420 mm	2 mm
Very coarse	300 µm	420 µm
Coarse	210 µm	300 µm
Fine	150 µm	210 µm
Very fine	105 µm	150 µm
Extremely fine	63 µm	105 µm

Table 6.6: sand particle size indication

The upper boundaries are taken for Figure 6.10. At *Re=100*, turbulence starts to occur for flow in porous media (Bear, 1972). As can be seen in Figure 6.10: Reynolds number for given injection rates through 7 mm screen for 4 types of soil particle diameter(D_{50}), there is turbulent flow in sandy types of soil, as *500 ml/min* equals *0.217 m/s* and used injection rates for the HPT are on average *500 ml/min*.

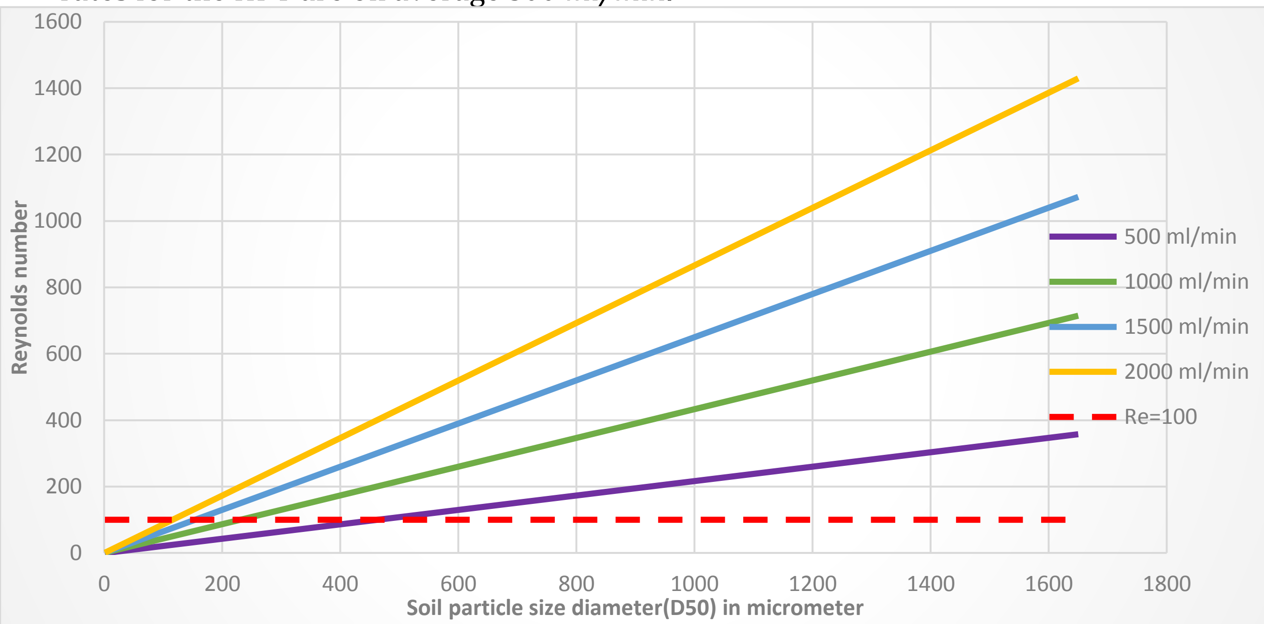

Figure 6.11: Reynolds number in relation to the D50 for a constant injection rate of 500, 1000, 1500 and 2000 ml/min, at the screen of the HPT

The injection rates are sometimes even higher than the standard 500 ml/min, in Table 6.7 the conversion from ml/min to m^3/s to m/s for the HPT probe can be seen.

ml/min	***m^3/s***	***m/s(HPT)***
500	8,33E-06	0,217
1000	1,67E-05	0,433
1500	2,50E-05	0,650
2000	3,33E-05	0,866
4000	6,67E-05	1,732
6000	1,00E-04	2,598

Table 6.7: Injection rates converted from ml/min to m^3/s and m/s for injection from the HPT injection screen

The Reynolds number shown in Figure 6.10 and Figure 6.11 is calculated directly at the opening of the injection point. As water starts to dissipate from the injection point, the surface area which the water flows through increases significantly. If spherical flow is assumed, this can be represented in Figure 6.12.

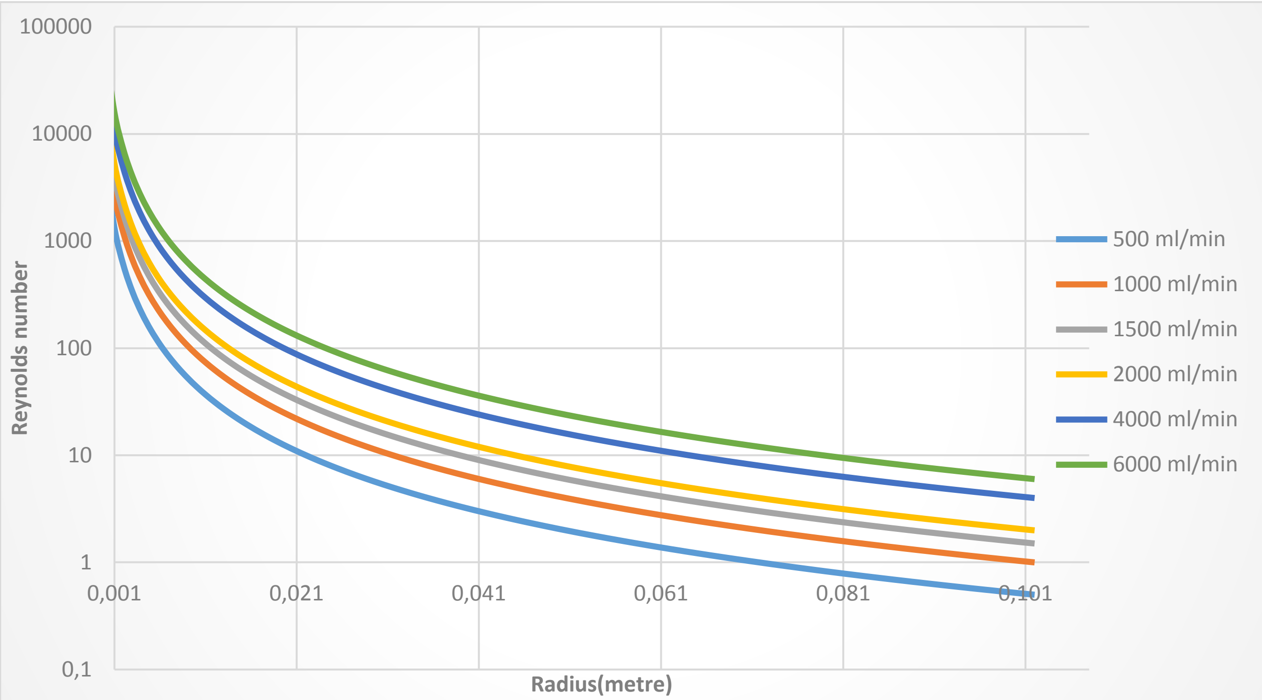

Figure 6.12: Reynolds number (note: logarithmic scale) for multiple injection rates at a certain spherical radius

The same can be done for anisotropic flow. The flow path will not follow a spherical flow, but an ellipsoidal/spheroidal flow. This means that the surface area which the water flows through must be the surface area of an oblate ellipsoid and defined in the different directions: x = y ≠ z. This can be calculated by the following formula (according to Wolfram Alpha):

$$A_{ellipsoid,oblate} = 2\pi a^2 (1 + (\frac{1-q^2}{q} tanh^{-1} q) \quad with \quad q = 1 - \frac{b^2}{a^2} \tag{6.3}$$

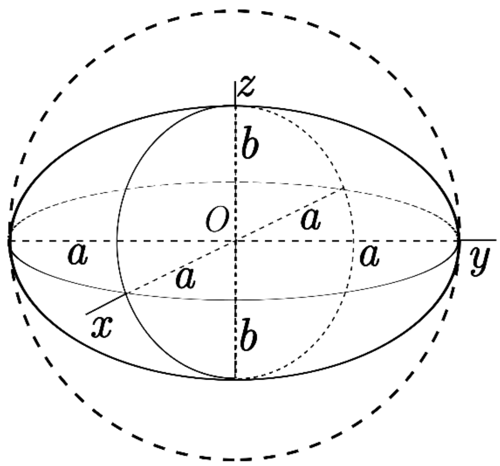

Figure 6.13: Oblate ellipsoid, with a the horizontal radius along the x,y-axis and b the vertical radius along the z-axis. (Wiki, 2016)

The horizontal to vertical hydraulic conductivity is usually given in a ratio, 1:1 to 1:10. If this ratio is translated to the spheroid in Figure 6.13, this is *b : a* . When a soil has a certain hydraulic conductivity ratio, it can be assumed to be continuous over the soil volume. Meaning q doesn't change when a or b increases. Using this approach in the surface area equation, based on 2 ratios q is calculated for both of the ratios. The only variable then left in the equation is a, which is the most important in this case because it shows the greatest length at which non-laminar flow can take place. 2 ratios were analysed, 10:1 and 2:1. Both were compared with a normal sphere, ratio 1:1. The result is shown in graph 4. The horizontal radius a is varied and is displayed along the x-axis.

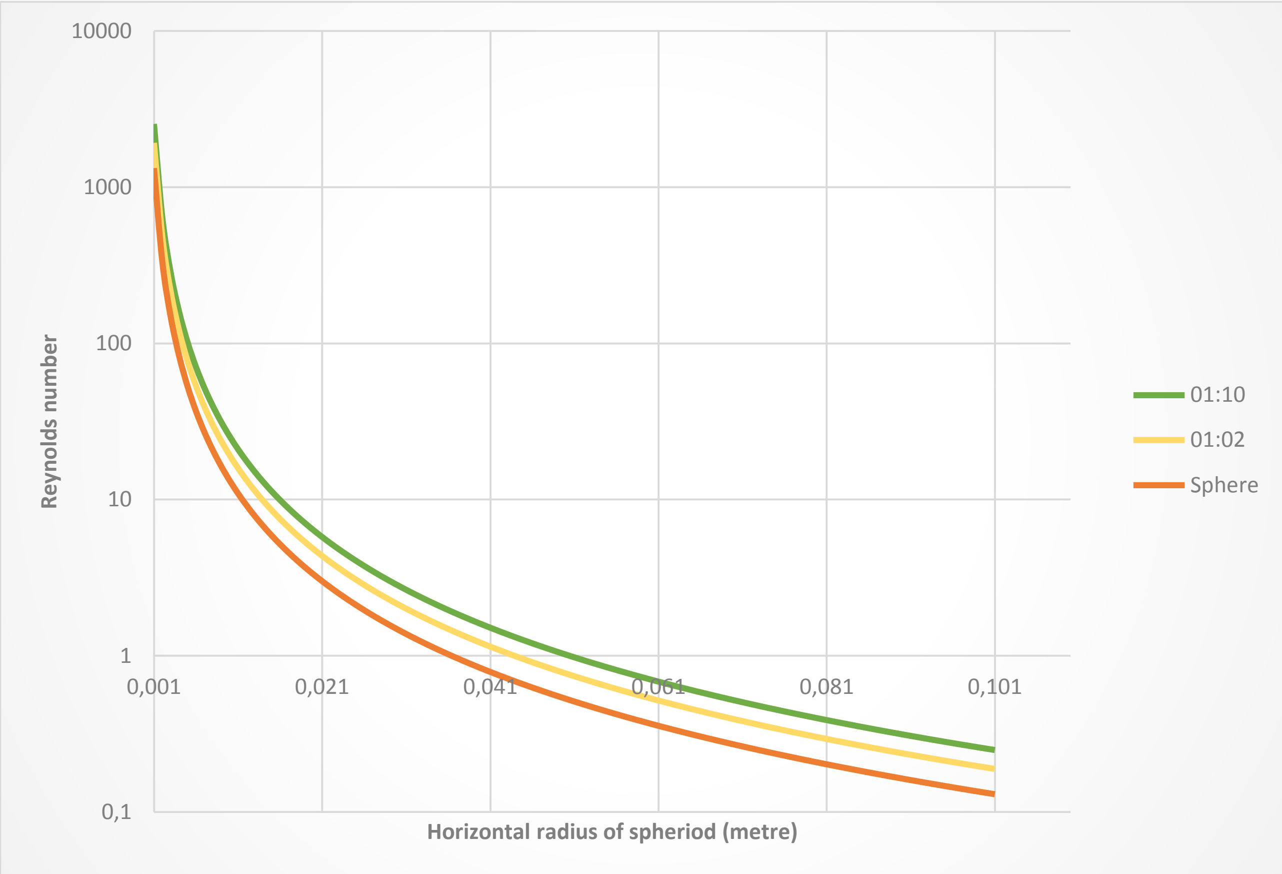

Figure 6.14: Reynolds number (note: logarithmic scale) for 2 types of vertical to horizontal ratio rates at a certain spherical radius

6.6.1 Conclusion Reynolds number

Darcy's law can be assumed, but it depends on the injection rate, the size of the injection filter and the type of soil which is analysed. For isotropic soils this results in a spherical shape volume in which the flowrate is too high to assume Darcy's law and for anisotropic soils this will result in an oblate spheroid volume. When Darcy's law is assumed, smaller injection flowrates and larger injection filters are preferred, because they reduce the chance of creating non-laminar flow.

7 HPT in practice

7.1 Introduction

The HPT is designed to determine the hydraulic conductivity from data that is acquired during movement of the probe into the ground. Because of this movement, the determination becomes much more difficult. This chapter will give a first insight in this topic, but further research is recommended.

7.2 Basic principles HPT measurement

The measurements from the HPT are non-stationary and therefor difficult to interpreted. The reasons are: First is the fact that excess pore pressures are generated by the displacement of water and soil by the movement of the probe. These pore pressure can dissipate, but this dissipation depends on the hydraulic conductivity of the soil. The probe moves down, into the zone where just excess pore pressures were generated. The total increase of excess pore pressure is hard to predict. It depends on the storage capacity of the surrounding soil, which depends on the porosity and compressibility of the soil matrix and water, and the hydraulic conductivity of the soil.
Second is the fact that a stationary situation might not be reached. This means that Darcy's law can't be used, because a stationary situation is necessary for applying Darcy's law. Every 1.5-2 centimetre a measurement is done and the probe moves with 2 cm/s into the ground. So only when a stationary situation is reached very fast (<2 seconds), Darcy's law can be applied.

7.3 Generated excess pore pressure by movement

The generation of excess pore pressures is a topic with a lot of research. In chapter 2.3 the methods that do not use water injection to create excess pore pressure are given. These methods determine the hydraulic conductivity from the excess pore pressure created by the movement of the probe. The problem with these methods is that they use dimensionless forms of the equations and a prediction of the excess pore pressure in absolute values can't be directly derived from them.

Fitzgerald and Elsworth (2010) and Elsworth (2013) did a numerical analysis on the generated pore pressures, which is given in paragraph 2.5.6.

7.4 Available solutions

Because the non-stationary conditions make it so hard to predict the hydraulic conductivity, the question rises if waiting for stationary conditions might be better. A relative simple solution, avoiding a complex analytical description of what takes place, is making an empirical relation.

The empirical relation given by the Geoprobe for the HPT is given as:

$$k = 0.3048 * (21.14 * ln(\frac{Q}{p} 6.894) - 41.71) \tag{7.1}$$

This equation is based only a small number of analysis where HPT and slug tests are done next to each other, and based on both results this relation is developed. The fact that the result can become negative for certain values of Q/p, shows that this equation is not correct. Internal analysis at Fugro also showed that this equation unnecessarily contains a logarithmic factor and results coming from the equation were not that good.

Therefore Fugro suggested to use the relation given by Bruggeman (1999):

$$k = \frac{Q}{4\pi \Delta h r} erfc(\frac{\beta r}{2\sqrt{t}}) \tag{7.2}$$

This relation is for a non-stationary point source. The complement error function(*erfc*) is the factor that makes it non-stationary or dependent on time and dependent on the storage capacity (β). Because this storage capacity is unknown, a value must be assumed based on expected soil types or CPT data taken at the same moment.

Liu et al. (2009) suggest to use a power-law relation of the form:

$$k = 10^b (\frac{Q}{\Delta h})^a \tag{7.3}$$

According to Liu et al. (2009), the factors are: a =2.5 and b = -9.0. According to Rogiers et al. (2013), the factors are a = 0.32 and b = -3.91.

Bohling et al. (2012) suggest a comparable power transform:

$$k = e^b (\frac{Q}{\Delta h})^a \tag{7.4}$$

Unfortunately, Bohling et al. (2012) do not give values for *an* and *b*.

Fugro also came up with a fixed value, assuming the relation to be linear.

$$k = 1.15 * \frac{Q}{\Delta h} \tag{7.5}$$

7.5 Data from practice

A dataset is taken with HPT injection rates/pressure and with that dataset the above mentioned relations are compared. Concluding from the results is that there is a large deviation of these methods, because they are correlated on data from specific sites.

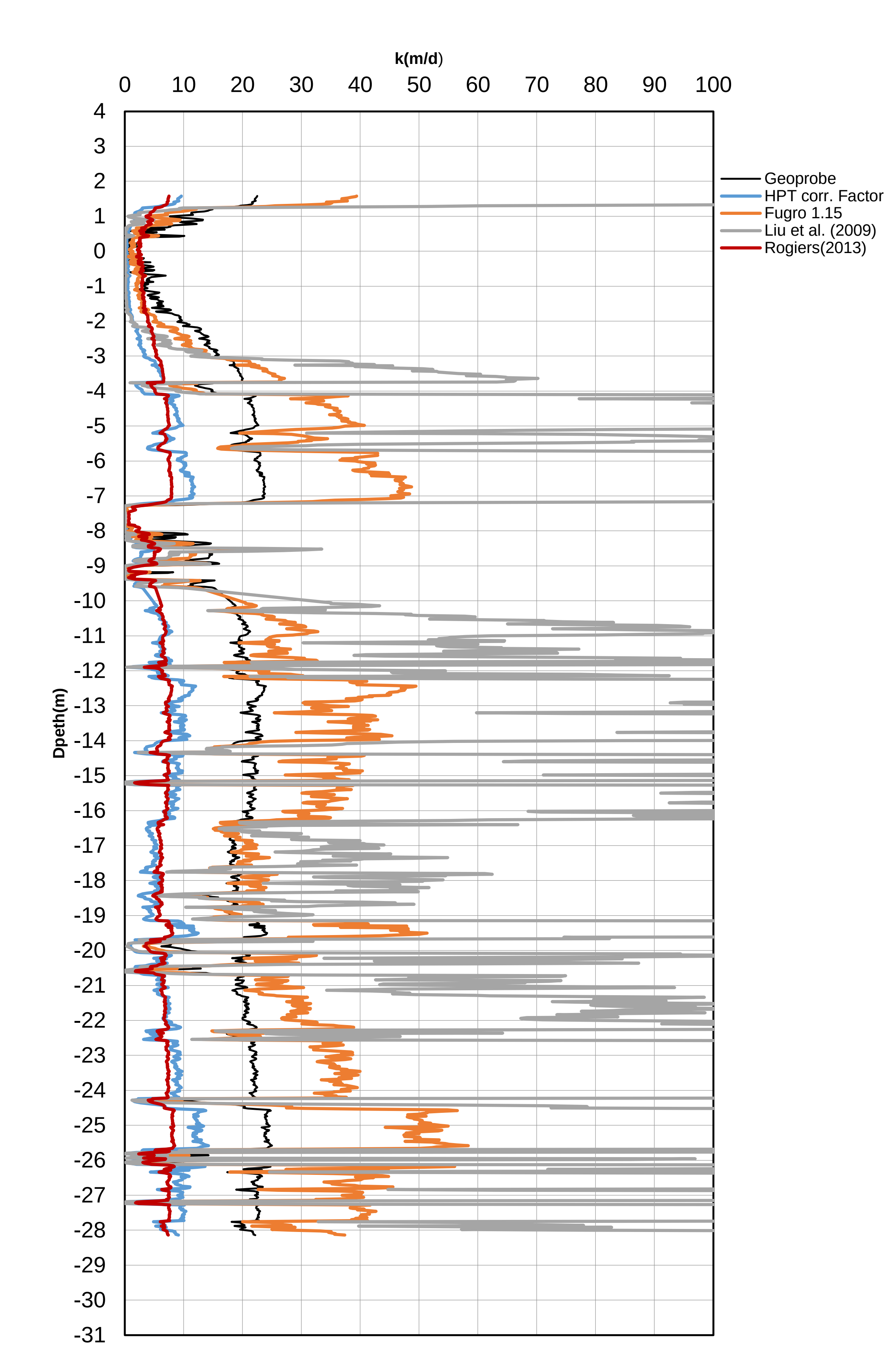

Figure 7.1: Multiple Q/P-k relation, applied on HPT data

7.6 Improving the results

These results vary a lot and can be improved. The Q/P-k relation can be improved, but also redesigning the probe could lead to an improved result.
First is to move the HPT injection upwards on the probe. By relocating the injection screen to upper levels, the measured pressure near the injection point is influenced less by excess pore pressures generated by movement of the probe.
Second is to decrease the penetration rate. The penetration rate is now 2 centimetres/second. This rate is based on the standard rate used for CPT cones. As can be seen in Figure 2.20and Figure 2.21, a lower penetration rate leads to lower excess pore pressures and results in an improved signal to noise ratio and measured excess pressures which only purely caused by the injection of water and not by movement of the probe. A lower penetration rate also increases the chance of reaching a stationary state, which means Darcy's law can be applied.
Third is to measure with two pressure transducers instead of one. Taking the *Δh* from these two pressure transducers give a faster stationary response (Liu et al., 2008).

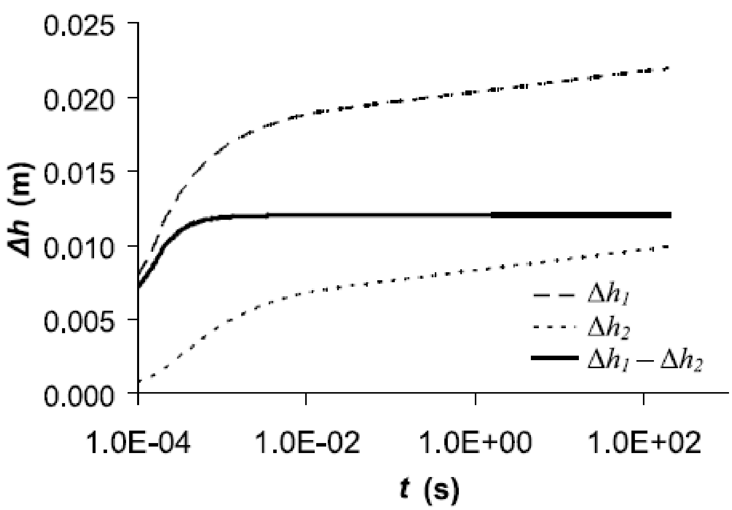

Figure 7.2: Δh_1- Δh_2 reaching a stationary situation much faster than the two separate signals (Liu et al. 2008)

This method is analysed in Comsol. A point source is created and two virtual pressure transducers are made. The soil is analysed using linearized storage. Figure 7.3 and Figure 7.4 both confirm the difference between the delta head and the two separate head signals. In Figure 7.3 the compressibility of the matrix is 1E-4 Pa^{-1} and in Figure 7.4 it is 1E-7 Pa^{-1}. A system with 2 or more pressure transducers is recommended, based on this result.

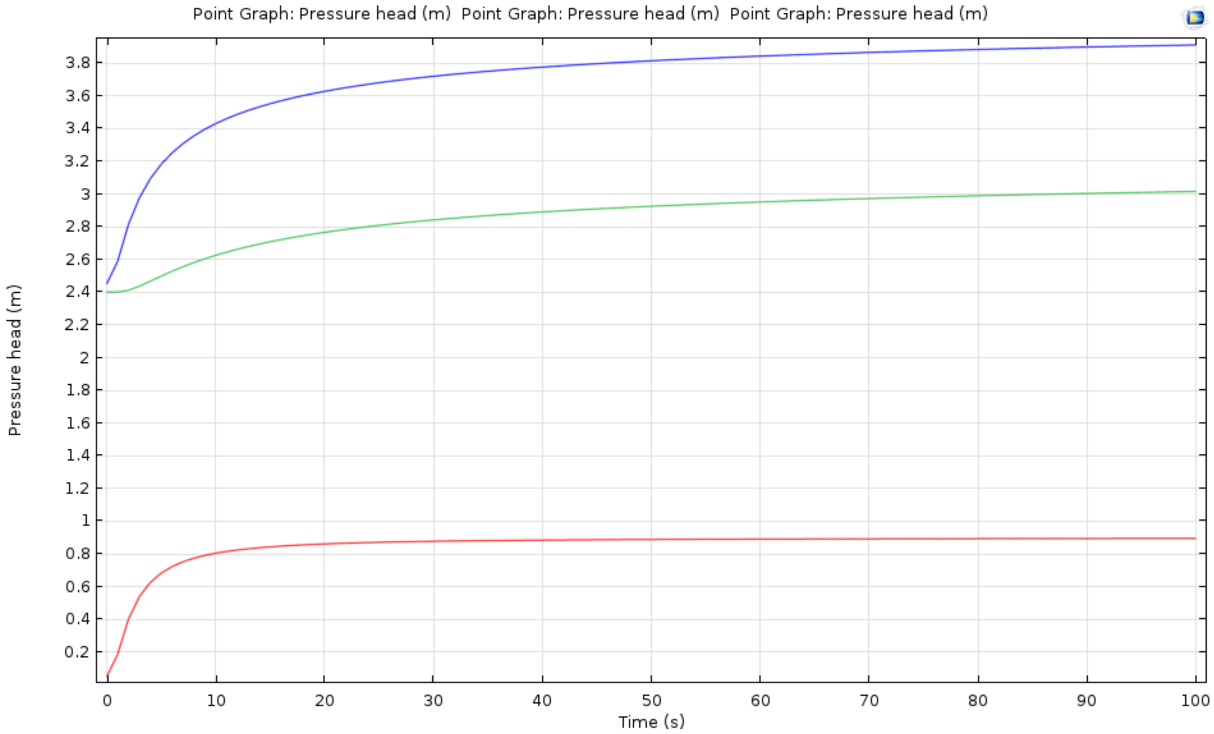

Figure 7.3: Δh_1- Δh_2 (red) reaching much faster stationary compared to two separate signals

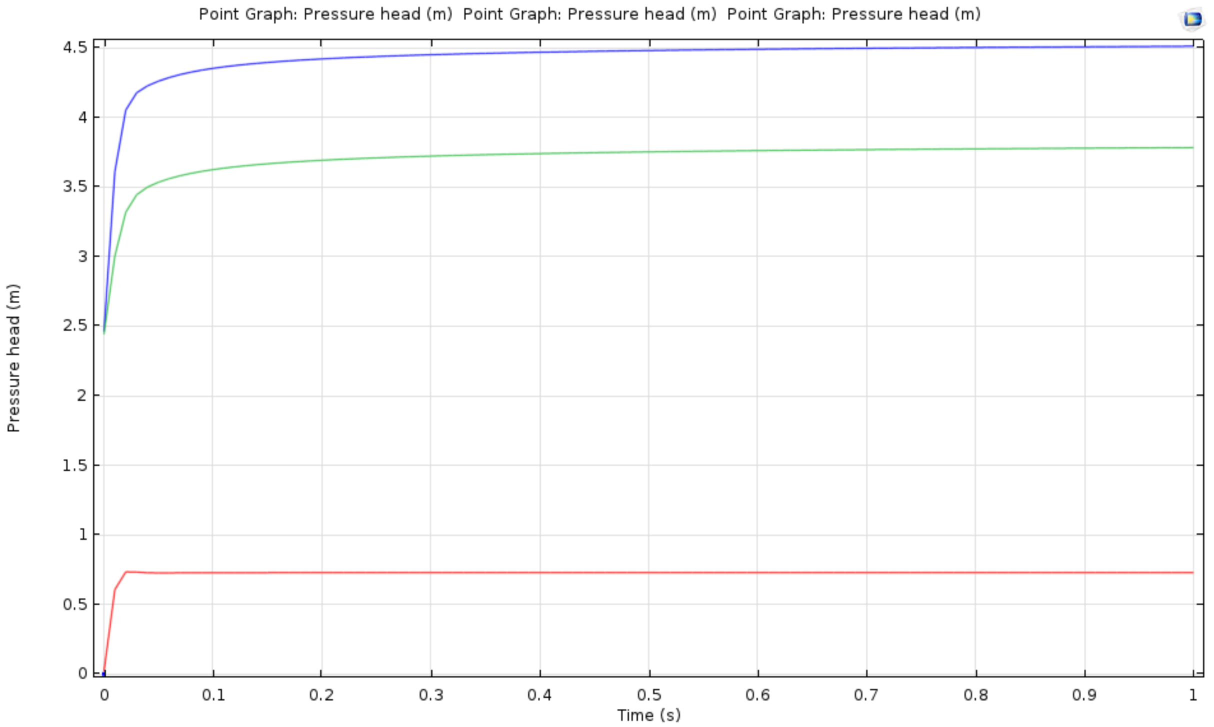

Figure 7.4: Δh_1- Δh_2 (red) reaching much faster stationary compared to two separate signals

7.7 Conclusion

Describing the full process that takes place during movement of the probe is complicated. Therefore multiple empirical relations were developed to relate the Q/P ratio to the hydraulic conductivity. Comparing these relations shows that there is a large deviation between results, which can be explained by the fact that these relations were based on site specific hydraulic conductivity values obtained using conventional methods. These methods give good results for that specific site, but for other locations this relation is not necessarily correct.

To improve the hydraulic conductivity determination, lower penetration rates are recommended and a redesign of the existing HPT probe should be considered. 2 pressure transducers located close to each other give a faster stationary response, which means that in a shorter timeframe the hydraulic conductivity can be determined. If the timeframe stays the same, because of limited time, the difference in head between the two pressure transducers will give a better approximation of the hydraulic conductivity.

8 Conclusion

8.1 Main research question

- ***Are analytical solutions the appropriate method to determine the hydraulic conductivity?*** *According to field experience lateral hydraulic conductivity is generally higher than vertical hydraulic conductivity. Which would indicate that the assumption of a perfect spherical flow is not valid.*

Empirical relations have shown to vary a lot when applied to the same set of data. This is because these empirical relations are developed using limited data of only one or two sites. Using this relation on another different site results on non-accurate values of the hydraulic conductivity (chapter 7.5). Analytical solutions have shown to be more accurate (chapter 4) for stationary analysis. This is because these have a scientific basis in the form of Darcy's law and are only used in stationary conditions. The non-stationary conditions that take place with a moving probe are at this moment unable to be analysed with just Darcy's law and need much more factors taken into account. These factors are the pore pressures generated by the moving probe and the fact that stable pressure head might not be reached.

Anisotropy can be incorporated in Darcy's law for spherical flow (chapter 6.2). The determined hydraulic conductivity of the injection-based direct push methods will result in the horizontal hydraulic conductivity. Changes in vertical hydraulic conductivity do not affect the result. This is only analysed in stationary conditions, how anisotropy affects the results of a moving probe.

8.2 Sub research questions

- ***How are the results affected by the compaction and creation of smear zone around the probe/cone?***

The effect of a smear or compacted zone depends on the location of the pressure transducer (chapter 6.3). Result of the Direct Push Permeameter from Lowry (1999) and Liu et al. (2008) show that the DPP is only minimally affected by a compacted zone with a lower conductivity around the probe. The DPP has two pressure transducers at 15 and 40 centimetres above the injection point.

The HPT probe is highly affected by a compacted zone (chapter 6.3). The hydraulic conductivity, determined by the measure pressure head, is close to the value of the compacted zone (Figure 6.5). This means that the zone of detection on the HPT hydraulic conductivity estimate is very small and that the result of the HPT probe is highly affected by a change of hydraulic conductivity by compaction near the injection point.

- ***If the system could be redesigned, where and how many pressure transducers would lead to a better hydraulic conductivity determination and at which location should water be injected?***

A minimum of 2 pressure transducers is highly recommended (chapter 7.6). The delta head over the 2 pressure transducers reaches a faster stationary state, which means it can be applied faster. Also 2 separate pressure transducers are only slightly affected by a compacted zone or clogging (chapters 6.3 and 2.5.4). The injection location should be away from the tip of the probe. Around the tip are the highest excess pore pressures generated. This means that dissipation with take the longest close to the tip. A location a few decimetres above the tip would already lead to earlier stationary conditions, which means that time is saved during stationary analysis.

- *There are systems that inject from a point screen in 1D (HPT and DPIL) and systems that inject from a cylindrical screen(DPP).* ***Which method is preferred and how does the geometry affect the k-Q/P relations mentioned above?***

Chapter 4 and 5 show that when homogeneous soil conditions are assumed, meaning no disturbance of the surrounding soil by water injection, and perfect laminar flow, the shape of the injection filter does not matter. A correction can be made for the different shapes (chapter 5), leading a comparable result. But the smaller screen does have an effect on the flow outside of the screen. A smaller screen means a smaller inflow area and higher generated pressures close to the screen. This could result in liquefaction (chapter 6.5), short circuiting (paragraph 2.5.5) or non-laminar flow (chapter 6.6). Higher pressures are preferred, because they reduce the signal-to-noise ratio (chapter 6.4) and the higher injection flowrate, because of the small screen, prevents from clogging taking place.

As a conclusion can be made that a smaller screen size is recommended, because large screens have proven to get clogged (monopoolsonde and dipoolsonde). Because injection into one direction or cylindrical direction only have a minor difference and a correction can be made, injection into one direction is recommended. Exact screen size must be based on the possibilities in constructing the probe and taken into account the injection flowrate.

- ***Which injection flowrates are recommended?*** *Should the injection flowrates be adjusted to different soil types in relation to short-circuiting? Can Darcy's law be assumed with the used injection flowrates of the HPT system? Should the injection rate be increased with depth? Until which depth can the HPT direct push methods be used?*

Based on clogging and signal-to-noise ratio, as high as possible injection rates are recommended. But based on liquefaction, short-circuiting and Reynolds number, lower injection rates are recommended. Injection rates also depend on the location of the pressure transducer. When the pressure transducer is at larger radius, the signal-to-noise ratio will increase much faster with depth than with a pressure transducer at the same location.
Darcy's law can be assumed for the HPT, but only when the injection rates are kept low (<500 ml/min).

Injection rates shouldn’t be increased with depth, but should be specific to a layer. A solution can be to inject not constant but create a constant head increase and vary the injection rate.
The depth depends on the soil type of interest and the injection rate. Soil with low conductivity and a low injection rate can be analysed only until a depth of a few metres (chapter 6.4).

9 Recommendations

9.1 Hydraulic conductivity from CPT data

Unfortunately, there was not enough time during this thesis to fully analyse and compare the methods mentioned in chapter 2.3. CPT data is available in enormous amounts. This data can all be analysed and methods should be compared.

9.2 Lab testing HPT

Lab testing should be done on the HPT to see what really takes place around the probe.

- What kind of deformation of the soil caused by the injection?
- How does heterogeneity affect the result?
- Where does the water go after it is injected in the soil?

A suggestion could be to inject warm water and based on that get a more insight of the flow path of the injected water. Modern techniques like glass fibre heat measuring sensors can be used around the probe and the data produced can be analysed. A good prediction can then be made of the flow path.

9.3 Improving Q/P-k relation

When the HPT is used more in practice, a lot of data will become available. This could be a great opportunity to create a new or improve exiting empirical relation, based on a larger amount of data. The limitations of the nowadays available methods have shown that creating an empirical relation on a specific site gives a relation only applicable to that site.

9.4 Material point method analysis

The Material point method is more used and still under development for use in the geotechnical software. The material point method is very interesting, because it is suitable for larger deformations. This is because the state parameters are not stored in the nodes, but in the material point which can move through the mesh. The movement of the probe causes a large deformation of the soil, so modelling the deformation of the soil around probe is something that is difficult to do correctly.

One of the disadvantages of the material point method is that is requires more computer calculation power and that it is not standard in geotechnical FEM-programs nowadays available. This is because there are still same issues which have to be improved to get useable in geotechnical software. In the near future more possibilities are expected, because Plaxis and Deltares are working on the implementation of MPM in software.

9.5 Using a different CPT cone

The HPT cone can be connected to a normal CPT cone. Now only a u1 pressure transducer cone is used. A u1, u3 cone could give a better result, based on the analysis given in chapter 7.6.

Bibliography

Barghava, S.C. (2012), Electrical and measuring instruments and measurements

Bear, J. (1972), Dynamics of flow in porous media, Dover Publications

Bohling, G.C. (2012), G. Liu, S.T. Knobbe, E.C. Reboulet, D.W. Hyndman, P. Dietrich, J.J. Butler Jr., Geostatistical analysis of centimetre-scale hydraulic conductivity variations at the MADE site, Water Resources Research, Volume 48,

Bruggeman, G.A. (1994), Verrassende uitkomsten in stromingen deel 1, Stromingen, Nederlandse Hydrologische vereniging

Bruggeman, G.A. (1999), Analytical solutions of geohydrological problems, Developments in water science 46

Butler, J.J. Jr. (2007), P. Dietrich, V. Wittig, T. Christy, Characterizing hydraulic conductivity with the direct-push pemeameter, Ground Water Vol 45. No. 4, July-August 2007

Chai, J.C. (2011), P.M.A. Agung, T. Hino, Y. Igaya and J.P. Carter, Estimating hydraulic conductivity from piezocone soundings, Geotechnique 61 No. 8, page 699-708

Darcy, H. (1856), Les fontaines publiques de la ville de Dijon. Victor Dalmont, Paris

Dietrich, P. (2008), J.J. Butler Jr. and K. Faiss, A rapid method for hydraulic profiling in unconsolidated formations, Ground Water Vol. 46 No. 2, pages 323-328, March-April 2008

Elsworth, D. (2005), D.S. Lee, Permeability determination from on-the-fly piezocone sounding, Journal of geotechnical and geoenvironmental engineering, pages 643-653

Elsworth, D. (2013), The evolution of pore pressure fields around standard and ball penetrometers: influence of penetration rate, Int. journal for numerical and analytical methods in geomechanics, number 37:2135-2153

Fargier, Y. (2013), Edouard Durand and R. Rousselet, Le Perméafor, un outil de diagnostic des ouvrages hydrauliques en terre et de leur foundation

Fitts, C.R.(2002), Groundwater Science, Academic press, Elsevier Science, London

Fitzgerald, M. (2010) and D. Elsworth, Evolution of the pore-pressure field around a moving conical penetrometer of finite size, Journal of Engineering Mechanics, March 2010

Fugro (2015), POV Piping: Continue doorlatendheidsprofielen: verdiepend inzicht in de bodem, Analyse vergelijking doorlatendheidsmetingen en HPT sonderingen, Juni 2015

Geoprobe (2013), Hydraulic profiling tool System, standard operating procedure, Technical bulletin No. MK3137

Hantush, M.S. (1961), Drawdown around a partially penetrating well. Journal of Hydraulics Division, ASCE 87, no. HY4, pages 171–195

Köber, R (2009), G. Hornbruch, C. Leven, L. Tischer, J. Großmann, P. Dietrich, H. Weiß, A. Dahmke, Evaluation of Combined Direct-Push Methods Used for Aquifer Model Generation, Ground Water Volume 47 No. 4, July-August 2009, pages 536-546.

Kruseman G.P. (2000), N.A. de Ridder, Analysis and Evaluation of Pumping Test Data, Second Edition, 1970-2000

Lambert, J. (1996), Doorlatendheidsmetingen: absolute noodzaak of luxe uit het verleden?, Brieven Stromingen 2 1996, Nederlandse Hydrologische Vereniging(NHV)

Lee, D.S. (2008) , D. Elsworth, R. Hryciw (2008), Hydraulic conductivity measurements from on-the-fly uCPT sounding and from VisCPT, Journal of geotechnical and geoenvironmental engineering, December 2008

Liu, G. (2008), G. C. Bohling, J. J. Butler Jr. , Simulation assessment of the direct-push permeameter for characterizing vertical variations in hydraulic conductivity, Water Resources research, Volume 44, W02432

Liu, G. (2009), J.J. Butler Jr., G.C. Bohling, E. Reboulet, S. Knobbe, D.W. Hyndman, A new method for high resolution characterization of hydraulic conductivity, water resources research vol. 45

Lowry, W. (1999), In-situ permeability measurments with direct push techniques: phase II topical report, Science and Engineering association

Lunne, T. (1997), P.K. Robertson and J.J.M. Powell, Cone Penetration Testing in Geotechnical Practice, Blackie Academic/Routledge Publishing, New York

McCall, W. (2011), Application of the Geoprobe HPT Logging System For Geo-Environmental Investigations, Geoprobe

McCall, W. (2013), HPT webinar, Geoprobe

Moran, J.H. (1962), and E.E. Finklea, Theoretical analysis of pressure phenomena associated with a wireline formation tester. Journal of Petroleum Technology 14, pages 899–908

Ree, van C.C.D.F. (2003), R.P. Heijer, J.A.C. Meekes, F. Debets, Demonstratie en kennisoverdracht Innovatieve Bodemonderzoektechnieken(DIB)

Rietsema, R.A. (1983), A new method for in situ measurements of hydraulic conductivity, Methods and Instrumentation for the investigation of groundwater systems, TNO

Roberson, P.K. (1990), Soil classification using the cone penetration test, Canadian Geotechnical Journal, 27, pages 151-158

Robertson, P.K. (2009), CPT interpretation – a unified approach, Canadian Geotechnical Journal, volume 46, pages 1-19

Roberson, P.K. (2010), Estimating in-situ soil permeability from CPT & CPTu

Rodgers, J.D. (2006), Subsurface Exploration Using the Standard Penetration Test and the Cone Penetrometer Test, Environmental & Engineering Geoscience, Vol. XII, No. 2, May 2006, pp. 161–179

Rogiers, B. (2013), T. Vienken, M. Gedeon, O. Batelaan, D. Mallants, M. Huysmans and A. Dassargues, Multi-scale aquifer characterization and groundwater flow model parameterization using direct push technologies, Environmental Earth Sciences 2014, 72:1303-1324

Zschornack, L. (2013), G.C. Bohling, J.J. Butler Jr., P. Dietrich, Hydraulic profiling with the direct-push permeameter: Assessment of probe configuration and analysis methodology, Journal of Hydrology 496, pages 195-204

Figure 1.2: Cone penetration test probe
Web address: https://en.wikipedia.org/wiki/Cone_penetration_test
Latest access: Februari 2016

Figure 1.3: Failure of soil around the cone, forming a zone of disturbance (Rodgers, 2006)
Rogers, J.D. (2006), Subsurface exploration using the SPT and CPT, Environmental & Engineering Geoscience, Vol. XII, No. 2, May 2006, pages 161–179

Figure 1.1: Piping under a dike, arrows indicate flow direction (WR, 2014
Waterschap rivierenland
Web address: https://www.youtube.com/watch?v=8-oZrG-Bi_E
Latest access: Februari 2016

Wiki, 2016
Figure 5.4: Cardioid shape
Web address: https://en.wikipedia.org/wiki/Cardioid
Latest access: Januari 2016

Appendix A

Comsol parameter equations:

*ρ = 838.466135+1.40050603*T^1-0.0030112376*T^2+3.71822313E-7*T^3*

*μ = 1.3799566804 - 0.021224019151*T^1 + 1.3604562827E-4*T^2 - 4.6454090319E-7*T^3 + 8.9042735735E-10*T^4 - 9.0790692686E-13*T^5 + 3.8457331488E-16*T^6*